DISSERTATION

# AN INVERSE PROBLEM AND MULTI-COMPARTMENT LUNG MODEL FOR THE ESTIMATION OF LUNG AIRWAY RESISTANCE THROUGHOUT THE BRONCHIAL TREE

Submitted by

Emily Heavner

Department of Mathematics

In partial fulfillment of the requirements

For the Degree of Doctor of Philosophy

Colorado State University

Fort Collins, Colorado

Fall 2022

Doctoral Committee:

Advisor: Jennifer Mueller

Patrick Shipman
Margaret Cheney
Marlis Rezende

ABSTRACT

AN INVERSE PROBLEM AND MULTI-COMPARTMENT LUNG MODEL FOR THE ESTIMATION OF LUNG AIRWAY RESISTANCE THROUGHOUT THE BRONCHIAL TREE

Mechanical ventilation is a vital treatment for patients with respiratory failure, but mechanically ventilated patients are also at risk of ventilator-induced lung injury. Optimal ventilator settings to prevent such injury could be guided by knowledge of the airway resistance throughout the lung. While the ventilator provides a single value estimating the total airway resistance of the patient, in reality the airway resistance varies along the bronchial tree. Multiple literature sources reveal a wide range of clinically used values for airway resistance along the bronchial tree, motivating an investigation to estimate the values of airway resistance in the alveolar tree and the relationship to disease state.

In this work, we introduce a multi-compartment asymmetric lung model based on resistor-capacitor circuits by using an analogy between electric circuits and the human lungs. A method for solving the inverse problem of computing the vector of airway resistance values in the alveolar tree is presented. The method uses a linear least squares optimization approach with several constraints. First, a symmetric lung model that makes use of parameters supplied by the mechanical ventilator of patients with acute respiratory distress syndrome (ARDS) is used. We then generalize the model to an asymmetric lung model. The asymmetric model takes regional information data from electrical impedance tomography, a medical imaging technique, and converts them to time dependent lung airway volumes. The linear least squares optimization inverse problem is embedded in an iterative method to update unknown parameters of the forward problem for the asymmetric case.

# ACKNOWLEDGEMENTS

Throughout this journey there were many people who encouraged me. Thank you to my advisor, Dr. Jennifer Mueller. My research would not have been possible without your aid and support. I am grateful for all your help to make this degree a reality. Thank you to my mom and dad for your encouragement toward exploring and pursuing my goals. A forever thank you to my husband, Steven, who knows first hand what this journey has been like. I am eternally grateful for your continuous love and support. To my fellow graduate students, thank you for making me a better mathematician and for the life long friendships we have created.

A big thank you to data collectors, Dr. Julie Dunn, Corey Mohnike, Patrick (PJ) Offner, and Dr. Ellen L. Burnham, for going above your already hefty work load to collect data for these projects. Also, to Nilton Barbosa da Rosa Jr. , thank you for running reconstructions and sending me volume data from the EIT machine so that I could properly apply it.

Thank you to the National Institutes of Health and Math Department of Colorado State University. Research reported in this paper was supported by the National Institute Of Biomedical Imaging And Bioengineering, a division of the National Institutes of Health under Award Number R01EB026710. During graduate school, I was also funded as a teaching assistant at Colorado State University.

TABLE OF CONTENTS

# Chapter 1

# Introduction

There is a long, rich history of mathematicians investigating the human body through mathematical models or systems of equations that describe the real world. We describe the respiratory function of the human body and its many aspects through an application of mathematical models to optimize patient specific ventilation and decrease the potential for damage. In this thesis, we predict and determine the airway resistance throughout a human lung by utilizing a multi-compartment lung model that relates the human lungs to electrical circuits through resistor-capacitor (RC) circuits. This RC-circuit Based (RCCB) lung model will be applied to data collected on mechanically ventilated patients with acute respiratory distress syndrome (ARDS), some of whom are COVID-19 positive. We will collect parameters for the RCCB lung model using ventilator screenshots and electrical impedance tomography (EIT).

Input parameters for the RCCB lung model are compliance (L/cm $H_20$), airway resistance (cm $H_20$/L/s), inhalation and exhalation breathing time (seconds), and applied pressure (cm $H_20$). The model outputs the lung volume at a given time per compartment. To ensure lung volume output is accurate, we need the correct input parameters, including airway resistance values. Airway resistance describes the resistance to airflow in an airway during inhalation and exhalation. Airway resistance is an opposition of flow in the lung caused by the forces of friction. If the airway resistance value is predicted incorrectly, then the total lung volume can be affected.

When studying the lungs, we find the literature presents wide ranges of airway resistance values. For example, [1] states the lung resistance is $0 - 0.09$ cm $H_20$/L/s per generation while [2, 3] claim the lung resistance per generation is $0 - 20$ cm $H_20$/L/s. Still others report airway resistance values from $2 - 3$ cm $H_20$/L/s or even $500 - 1500$ cm $H_20$/L/s [4, 5]. The reason for this may be based on the type of technique used to open one's airway which differs depending on the type of airway obstruction and the size of the oral airway [6]. These varying resistance values motivate us to investigate further into determining airway resistance throughout the bronchial tree.

As mentioned, we collect parameters for the RCCB lung model using ventilator screenshots and EIT. We introduce two studies. The first study, in chapter 6, focuses on modeling a symmetric lung and is completed with patients on the Hamilton G5 series as a mechanical ventilator. The Hamilton G5 series includes an airway resistance value which represents the total overall airway resistance in the bronchial tree [7, 8]. An example of a ventilator screenshot collected is seen in Figure 1.1. Although the Hamilton G5 series ventilator has a reported compliance value, the manual states it is not reliable; and thus, in the first study, we manually calculate compliance based on the definition [7].

The second study, discussed in chapter 9, focuses on modeling an asymmetric lung and uses both the Hamilton series and the Puritan Bennett 980 Series Ventilator. Both ventilators provide minimum and maximum pressure values, volume curves, compliance, and a ventilator reported airway resistance value, which represents the total overall airway resistance in the bronchial tree [7, 8]. Examples of ventilator screenshots can be seen in figures 1.1 and 1.2.

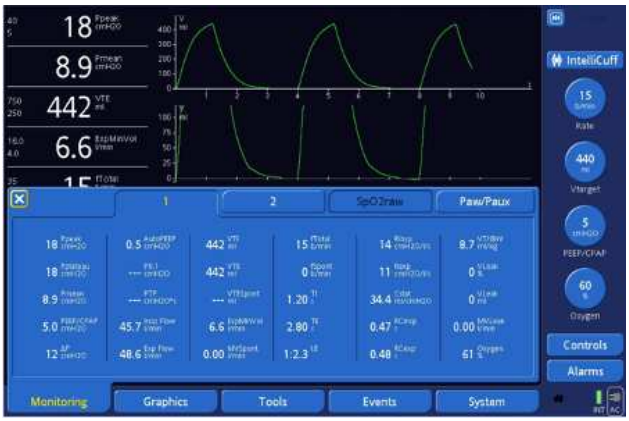


**Figure 1.1:** A screenshot of ventilator settings including two volume curves in green with time in seconds on the horizontal axis and volume in mL on the vertical axis. The two volume curves are over the same time with different mL scales. The bottom half of the screenshot includes parameters like inhalation time, exhalation time, pressure values, and others.


**Figure 1.2:** Two screenshot of the Puritan Bennett 980 Series Ventilator. Both screenshots come from one patient and are discussed in chapter 9. The screenshot on the left includes curves like pressure and airflow rate. The screenshot on the right includes the resistance value, compliance, and minimum and maximum pressures.

Starting in December 2019, the world was hit with a novel strain of coronavirus, called coronavirus disease 2019 (COVID-19) [9]. This virus rapidly spread through many countries, causing travel restrictions and quarantines. COVID-19 effected the respiratory system which resulted in many hospitals reaching or surpassing their maximum capacity because so many patients were relying on mechanical ventilators. One of the challenges the medical field has faced when working with COVID-19 positive patients is determining the protocol to use, or the steps to ensure the patients' safety and recovery [10–12]. Studying COVID-19 patients allows us to determine if there are statistically significant differences in airway resistance values between COVID-19 positive patients and COVID-19 negative patients.

Currently, there is no direct method to measure resistance values along the bronchial tree. In this work, a $2^n$-generation model of airway resistance in mechanically ventilated patients is estimated from the solution of an inverse problem with ventilator data as input. A multi-compartment lung model based on resistor-capacitor circuits is presented to estimate the ventilation volume throughout the breathing cycle. Resistance in the pulmonary system can include both airway resistance and viscoelastic resistance, which help describe how much the lung walls can expand. The

model presented in this thesis does account for viscoelasticity in parameters including compliance, but the focus is on determining airway resistance.

To estimate the resistance values along the bronchial tree, a constrained regularized inverse problem is formulated to obtain the best least-squares fit to the ventilation volume curves obtained from the ventilator. In this work, a multi-generation lung model is implemented and studied using data from two studies. The resistance in the endotracheal tube is assumed to be a part of the $0^{th}$ generation. In the first study, estimated resistance values were statistically compared in terms of sex and COVID-19 diagnosis. Airway resistance vectors of a nine-generation lung along the bronchial tree are compared to the single-value airway resistance parameter from the ventilator.

In the second study, we update the lung model and use medical imaging to reflect asymmetries, regional lung volume, and total lung volume. We use a 5-generation system to study COVID-19 negative patients who have ARDS. We develop a multi-compartment asymmetric lung model that accounts for collapsed or blocked airways. This updated RCCB lung model defines a unique lung structure for each patient by using medical images. We detect where asymmetries in the lung are by collecting data using the GE GENESIS EIT system, reconstruct the data, and calculate lung volumes. We then estimate lung volume in each airway at a given time. These airway volume estimates are applied and used on the RCCB asymmetric lung model for each individual patient.

In this thesis, we give background on the human lungs, develop and describe the RC-circuit Based (RCCB) lung model, and include a literature review of other lung models to explain and motivate the importance of this study. We introduce and discuss a study to determine the airway resistance values throughout the bronchial tree including the data collection process and results. We update the RCCB lung model to include asymmetric flows to determine the airway resistance of ARDS patients using mechanical ventilators.

# Chapter 2

# Introduction to Pulmonary Physiology

Before introducing the RC-circuit Based (RCCB) lung model, we provide some background on the human lungs. The RCCB lung model describes respiratory mechanics which include resistance and compliance [13]. The main purpose of the lungs is to transfer oxygen to the bloodstream and remove carbon dioxide [1]. The human lung has a tree-like structure which consists of a series of branching tubes [1]. For our lung model, we assume a dichotomous structure, meaning each branch leads into another two branches. We start with the main bronchi, and, as we move further down the lung, the branches become narrower and shorter until we reach the terminal branches [1]. Besides branching, human lungs also have generations. We view generations like generations on a family tree; the main bronchi starts at the $0^{\text{th}}$ generation and the generations end at the terminal branch, which is the $23^{\text{rd}}$ generation. Overall, the average human lungs have a total of 24 generations [1]. Visuals of lung branching and lung generations can be found in [1].

When humans inhale, or participate in inspiration, lung volume increases [1]. Expiration, or the act of exhaling, is passive; since the lungs are elastic, they naturally release air [1]. However, when the lungs are under stress (like during a cardiovascular workout) exhaling is not passive and there is a certain amount of force the lungs apply to release air. For ventilated patients, we assume the lungs are not under stress and exhalation is passive.

It is also important to understand common terminology used when talking about the lungs. Applied pressure is the amount of pressure applied to the lungs. If we think about a mechanical ventilator, or a medical device that assists in breathing for a patient, a certain amount of pressure is applied to the airway, allowing oxygen to be pushed into the lungs. Mechanical ventilation is used in hospitals and is common in intensive care units. During the COVID-19 outbreak, the use of mechanical ventilators in intensive care units increased. This increase is due to COVID-19 being a pulmonary disease that effects the lungs [9]. However, not all COVID-19 patients require mechanical ventilation and not all ventilated patients during this pandemic have COVID-19. For

more extreme COVID-19 patients, ventilators are utilized to help assist the patient in breathing. The condition that causes COVID-19 patients to need mechanical ventilation is acute respiratory distress syndrome (ARDS).

Acute respiratory distress syndrome (ARDS) is a clinical condition of lung injury. Patients with ARDS tend to have more complications and higher morbidity rate [14]. This has caused an increase in studies examining the cause, prevention, and care of ARDS. ARDS is a complex clinical condition in which inflammation of lungs and fluid in the alveoli lead to low blood oxygen levels. It is treated with mechanical ventilation through an endotracheal tube, but potential side-effects include ventilator-induced pneumonia and lung damage. Risks of ventilator-induced lung injury (VILI) are reduced when the proper ventilator settings are applied [15]. Typical ARDS patients have higher elastance and reduced gas exchange and can be challenging to ventilate.

It has been recognized that COVID-19 ARDS differs from the "typical" ARDS [12]. COVID-19 patients have been found to have relatively high respiratory compliance accompanied by severe hypoxia, with a discrepancy rarely seen in most forms of ARDS [12]. The high compliance indicates well preserved gas volume and a poorly recruitable lung, also uncommon in severe ARDS [16]. This unusual discrepancy suggests that the standard ventilation protocol for treating ARDS patients may not be optimal for patients with COVID-19. A better understanding of airway resistance along the bronchial tree can inform ventilator strategies to optimize outcomes.

Compliance is another common terminology used when discussing the lungs. The change in volume between inspiration and expiration per unit pressure is known as compliance, given by, $C = \frac{\Delta V}{\Delta p}$ [1]. Compliance, "is the measure of how difficult it is to stretch the lung tissue in order to increase lung volume" [17]. Another important variable that effects lung volume is airway resistance, which is the pressure difference divided by air flow rate. Flow rate is a measure of the velocity of the air through the bronchi and other airways. Flow rate describes the gas moving around in the lungs and is dependent on the individual. For example, someone with asthma will have more airway resistance because their flow rate is smaller than someone without asthma [18].

Airway resistance in the bronchi is estimated as a single parameter from the ventilator in patients receiving mechanical ventilation. However, airway resistance varies along the bronchial tree, decreasing proportionally to the fourth power of the radius of the airway under laminar flow. In human lungs, airflow is both laminar and turbulent, resulting in a complex and nonlinear relationship between airway geometry and resistance. Furthermore, the airways are connected in both series and parallel, and the exact structure is unique for each individual. Knowledge of airway resistance along the tree can provide important clinical information, such as location of airway obstruction and response to bronchodilators [19]. We further hypothesize that such knowledge could aid in individualizing ventilator settings for patients with acute respiratory distress syndrome (ARDS).

Since we are using mathematics to describe the real world it is important to note the physical constraints. The total lung volume that the average adult human lung can physically expand to is around 5 liters (L). However, this number can change up to a half liter due to altitude, gender, height, and health [1, 20, 21]. For accuracy, we will assume a max of 5 L for total lung volume but when modeling patients on a ventilator, volumes should not surpass 5 liters. Now that we have some background on what the lungs are, we can represent the human lungs through mathematical equations using an analogy to electrical circuits.

# Chapter 3

# Literature Review

When studying the lungs and mathematical models that represent respiratory function, we found ourselves asking what the airway resistance is throughout the bronchial tree. There are varying reported values of airway resistance in the human lungs [1–5]. Despite these conflicting and varied values, the shape of the resistance curve is consistent throughout each source. The resistance curve represents the resistance value throughout each generation of the lung, and is plotted as a generation versus resistance graph. An example of a lung generation versus airway resistance curve can be seen in figure 3.1, where the horizontal axis represents the generation in the lung and the vertical axis is the resistance value, with varying scales. The resistance value tends to start off near the peak, peak within the first few generations, and then decrease. Airway resistance, "is predominately affected by the large branch [and] overall resistance of the small airway is negligible" [22]. Airway resistance for larger airways is nonlinear due to "turbulent flow effects" [23].

Multiple mathematical models that describe ventilation, diffusion, and perfusion as gas exchange in the lungs are presented in [13]. Although this is related to lung volume, the equations focus on describing and modeling gas exchange and ventilation as opposed to parameters of respiratory mechanics such as resistance and compliance. We wish to describe lung mechanics as opposed to pulmonary gas exchange. Since the models from [13] are not the best model for our case, we explore other mathematical models that describe respiratory function.

Many sources have related lung mechanics to electric circuits, including [23–29]. More specifically, there is an analogy between lungs and circuits; the summary of the relation can be seen in table 3.1, which is based on work from [26]. We will explore the analogy in depth in Chapter 4. The work done in [25] introduces a multi-compartment model that describes dynamic conditions of respiratory mechanics. In the study from [25], the model was validated against experimental data. The model requires multiple pressure values and resistance values used throughout the ventilation system that we cannot collect in our study.

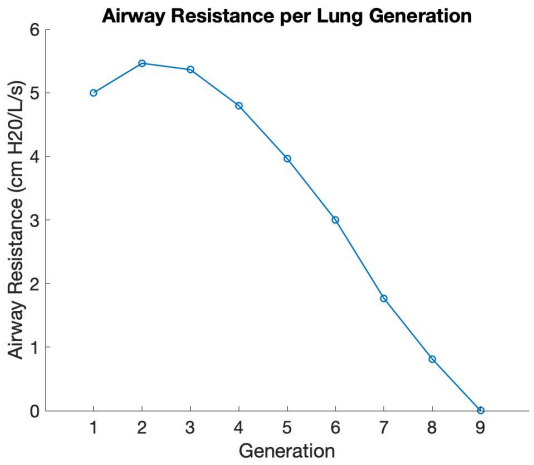


**Figure 3.1:** An example of a resistance curve with lung generation versus airway resistance. Although the reported vertical axises scale varies the overall shape is consistent.

**Table 3.1:** Summary of the analogy between electrical circuits (on the left) and the human lung (on the right).

| **Electrical Component (units)** | **Respiratory Component (units)** |
|---|---|
| Voltage (volts) | Pressure (cm $H_20$) |
| Current Flow (amps) | Gas Flow (L/s) |
| Electrical Resistance (ohms) | Airway Resistance (cm $H_20$/L/s) |
| Quantity (coulombs) | Volume (L) |
| Capacitance (farads) | Compliance (L/cm $H_20$) |

During research into other models, we found a model that focuses on the relationship of the cardiovascular and respiratory system to create a cardiopulmonary model [29]. This approach focuses on modeling two systems of the body; the model is a single compartment model made up of 78 differential equations and 240 parameters. Although we can simulate data using this model, actually collecting 240 parameters from both the respiratory system and the cardiovascular system would be a challenge. We would also have to adapt this 78 differential equation system to represent a multi-compartment lung. Since we assume a dichotomous structure, converting

this model into a multi-compartment lung model could require $(2^n)(78)$ equations where $n$ is the number of generations. This model is mathematically more complex than we want, but studying this model closely allows us to see a numerical simulation of a time versus volume graph that outputs the same shape we expect from ventilator volume curves. Although this model requires parameters we would not be able to physically collect, we found it useful as it related the pulmonary and cardiovascular systems to electrical circuits. Many of the parameters in [29] including volume, resistance, and compliance required decomposing the values into different sections of the lungs that we would not be able to account for or collect. Although we do not use the model from [29], we do use the analogy of lungs and circuits it introduces.

As mentioned, [23, 24] both utilize electric circuits to model the lung. The study conducted in [24] presents a single compartment first order model to describe respiratory mechanics and uses data from mechanical ventilation. In [23], we are introduced to multiple mathematical models of lung mechanics, from first order single compartment lung models to more complex multi-compartment models. The first order equation assumes constant resistance and constant compliances value in a single compartment lung. The first order model presented in [23, 24] describes applied pressure over some time and takes the form of

$$p = r\dot{V} + \frac{1}{c}V + p_0 \tag{3.1}$$

where $p$ is applied pressure, $r$ is resistance, $\dot{V}$ is flow, $V$ is volume, $c$ is compliance, and $p_0$ is positive end-expiratory pressure (PEEP). Since these models are comparing circuits and the human lung we can use the analogy from table 3.1 to see the solution to equation (3.1) also describes a resistance-capacitor circuit charging and discharging. We found resistance and capacitor circuits (RC-circuits) produce a time versus capacitor voltage graph with the shape we see in our ventilator screenshots.

The multi-compartment model introduced in [23] is the Horsfield model named after British medical doctor, Keith Horsfield. This model assumes a dichotomous structure and is based on the data obtained from a resin cast of the bronchial tree. The Horsfield model assumes every airway is

a rigid tube and uses the, “law of propagation of sound waves in a cylindrical tube” to describe lung mechanics [23]. The equation representing resistance in the Horsfield model requires knowledge of a patient’s radius and length per each tube segment as well as gas viscosity. Unfortunately, we do not have the patient’s radius and tube length for each segment along the bronchial tree, so we do not use this equation. This model does not account for resistance differences between inhale and exhale either.

So far, the models we have discussed are either too complex, require more parameters than we are able to collect, or are based off a single compartment lung. Since we want to determine the airway resistance throughout the entire lung, we need a model that represents and predicts parameters that consider each generation. To do this, we need to develop a multi-compartment model. According to [21], many mathematical models have described respiratory function with the goal of better understanding the process of mechanical ventilation including [26, 30–33]. These models have all assumed a homogeneous lung function with a single compartment. Although there have been some models that have expanded to a two-compartment lung, the true lung is composed of multiple airways. Compartmental lung models can be described by vectors and matrices, whose components are volumes of the individual compartments [21].

The model developed in [21] has the attributes of being a multi-compartmental dynamical system lung model to predict time-dependent lung volume in each compartment given the compliance, airway resistance, and pressure, but the shape of the resulting volume curve is not a good match to the observed shape from a patient receiving mechanical ventilation. Figure 3.2 includes a numerical simulation based on the dynamical system model in [21]. The exhale does not decay as fast as expected and the curve appears more like a mountain peak as opposed to a “shark fin" we see in the ventilator volume curves. The dynamical system lung model from [21] takes time and multiple breaths to reach its stability point. This means, the model must run through multiple iterations before yielding its results. Even though this model does not reflect the accurate shape of volume we expect, we can utilize the concept of the multi-compartment vector, where each element of the vector represents the volume of each compartment.

We utilize the first order model presented in equation (3.1), the analogy between electrical circuits and the lungs, as well as the multi-compartment aspects of the dynamical system lung model in [21] to determine the airway resistance throughout the bronchial tree. We expand on the first order model to include parameters throughout the lung.

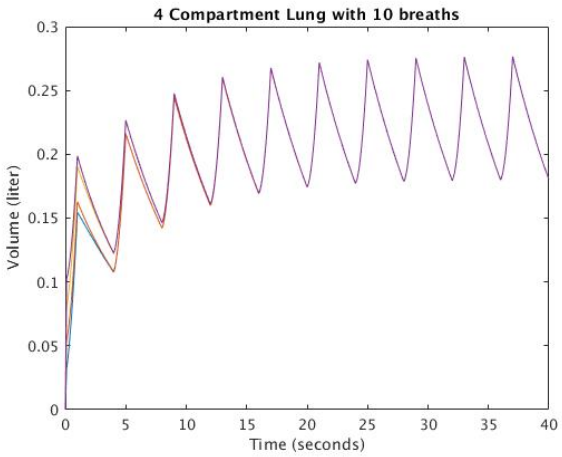


**Figure 3.2:** A time versus volume numerical simulation of a 4 compartment, 2-generation lung with 10 breaths based on the model introduced in [21]. Each $x_i$ represents the volume of the $i^{th}$ compartment. For example, $x_1$ is the volume of the first compartment.

# Part I Reconstruction of Airway Resistance in a Symmetric Lung

# Chapter 4

# Forward Problem for a Symmetric Lung

To actually describe and determine parameters in the real world, we need a mathematical model. The RC-circuit Based (RCCB) multi-compartment lung model is introduced in this paper. We create a mathematical model using knowledge from the multi-compartment aspects of [21] and the first order equations and analogy of lung to circuits in [23, 24, 29]. The RCCB lung model takes in time (seconds), airway resistance (cm $H_20$/L/s), compliance (L/cm $H_20$), and pressure (cm $H_20$) and outputs lung volume (L) at a given time. Many sources [24–29, 34, 35] make the connections between electrical circuits and the lungs. The RCCB lung model proposed in this work uses the analogy between electrical circuits and the lungs to describe respiratory mechanics in the human lung. The RCCB model relies on lung volume information as it can be found using both the mechanical ventilator and electrical impedance tomography.

Based on the data we collect, we create a model that describes the lung volume at a given time. Consider the patient's volume curve in figure 4.1. We see two consistent "shark fin" shapes where the patient's inhale takes the form of a logistic growth curve until it plateaus and the exhalation decays exponentially. From the shape of the inhalation and exhalation curves, we see this time versus volume curve is similar to a resistor-capacitor (RC) circuit curve charging and discharging a capacitor. In a resistor-capacitor (RC) circuit, the resistor and capacitor are connected. With the presence of a resistor, the capacitor charges slowly. A capacitor has a time delay that represents the amount of time required to charge the capacitor to full capacitance. When voltage is initially applied to a RC circuit, the capacitor is charging at its fastest rate because the voltage difference is highest. In the lungs, this is reflected by the volume increasing the fastest at the start of an inhale due to the driving pressure in the lung. The charging rate of the circuit begins to exponentially decrease to a slower rate when the voltage is not applied. In order to discharge a RC circuit, the voltage supply is removed and the circuit discharges at a variable rate. The curve shape of a RC

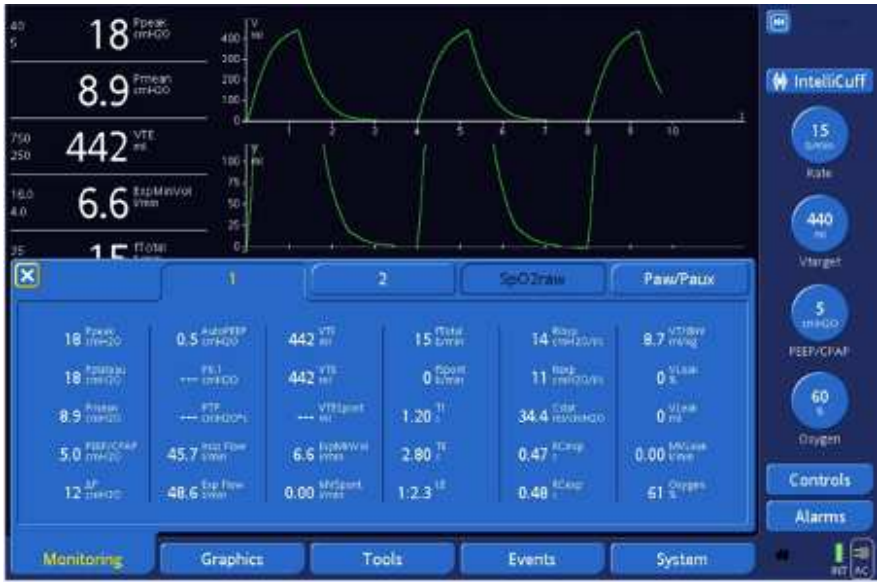


**Figure 4.1:** A screenshot of the mechanical ventilator Hamilton G5 series. The patient is a female with a 7.5 endotracheal tube, a plastic tube that goes from a ventilator to the patient's trachea. The green volume curve is one of the most important data pieces we collect. It displays time in seconds on the horizontal axis and volume in milliliters (mL) on the vertical axis.

circuit charging and discharging, seen in [36], is similar to the volume of a lung inhaling and exhaling on a mechanical ventilator.

There are known equations that describe a RC circuit charging and discharging and we make an analogy from these parameters to the human lung. Equations (4.1) and (4.2) describe the voltage across a RC circuit,

$$v = v_u \left(1 - \exp\left[-\frac{t}{\rho a}\right]\right) \tag{4.1}$$

$$v = v_u \left(\exp\left[-\frac{t}{\rho a}\right]\right) \tag{4.2}$$

where $v$ is the voltage during charge and discharge (equation (4.1) and equation (4.2), respectively), $v_u$ is the supply voltage, $t$ is time, $\rho$ is electrical resistance, and $a$ is capacitance. We apply the analogy between lungs and circuits, seen in Table 3.1, to convert equations (4.1) and (4.2) into

equations (4.3) and (4.4) which describe the pressure of the lungs over time.

$$p = p_u \left(1 - \exp\left[-\frac{t}{rc}\right]\right) \tag{4.3}$$

$$p = p_u \left(\exp\left[-\frac{t}{rc}\right]\right) \tag{4.4}$$

where $p$ is the total pressure during inhalation and exhalation (equation (4.3) and equation (4.4), respectively), $p_u$ is the supply pressure, $t$ is time, $r$ is airway resistance, and $c$ is compliance.

Equations (4.3) and (4.4) describe the lungs in terms of pressure, but the time-dependent lung volume curve from mechanical ventilator data will be used in the inverse problem of estimating airway resistance. Thus, we need to include volume as a parameter in the model. Returning to the analogy of circuits, the electrical charge, $q$, stored on plates of the capacitor is given by the product of capacitance, $a$, and voltage, $l$, such that $q = al$ [36]. In terms of the lung, this equation becomes the product of compliance and pressure which describes volume. Thus, the equations for volume at a given time of a single compartment lung are

$$v_{in}(t) = pc \left(1 - \exp\left[-\frac{t}{rc}\right]\right) \qquad t \in [0, T_{in}], \tag{4.5}$$

$$v_{ex}(t) = pc \left(\exp\left[-\frac{t}{rc}\right]\right) \qquad t \in [T_{in}, T_{total}]. \tag{4.6}$$

where $v_{in}$ is inspiration volume, $v_{ex}$ is expiration volume, $c$ is compliance, $p$ is pressure, $r$ is resistance, $t$ is time, $T_{in}$ is the total inhale time, and $T_{total}$ is the total breath time for one inhale and one exhale.

Just like in RC-circuits, equations (4.5) and (4.6) have a time constant represented by product of compliance and resistance in the exponential term [22]. The time constant in an RC-circuit is the product of the resistor and capacitance in the exponential term. Lungs with, "higher resistance and or compliance will have a longer time constant and require more time to" fill or empty [37].

Equations (4.5) and (4.6) are the solutions to the first order single compartment lung model discussed in [24] given appropriate initial conditions. Our goal is to use equations (4.5) and (4.6)

to describe airway resistance throughout the lung, so we extend this single compartment model to a multi-compartment lung model by converting scalar equations into equations that utilize vectors and matrices. The multi-compartment model should return a vector of volume at a given time where each element in the resulting vector will represent the volume of a lung generation. The multi-compartment conversion is based on the model presented in [21]. We assume each branch of the lung divides into two more branches, resulting in $2^n$ compartments, where $n$ is the number of generations throughout the lung. This results in a dichotomous lung structure for our model.

We work with a $2^n$ compartment lung model where $n$ is the number of generations throughout the lungs, and we assume each branch of the lung divides into two more. We also assume the shape of the resistance value curve starts near the peak, peaks, then decreases, as discussed in Chapter 3. Based on [21], both the resistance value and compliance value can be converted into $2^n \times 2^n$ matrices. The compliance matrix is a diagonal matrix with the compliance values throughout the lungs along the diagonal [21].

From the single compartment model, we know each compartment needs compliance and resistance values for each generation. Let $c_i, i = 1, 2, \ldots, 2^n$ be the compliance for the $i^{\text{th}}$ compartment and $R^{in}_{j,k}$, where $k = 1, 2, \ldots, 2^j, j = 0, \ldots, n$ be the airway resistance value in the $k^{th}$ airway in the $j^{th}$ generation during inspiration as in reference [21]. Our inspiratory resistance values are then $R^{in}_{1,1}$ and $R^{in}_{1,2}$, which represent the resistance in the first generation and the first and second airway, respectively. An example is seen in figure 4.2. The resistance value when exhaling, $R^{ex}_{j,k}$, is defined in a similar manner.

We know from [2, 19, 35, 38, 39] airway resistance along the tree starts near its peak value and rises until around the beginning of the middle generations. From there, the subsequent generations drop in resistance values, revealing a concave down shape. Overall, generation resistance values drop further into the lungs since resistance to airflow depends on the number of parallel pathways present, and the larger and medium sized airways provide a greater resistance to flow than the numerous small airways [38].

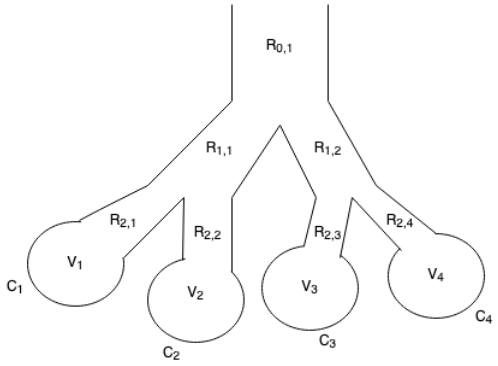


**Figure 4.2:** A four compartment, two generation, lung model based off work from [21]. Each compartment has its own compliance value, $c_i$, although we assume it is the same value regardless of compartment for the RCCB lung model. $V_i$ is the volume of compartment $i$, and $R_{j,k}$ is the resistance value that corresponds to the $j^{th}$ generation and the $k^{th}$ airway in the generation. We read airways from left to right in a generation.

Since a dichotomous lung structure results in a system of $2^n$ equations, both the resistance value and compliance value can be converted into $2^n \times 2^n$ matrices. The compliance matrix is a diagonal matrix with the compliance values of each compartment along the diagonal [21]. Let $c_i, i = 1, 2, \ldots, 2^n$ be the compliance for the $i^{th}$ compartment. We define the compliance matrix $C$ to be a diagonal matrix with $c_i$ on the diagonal. We assume the compliance is equal throughout each airway in a generation. The overall lung compliance was assumed to be uniform along each terminal airway, and so the overall total lung compliance, $C_{total}$ is divided by $2^n$, with $C_{total}/(2^n)$ becoming the entries of the $2^n \times 2^n$ diagonal compliance matrix, $C$.

The resistance values in the bronchial tree are represented by a matrix using the method introduced in [21], defining $R_{j,k}$, $j = 0, \ldots, n$, and $k = 1, 2, \ldots, 2^j$, to be the airway resistance value in the $k^{th}$ airway in the $j^{th}$ generation. For example, $R_{2,3}$ is the airway resistance value in the third airway of the second generation. The $2^n \times 2^n$ matrix $R$ is then formed by taking the sum:

$$R = \sum_{j=0}^{n} \sum_{k=1}^{2^j} R_{j,k} Z_{j,k} Z_{j,k}^T, \tag{4.7}$$

where $R_{j,k}$ is a scalar representing the resistance in the $k$th airway in the $j$th generation and $Z_{j,k}$ is a vector defined as follows. The vector $Z_{j,k} \in \mathbb{R}^{2^n}$ is defined such that the $l^{th}$ element of the vector $Z_{j,k}$ is 1 for all $l = (k-1)2^{n-j}+1, (k-1)2^{n-j}+2, \ldots, k2^{n-j}, k = 1, 2, \ldots, 2^j, j = 0, \ldots, n$ and

zero elsewhere [21]. Thus, $Z_{j,k}Z_{j,k}^T$ is a $2^n \times 2^n$ matrix. An example of finding the matrix $R$ for a 4 ($n = 2$) compartment model, seen in figure 4.2, is

$$\begin{aligned} R &= \sum_{j=0}^{2}\sum_{k=1}^{2^j} R_{j,k}Z_{j,k}Z_{j,k}^T \qquad (4.8)\\ &= R_{0,1}Z_{0,1}Z_{0,1}^T + R_{1,1}Z_{1,1}Z_{1,1}^T + R_{1,2}Z_{1,2}Z_{1,2}^T + R_{2,1}Z_{2,1}Z_{2,1}^T + R_{2,2}Z_{2,2}Z_{2,2}^T \\ &+ R_{2,3}Z_{2,3}Z_{2,3}^T + R_{2,4}Z_{2,4}Z_{2,4}^T \\ &= R_{0,1}[1,1,1,1][1,1,1,1]^T + R_{1,1}[1,1,0,0][1,1,0,0]^T + R_{1,2}[0,0,1,1][0,0,1,1]^T \\ &+ R_{2,1}[1,0,0,0][1,0,0,0]^T + R_{2,2}[0,1,0,0][0,1,0,0]^T + R_{2,3}[0,0,1,0][0,0,1,0]^T \\ &+ R_{2,4}[0,0,0,1][0,0,0,1]^T. \end{aligned}$$

Notice, that $R$ by definition is row-equivalent and column-equivalent, so the matrix $R$ is invertible. More detail on the invertibility of these matrices can be found in [21].

Using this knowledge enables one to convert the exponential term in equations (4.5) and (4.6) to a $2^n \times 2^n$ exponential matrix. Note that this $2^n \times 2^n$ matrix represents the resistance in every airway for an $n$ generation lung, whereas a vector of length $(n+1)$ represents the total resistance in each generation. For example, equation (4.8) defines the airway resistance as a matrix of a $2^2 = 4$ compartment lung which can be written as a vector of length 3 with $[R_0, R_1, R_2]$ representing the total airway resistance in generation $0, 1$ and $2$ respectively.

The division of the resistance and compliance product, seen in equations (4.5) and (4.6) becomes the inverse of the product in the exponential matrix. The pressure term is a $1 \times 2^n$ vector where each element represents the total pressure in a generation. Volume, $\vec{V}(t)$, is a $1 \times 2^n$ vector where each entry represents the volume in one of the $2^n$ compartments at a given time, $t$. In this model, we assume time starts over at every inhale.

Given the total inhale time $T_{in}$ and total breathing time $T_{total}$, the volume of air in the lungs over a single breath is given by the RCCB lung model:

$$V(t) = \begin{cases} \vec{V_{in}}(t) = \vec{p}^T C \left(\mathbb{I} - \exp\left[-t(RC)^{-1}\right]\right) & t \in [t_0, T_{in}] \\ \vec{V_{ex}}(t) = \vec{p}^T C \exp\left[-t(RC)^{-1}\right] & t \in [T_{in}, T_{total}], \end{cases} \tag{4.9}$$

where $\vec{V_{in}}$ $(1 \times 2^n)$ is inhalation volume, $\vec{V_{ex}}$ $(1 \times 2^n)$ is exhalation volume, $C$ $(2^n \times 2^n)$ is compliance, $\vec{p}$ $(1 \times 2^n)$ is pressure, $R$ $(2^n \times 2^n)$ is resistance, $\mathbb{I}$ is an $2^n \times 2^n$ identity matrix. To determine the total volume per breath, $V(t)$, we can combine or append $\vec{V_{in}}(t)$ and $\vec{V_{ex}}(t)$ such that $V(t) = [\vec{V_{in}}(t) \;\; \vec{V_{ex}}(t)]$ for all time $t \in [t_0, T_{total}]$. The resistance in equation (4.9) does not include the resistance in the endotracheal tube, but we assume this value is taken into account as part of the $0^{th}$ generation.

This yields the RCCB lung model. This model describes respiratory mechanics for an adult lung as infants and newborns have different respiratory characteristics like low compliance and high resistance values [34]. Using the RCCB lung model for our studies, $R$ is unknown and all other parameters are known from data sets or literature. Unfortunately, we can not easily solve equation (4.9) for the unknown vector $R$. To determine resistance, we will solve an inverse problem.

## 4.1 Model Improvements

For this model, we assume a symmetric lung, meaning every airway in a generation has the same parameter values and is essentially identical. This assumption, especially for patients on mechanical ventilators with ARDS, is not realistic. Many patients on ventilators have diseased lungs with potential areas of mucus or air trapping blocking certain airways. Applying asymmetries to the model would add complexties to matrices and equations. Even though it is less realistic, for now we assume a symmetric lung to test the RCCB lung model. In chapter 7, we add asymmetries to the RCCB lung model.

In the RCCB model we assume the resistance value throughout a generation is equal. We also assume resistance has a linear relationship. However, this is inaccurate to the real world as many sources ( [17, 40–42]) have defined resistance as a function of flow, such that,

$$R = k_1 + k_2\dot{V(t)} \tag{4.10}$$

where $R$ is a numerical value that represents the total airway resistance in the lung, $k_1$ is the coefficient for laminar flow, $k_2$ is the coefficient for turbulent flow, and $\dot{V(t)}$ represents the rate at which volume changes over time or the derivative of volume with respect to time. If $k_1$, $k_2$, and $\dot{V(t)}$ are known, $R$ can be determined and if $\dot{V(t)}$ and $R$ are known, $k_1$ and $k_2$ can be determine by using least squares, as equation (4.10) is in the slope-intercept form where $k_1$ is the y-intercept and $k_2$ is the slope [40]. However, adding in this realistic knowledge of resistance is impractical for our model as representing resistance in this way, requires us to solve for two unknowns. If we know resistance, $R$, we can determine $k_1$ and $k_2$ by plotting $\dot{V}$ versus resistance and find the slope and y-intercept of the resulting line. However, in this case we have too many unknowns and since the goal is to determine resistance, adding in nonlinear resistance is not realistic but a good hope for future studies to update the model to better real world accuracy. The goal of this study is to predict airway resistance throughout the entire bronchial tree and in every airway. If the RCCB lung model includes equation (4.10) as resistance, we would then be solving for 2 unknown parameters ($k_1$ and $k_2$) per each airway.

In the RCCB lung model, we assume compliance is linear and equal throughout each compartment $k$, for $k = 1, 2, ..., 2^n$. However, previous work has been completed to include nonlinear compliance, as seen in [43]. This work is based off pressure-volume loops or plots of volume versus pressure curves. Compliance is defined to be the derivative of volume with respect to pressure so using pressure-volume loops to determine compliance works well.

In [43], Li and Haddad found for inhalation, compliance starts off low then increases until reaching some specified volume value, the compliance then holds steady until the lungs volume reaches another volume value at which time the compliance will start to decrease. Compliance

associated with exhalation has a similar shape. Using this understanding of compliance, we can conclude compliance is a function of volume. A visual of these increasing, steady, and decreasing nonlinear compliance values can be seen in figure 4.3 for one airway, $k$. As an equation, this becomes,

$$C_k(V_k) = \begin{cases} a_k + b_k V_k, & 0 \leq V_k \leq V_\alpha \\ d_k & V_\alpha \leq V_k \leq V_\beta \\ f_k + j_k V_k, & V_\beta \leq V_k \leq V_\gamma \end{cases} \tag{4.11}$$

which describes the compliance for compartment $k$ where $a_k$, $b_k$, $d_k$, $f_k$, and $j_k$,describe the slope or y-intercept for each compliance value at various volume value $V_k$ including transitional volumes, $V_\alpha$, $V_\beta$, and $V_\gamma$ that trigger the compliance value to hold steady, decrease, or increase. Each volume value depends on time.

To apply nonlinear compliance, we would need to determine $a_k$, $b_k$, $d_k$, $f_k$, $j_k$, $V_\alpha$, $V_\beta$, and $V_\gamma$ for each compartment. The forward and inverse problem would also need to be updated to reflect a nonlinear compliance matrix that depends on volume. Like the work done in [43], we can determine these unknowns by utilizing knowledge on pressure and overall lung volume.

Recall that compliance is defined by the change in volume divided by the change in time. Unfortunately, pressure for mechanical ventilators has a similar shape to compliance, seen in figure 4.3. Where pressure starts low, increases as time increases, then holds steady until the end of inhalation, where pressure then decreases at the start of an exhale, visually seen in figure 6.1. Because of this, for some time the change in pressure is zero which causes the compliance to blow up instead of hold steady as we would be dividing by zero. Due to the amount of unknowns and the type of ventilator techniques we use in the studies, nonlinear pressure would not be appropriate to add in these studies but may be helpful to apply to future studies.

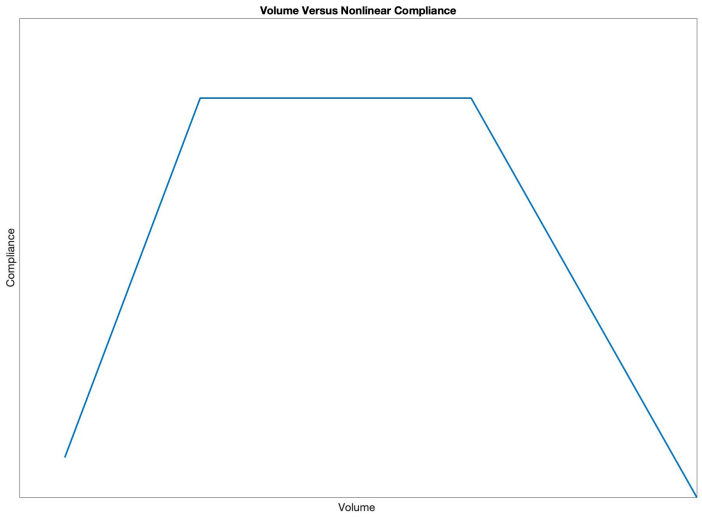


**Figure 4.3:** A plot of volume versus compliance based on the work done in [43]. This plot shows an example of what a compliance might do while lung volume changes.

# Chapter 5

# Inverse Problem for a Symmetric Lung

An inverse problem determines parameters of a system which can only be observed indirectly. In the medical field, inverse problems are a common tool to observe inside a patient indirectly without invasive procedures. We solve an inverse problem to predict the matrix $R$ representing airway resistance along the bronchial tree from the time-dependent measurements of lung volume provided by the ventilator. We solve inverse problems by approximately determining the value or parameter of a model. We know the output of the model and approximate the input of the model that leads to our output using experimental data. The RCCB model's output and the observed data are both given in liters of volume. We use both data from the ventilator and the RCCB model to approximate the resistance vector as the input. A common technique used when solving inverse problems and determining unknown parameters is least-squares minimization with Tikhonov regularization. The inversion approach used here is to solve a constrained least-squares minimization problem with Tikhonov regularization.

There are three constraints included in the minimization problem. First, we constrain the total resistance $R^{tot}$ over all airways to be bounded by and within a specified tolerance $\epsilon$ of the resistance value $R_{vent}$ provided by the ventilator. That is, we require

$$R^{tot} + \epsilon \leq R_{vent}. \tag{5.1}$$

The resistances in successive generation are modeled by resistors in serial and so

$$R^{tot} = \sum_{j=0}^{n} R_{tot}^{j}, \tag{5.2}$$

where $R_{tot}^{j}$ is the total resistance in the $j$th airway.

The airway resistances in the $j$th generation are modeled as resistors in parallel. In electrical circuits, the total resistance of resistors in parallel is computed differently from resistors in series. For example, three resistances $r_1, r_2$, and $r_3$ have total resistance $r_{tot}$ given by

$$\frac{1}{r_{tot}} = \frac{1}{r_1} + \frac{1}{r_2} + \frac{1}{r_3}.$$

Thus, in the $j$th generation the total resistance $R_{tot}^j$ is

$$\frac{1}{R_{tot}^j} = \frac{1}{R_{j,1}} + \frac{1}{R_{j,2}} + \cdots + \frac{1}{R_{j,2^j}} = \sum_{k=1}^{2^j} \frac{1}{R_{j,k}}. \tag{5.3}$$

Under the assumption that all resistances in the $j$th generation are the same, and denoting that value by $R_j$,

$$\frac{1}{R_{tot}^j} = \sum_{k=1}^{2^j} \frac{1}{R_{j,k}} = \sum_{k=1}^{2^j} \frac{1}{R_j} = \frac{2^j}{R_j}. \tag{5.4}$$

So

$$R_{tot}^j = \frac{R_j}{2^j}, \tag{5.5}$$

and the total resistance in the airways is given by

$$R^{tot} = \sum_{j=0}^{n} R_{tot}^j = \sum_{j=0}^{n} \frac{R_j}{2^j} = \sum_{j=0}^{n} \frac{1}{\sum_{k=1}^{2^j} \frac{1}{R_{j,k}}}. \tag{5.6}$$

Since we assume all resistances in the $j$th generation are equal, the unknown resistances can be expressed as the vector $\vec{R} = [R_0, R_1, \ldots, R_n]^T$, to formulate the minimization problem. That is,

$$\vec{R} = \begin{bmatrix} R_{0,1} \\ \frac{R_{1,1}+R_{1,2}}{2} \\ \frac{R_{2,1}+R_{2,2}+R_{2,3}+R_{2,4}}{4} \\ \vdots \\ \frac{R_{n,1}+R_{n,2}+\ldots+R_{n,n}}{2^n} \end{bmatrix} = \begin{bmatrix} R_0 \\ R_1 \\ R_2 \\ \vdots \\ R_n \end{bmatrix}. \tag{5.7}$$

We formulate the model output as $V(\vec{R})$, which represents the volume in the time-dependent RCCB lung model as a function of $\vec{R}$ with time dependence suppressed in the notation. Thus, $V$ is a $1 \times 2^n$ vector at each known discrete time point, $t$. Each element in $V$ represents the volume per generation. Thus, the least-squares minimization problem takes the form

$$\min_{\vec{R}} \left\{ \left\| V(\vec{R}) - V_{vent} \right\|_2^2 + \alpha^2 \left\| \vec{R} \right\|_2^2 \right\}, \tag{5.8}$$

where $V(\vec{R})$ for a single breath is computed at the discrete time points from equation (4.9), converting the vector $\vec{R}$ to the matrix $R$ using the fact that $R_{j,k} = R_j$ for all $k = 1, \ldots, 2^j$. $V_{vent}$ is the measured volume inside a human lung at a given time taken from our mechanical ventilator.

Two additional constraints are applied to the minimization problem based on knowledge of the per–generation resistance in the bronchial tree from clinical literature. Define a minimum and a maximum resistance vector, $\vec{R}_{min}$ and $\vec{R}_{max}$, and require $\vec{R}_{min} \leq \vec{R} \leq \vec{R}_{max}$. In our implementation, $\vec{R}_{min}$ and $\vec{R}_{max}$ were chosen based on the ventilator reported resistance value $R_{vent}$ for each patient and values given in [2,19,35,38,39] based on resistance curves. The vectors were defined as

$$\begin{aligned} \vec{R}_{max} &= [R_{vent}, R_{vent}, R_{vent}, \frac{R_{vent}}{2}, \frac{R_{vent}}{2}, \frac{R_{vent}}{2}, \frac{R_{vent}}{4}, \frac{R_{vent}}{4}, \frac{R_{vent}}{4}]^T \\ \vec{R}_{min} &= [\frac{R_{vent}}{4}, \frac{R_{vent}}{4}, \frac{R_{vent}}{4}, 1, 1, 1, 0.001, 0.001, 0.001]^T. \end{aligned}$$

These vectors were defined consistently for each patient except for a patient that had a smaller reported resistance value than the others of $R_{vent} = 4$. For that patient we defined $\vec{R}_{min} = [0.75, 0.5, 0.1, 0.1, 1e-6, 1e-6; 1e-6; 1e-10; .1e-10; 1e-10]$.

The final constraint is based on the expected shape of the resistance curve, which is concave down, as seen in [2, 19, 35, 38, 39]. This motivates including the constraint $L\vec{R} \leq \vec{b}$, where $L$ is the second derivative discrete operator using centered differences. The vector $\vec{b}$ controls the concavity of $\vec{R}$ and changes per patient based on the reported ventilator resistance value, $R_{vent}$. For $R_{vent} \geq 16$, $\vec{b} = [-1, -1, -1, -0.5, -0.3, -0.2, 0.1, 0.2, 0.3]$. If $8 \leq R_{vent} \leq 15$, then $b = [-0.5, -0.5, -0.5, -0.3, -0.2, -0.15, 0.05, 0.15, 0.1]$. If $R_{vent} < 8$, then $\vec{b} = [-0.3, -0.2, -0.2, -0.1, -0.07, -0.06, 0.1, 0.1, 0.05]$.

Now, letting $n$ denote the number of generations in the model, $V_{vent}$ the ventilator volume, $\alpha$ the regularization parameter, $\epsilon$ a small tolerance, and $\vec{b}$ a bound on the concavity, the constrained minimization problem for the solution of the inverse problem is:

$$\min_{\vec{R}} \left\{ \left\| V(\vec{R}) - V_{vent} \right\|_2^2 + \alpha^2 \left\| \vec{R} \right\|_2^2 \right\} \tag{5.9}$$

$$\text{subject to} \begin{cases} \vec{R}_{min} \leq \vec{R} \leq \vec{R}_{max} \\ L\vec{R} \leq \vec{b} \\ \sum_{j=0}^{n} \frac{R_j}{2^j} + \epsilon \leq R_{vent} \end{cases} \tag{5.10}$$

The function `fmincon` in MATLAB [44] was used to solve the constrained minimization problem for $\vec{R}$, the resistance vector throughout the lung.

The resistance in the endotracheal tube (ETT) is assumed to be a part of the $0^{th}$ generation. The work in [45] included measuring ETT resistance values for multiple sizes in both a controlled setting and after the tube was inside a ventilated human. On average, the measured ETT resistance differed outside the found control range by 3 standard deviations [45]. The measured resistance value of an ex-vivo ETT was found to be consistent across multiple tubes whereas their were many inconsistencies outside of the controlled measurement of in vivo ETTs [45]. Due to these findings,

we do not give a strong constraint on the $0^{th}$ generation. Instead, we take $10\%$ of the reported controlled resistance value for a ETT based on the findings in [45–47]. This value is represented as the tolerance, $\epsilon$ for each patient to account for any potential errors in the ETT resistance value. Over half of the patients in this study had a reported ETT internal diameter of 7.5 mm. In a controlled setting the ETT of size 7.5 has a resistance value of 6 cm $H_20$/L/s. Due to this, the tolerance was set as $\epsilon = 0.6$ for all patients.

The solution method was tested on synthetic data, and a range of values for the regularization parameter was explored to find the optimal value, which was then used for the clinical data sets. Empirically, $\alpha = 0.069$ was found to be optimal for the synthetic data and was used for the experimental data sets.

## 5.1 Inverse Crime for a Symmetric Lung

We solve an inverse crime to test the set up of our inverse problem. An inverse crime is a technique where we input a known parameter into our forward model to then determine the output of our model. In an inverse crime, the RCCB model, or forward model, is used to generate the data as well as predict the data. In this case, we choose and input a known resistance vector, $\vec{R}$, in the RCCB model which then outputs the volume, $V(\vec{R})$. We then use that volume output, $V(\vec{R})$, as our data, $V_{vent}$, in the inverse problem to solve for the known resistance vector, $\vec{R}$ . In this study, we take our model $V(\vec{R})$ and input a $\vec{R}$ vector we create to synthetically create data, $V_{vent}$. The output value of $V(\vec{R})$ becomes $V_{vent}$ and we solve this minimization problem for $\vec{R}$. The results from our inverse problem should approximate the $\vec{R}$ we originally created. If that is not the case, then the inverse problem or model is not reliable. This method is called an inverse crime because one should never claim this is the most accurate model without applying real world data. If the RCCB lung model does not solve an inverse crime, then it has no way of solving the problem with real data.

The solution method was tested on a set of synthetic data, and a range of values for the regularization parameter was explored to find the optimal value, which was then used for the clinical

data sets. Figure 5.1 shows the output lung volume data computed from the forward model seen in equation 4.9 with resistance vector $\vec{R} = [6, 6.7, 6.3, 5.25, 4, 2.93, 2, 1.1, 0.1]$. The resistance vector is shown in blue in figure 5.2. The total time for the two breaths for the volume curve was 7 seconds with an inhale time of 1.5 seconds and an exhale time of 2 seconds. The minimum pressure was set to 5 cm $H_20$, the maximum pressure was 25 cm $H_20$, and a synthetic pressure curve was computed. The compliance was chosen to be 0.032 L/cm $H_20$. The results of our inverse crime can be seen in figure 5.2. Figure 5.2 shows the reconstructed resistance curve in red, using the optimal regularization parameter $\alpha = 0.069$. The computed volume curve corresponding to the reconstructed resistance vector and the true vector are plotted on the left in figure 5.2. The curves are visually indistinguishable with a relative error 2-norm error of 8.8e-7%. This tiny relative error illustrates the ill-posedness of the inverse problem. After confirming the method works when an inverse crime is committed, we can then apply the model to measured data.

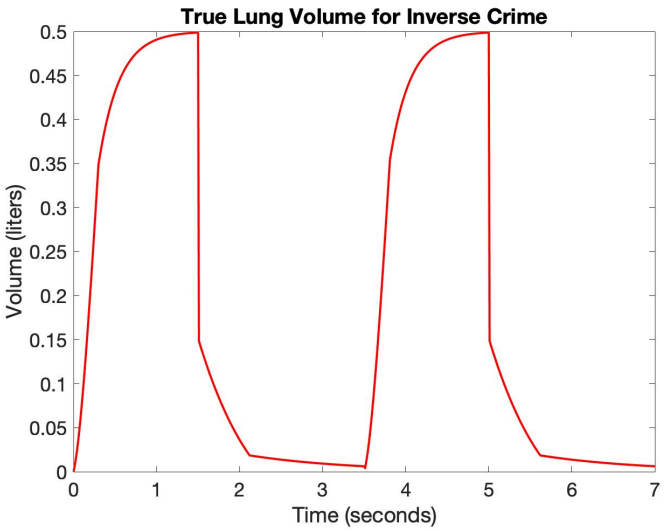


**Figure 5.1:** Synthetically generated lung volume from the forward problem with resistance vector $[6, 6.7, 6.3, 5.25, 4, 2.93, 2, 1.1, 0.1]$ and compliance 0.032 L/cm $H_20$.

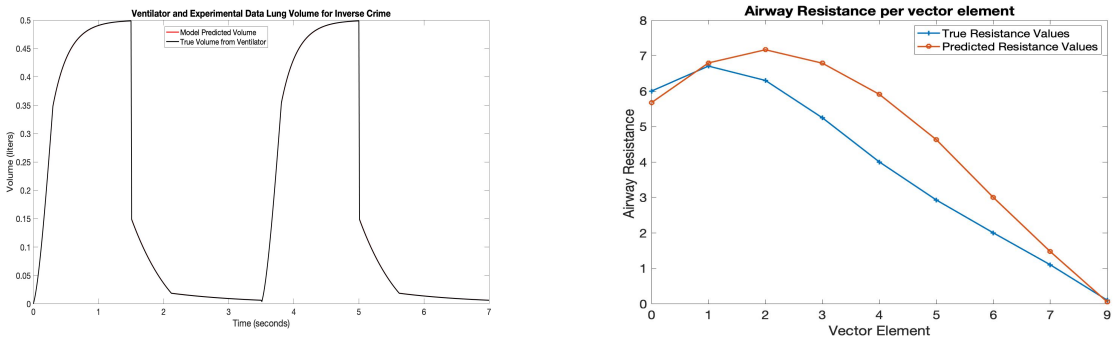


**Figure 5.2:** Left: Comparison of the synthetic volume curve (black) and from the inverse problem (red). The $2-$norm relative error is $8.8e-7\%$. Right: Reconstructed resistance vector curve of $[5.67, 6.79, 7.17, 6.79, 5.9, 4.6, 3, 1.47, 0.05]$ (red) and true resistance vector (blue).

# Chapter 6

# Estimating Airway Resistance from Mechanical Ventilation Data

To determine airway resistance throughout the lung, we use a mathematical model and real–world data. This technique allows us to apply known information and understandings, like constraints on airway resistance. Thanks to the help of Respiratory Therapist, Corey Mohnike, General Surgeon, Dr. Julie Dunn, and Trauma and Acute Care Surgery Research Manager, Omar Alnachoukati, at UCHealth's Medical Center of the Rockies, our data was collected. Thanks to the efforts of Dr. Kim McFann, a Project Coordinator and Biostatistician for Medical Center of the Rockies, our sample size and statistical analysis were completed. We set up a data collection process that involves 32 total patients: 5 female COVID-19 positive patients, 7 male COVID-19 positive patients, 9 female COVID-19 negative patients, 11 male COVID-19 negative patients, and their mechanical ventilation data. Each patient is between 30 and 80 years old with varying levels of lung health including chronic obstructive pulmonary disease (COPD), asthma, or no history. The endotracheal tubes used in this study had an internal diameter of 6 to 8 millimeter. This study uses mechanical ventilation waveform data and the RCCB lung model to determine the lung resistance of a patient using an inverse problem.

The RCCB lung model takes in ventilated reported compliance, resistance, and applied pressure, and outputs the lung volume at a given time. If the airway resistance value is not correct, then the lung volume size is affected. Having an accurate lung volume is important as machines like mechanical ventilators rely on maintaining lung volume. If literature is reporting varying values for airway resistance, it is important to determine a more accurate value throughout the lung to continue using mathematical equations to learn more and describe the human body. In this chapter, we introduce this study including the data collection process and parameters collected, we show

results for all 32 patients, analyze the results with a statistical and sensitivity analysis, and then state conclusions from the results.

## 6.1 Data Collection

Thanks to the work of Dr. Julie Dunn and Corey Mohnike at UCHealth's Medical Center of the Rockies in Northern Colorado, we received data from 32 patients between the age of 30 and 80 years old. These patients had no prior lung or respiratory injuries before being put on a mechanical ventilator. The endotracheal tubes used in this study had an internal diameter of 6 to 8 mm. The data was given to us de-identified through screenshots of the Hamilton G5 mechanical ventilator as seen in figures 6.1 and 6.2. We take parameters like minimum and maximum pressure, volume, and compliance from the ventilator screenshots to use as fixed variables for the RCCB lung model. Along with ventilator screenshots that included the ventilator parameters compliance, resistance, and pressure, the patients' age (years), sex (male or female), weight (kg), endotracheal tube (ETT) internal diameter (mm), pulmonary history (if known), and COVID-19 status were also recorded.

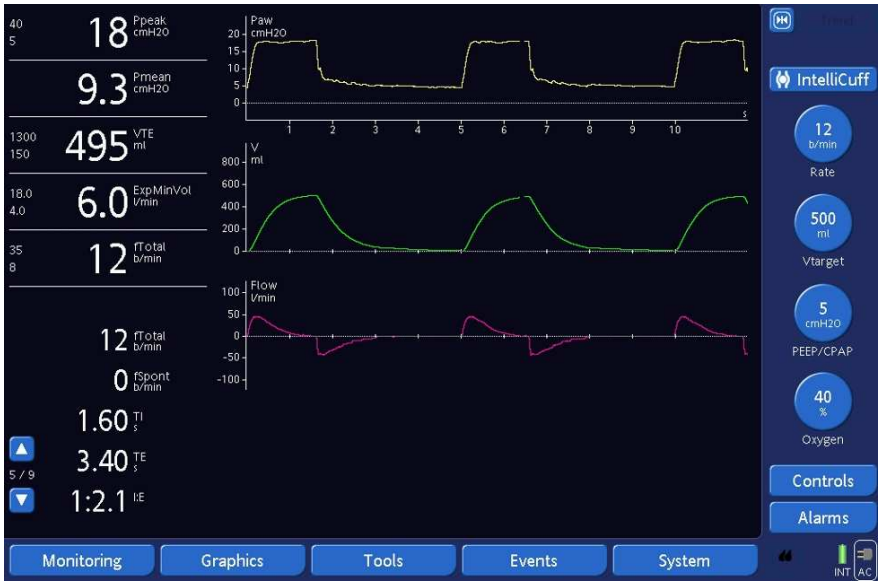


**Figure 6.1:** A screenshot of the mechanical ventilator Hamilton G5 series. The patient is a female with a 7.5 endotracheal tube. The yellow top curve is time versus applied pressure. The middle green volume curve represents time in seconds on the horizontal axis and volume in mL on the vertical axis. This curve tells us the patient's lung volume at a given time.

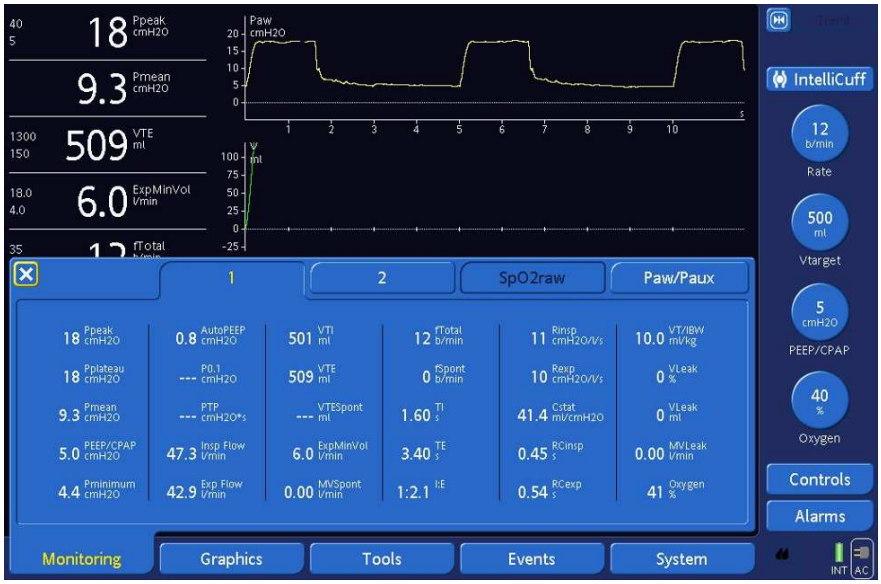


**Figure 6.2:** A screenshot of the mechanical ventilator Hamilton G5 series. The patient is a female with a 7.5 endotracheal tube. The blue box on the bottom half of the screenshot is important as it shows many parameters that we will use in our model as inputs like PEEP and inspiratory and expiratory time.

The last piece of information we extract from the ventilator screenshots is the plot of a volume curve in time (seconds) versus volume (mL). To pull the volume curve information from the screenshots we wrote a Python script to identify the Hue, Saturation, value (HSV) color of the plot and output a vector of pixels at those specific HSV locations. We then convert these pixel values into time and volume vectors which we scale to be in seconds and liters, respectively. This volume (per time) vector represents $V_{vent}$ data for the inverse problem seen in equation (5.9). After receiving and converting data, we solve the inverse problem.

This study excluded patients with triggered spontaneous breaths, a mode on the ventilator which permits a patient to override the start of an inhale. Spontaneous breathing is a mode in mechanical ventilation where patients can trigger their own breathing. Instead of the machine controlling the start of an inhale, the patient controls it instead. In patient triggering, the patient overrides the machine's breath. Some ventilator modes allow for triggered breaths from patients anywhere in the breath cycle. This study does not include patients who took spontaneous or triggered breaths on the ventilator.

## 6.2 Parameters Collected

We were able to collect screenshots from the Hamilton G5 mechanical ventilator which included a time in seconds versus volume in mL curve as well as parameters like PEEP, max pressure, and inhale and exhale time. An example, of one of these screenshots can be seen in figures 6.1 and 6.2. Overall, the 32 patients we collected data from include 5 female COVID-19 positive patients, 7 male COVID-19 positive patients, 9 female COVID-19 negative patients, and 11 male COVID-19 negative patients in this study. Since we do not collect any identifying information from our patients, an IRB found this study to be exempt.

From the screenshots of the mechanical ventilator, we can determine the time versus volume curve of each patient by running a Python script that scales and pulls the volume in liters at the respected time. For example, the curve in figure 4.1 reads $0.0068$ L at time $t = 2.9$ seconds.

A total of three patients had pressure curves in their data collection, and we use the same technique employed on the volume curve, relying on Python to process the information of the lung pressure at a given time. We then divide the pressure value by $2^n$ to represent the pressure vector throughout each generation in the lungs. For this model, we assume the pressure is the same throughout each generation. These assumptions give us a pressure vector at a given time per each patient.

For the remaining 29 patients that did not have pressure curves in their screenshots, we estimated the pressure at a given time by recreating the curves from the parameters given. The screenshot may not include the pressure curve, but they do include the mean, peak, plateau, and minimum pressure. We use these values to create a synthetic pressure curve for the patients that do not have the pressure curve included in their ventilator screenshots. The method for creating the pressure curve is explained in section 6.2.1.

A patient's compliance value comes from the total lung volume and total lung pressure throughout the lungs at a given time. By definition, compliance is the change in volume over change in pressure, so we can calculate compliance at each given time to determine the overall compliance throughout the lung. Since we assume compliance is uniform along each lung generation, we take

the compliance value and divide it by $2^n$, where $n$ is the number of generations. Those values then become the diagonals of a $2^n \times 2^n$ diagonal matrix. All parameters are taken from ventilator screenshots to help determine the overall airway resistance values throughout the lung using the RCCB model.

The collected ventilator compliance is helpful in validating calculated compliance but is not used in the RCCB model. The Hamilton G5 Operator's Manual states compliance should not be used for reliable analysis,"[d]ue to the changing and unpredictable amount of leakage" [7]. Since there may be inaccuracies in the total reported compliance value, we calculate a patient's total lung compliance based on the definition. By definition, compliance is the change in volume over the change in pressure, $C = \frac{\Delta V}{\Delta P}$, and so we calculate compliance at each time point based on the volume and pressure at that time using MATLAB's `diff` function [44].

Overall, the calculated compliance and the ventilator reported compliance values were close. Out of the 32 patients, the average calculated total compliance was 0.0366 $\pm$ 0.0135 L/cm $H_20$, and the average ventilator compliance was 0.0356 $\pm$ 0.0173 L/cm $H_20$. The average absolute difference between the calculated compliance and the ventilator compliance was $0.0073 \pm 0.0084$ L/cm $H_20$. When we consider that this value is divided by $2^n$ generations, for this study, where $n = 9$, that leads to an average difference of $0.000014 \pm 0.000018$ L/cm $H_20$ per entry in the compliance matrix. We also note the smallest absolute difference between the total calculated compliance and the total reported ventilator resistance was 0.001 L/cm $H_20$ while the largest was 0.0387 L/cm $H_20$.

### 6.2.1 Airway Pressure

For some patients, pressure curves from the ventilator screenshots are available and allow us to see pressure applied from the ventilator to the patient at a given time. Not all patients had a pressure curve collected as data. To create this curve for other patients, we use the information given from the 3 patients to create "synthetic" data. At the beginning of an inhale, the applied pressure is at its minimum value and then then moves to maximum pressure at some time, $t_\alpha$. The

applied pressure plateaus and stays at the maximum value until the start of an exhale. The pressure value then decreases back down to the minimum at time $t_\beta$ until the start of the next inhale.

The applied pressure curve data from the ventilator screenshots, seen in figure 6.3 were only provided for three patients, and so the minimum and maximum values of the applied pressure were used along with properties of the known pressure curves to create synthetic pressure curves for the remaining patients as follows. Measured pressure curves were observed to increase at the start of an inhale until peak pressure was reached, and then remain constant at that peak pressure until the start of an exhale when the pressure decreases again. Once the next inhale starts the applied pressure increases anew. Figure 6.4 includes a measured volume curve scaled to have a better visual of the pressure peaks at the appropriate locations. For the collected data, the average time over all pressure changes and patients for the pressure to increase from its minimum to its maximum pressure was $0.29 \pm 0.07$ seconds while the average time to decrease from maximum to minimum pressure was $0.60 \pm 0.08$ seconds. These average times along with the unique minimum and unique maximum pressure for each patient were used to create a function that outputs a simulated pressure curve for the patients without a measured pressure curve.

We recreate synthetic pressure curves from this pattern. We calculate the average time it takes to go from minimum pressure to maximum pressure and vice versa for the 3 known patients. We then apply this time to create a function that outputs a pressure curve. In figure 6.4, we see a plot with both a pressure curve (in blue) and volume curve (in red). The volume curve is scaled to have a better visual of the pressure peaks at the appropriate locations.

Figure 6.5 includes two examples of comparing the true pressure curves taken from the ventilator, for available patients, to the synthetic pressure curve function. We notice, there are times when pressure is not applied to the patient on the ventilator but the synthetic pressure is applied. Synthetic pressure is still synthetic at its core but overall, this function does allow for us to “fill in" missing data.

Using pressure curves from the ventilator introduces noise to the final volume result, but overall there is little difference between using the synthetic pressure data and the pressure from ventilators.

We can see this in figure 6.6. Figure 6.7 shows the synthetic curve in red and the true pressure curve from the ventilator in black for all three patients.

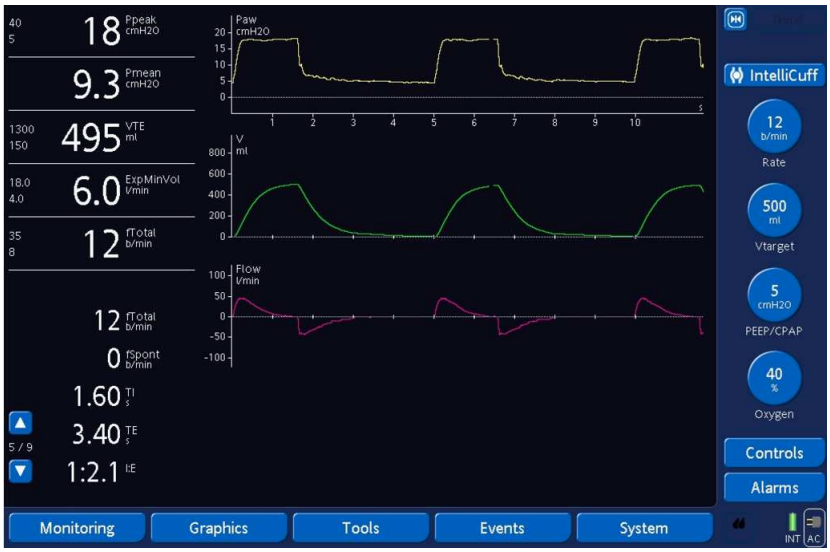


**Figure 6.3:** A screenshot of a pressure curve on the mechanical ventilator Hamilton G5 series. The female patient has a 7.5 endotracheal tube. During inhalation, the applied pressure goes from the minimum pressure value to the maximum pressure value where it stays until the start of the exhale. From there, the pressure decreases to the minimum pressure value until the start of the next inhale where it increases to the maximum pressure.

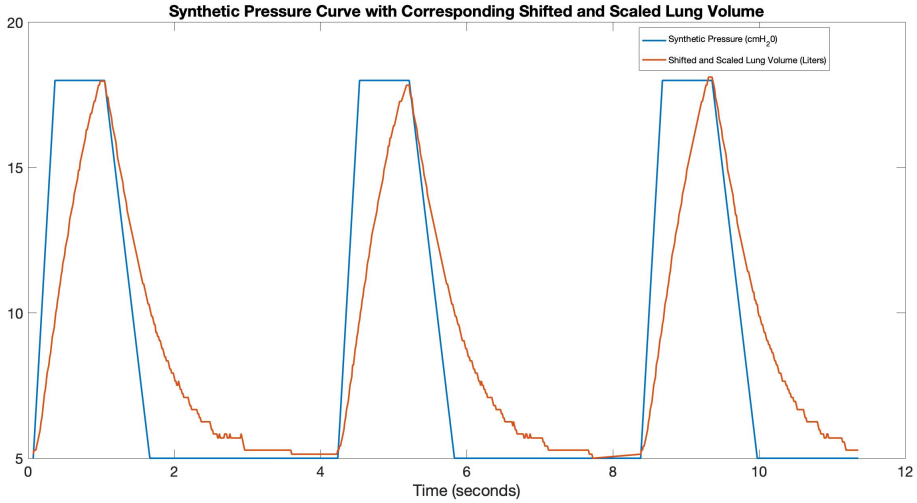


**Figure 6.4:** A plot of a synthetic pressure curve (blue) based on the minimum and maximum pressure values from the mechanical ventilator. This image also includes the volume curve (red) scaled to better visualize the increase and decrease in pressure at the start of inspiration and expiration, respectively.

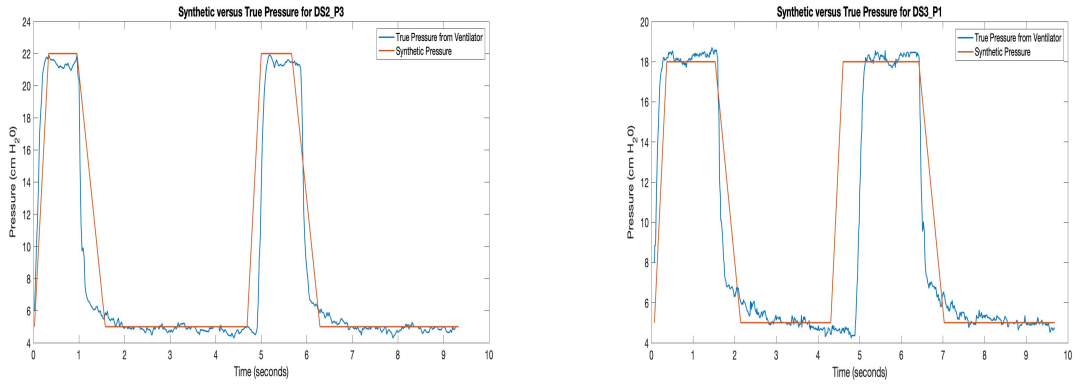


**Figure 6.5:** Time (seconds) versus synthetic pressure (cm $H_20$) and true pressure (cm $H_20$) curves from ventilator. Note the true pressure curve includes noise based on the Python script using a range of hues. Left: True pressure from ventilator (blue) and synthetic pressure (red) for a female COVID-19 negative patient. Right: True pressure from ventilator (blue) and synthetic pressure (red) for female COVID-19 negative patient.

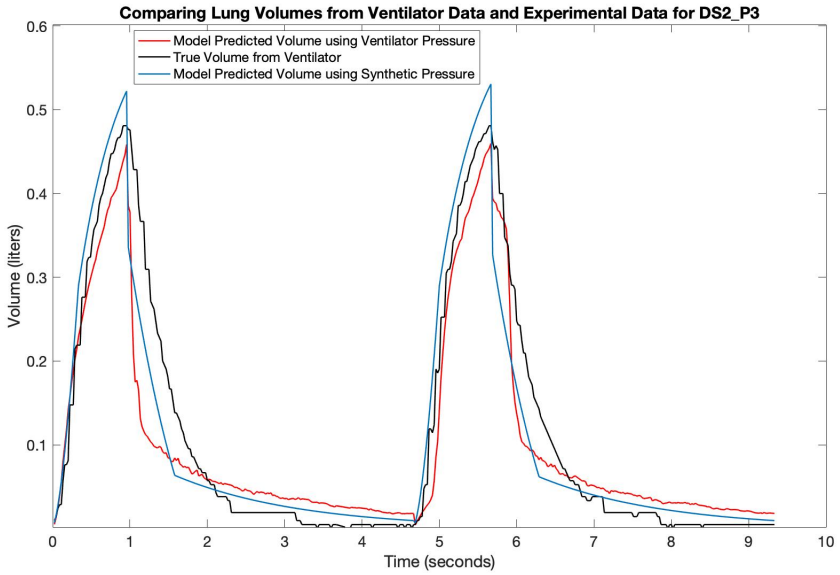


**Figure 6.6:** Three volume curves for data set 2 patient 3. The black curve is the true patient volume from the ventilator. The tallest volume curve in blue is the model predicted volume curve using the synthetic pressure curve based on the minimum and maximum pressure values. This curve is smooth because the pressure curve we are using in the model is not noisy. The $2-$norm error for this model was 24.47%. The lowest red volume curve is the model predicted volume using the pressure curve from the ventilator. The $2-$norm error for the red curve is 28%. Besides the pressure value, all other parameters in the model used were identical between the red and blue curve.

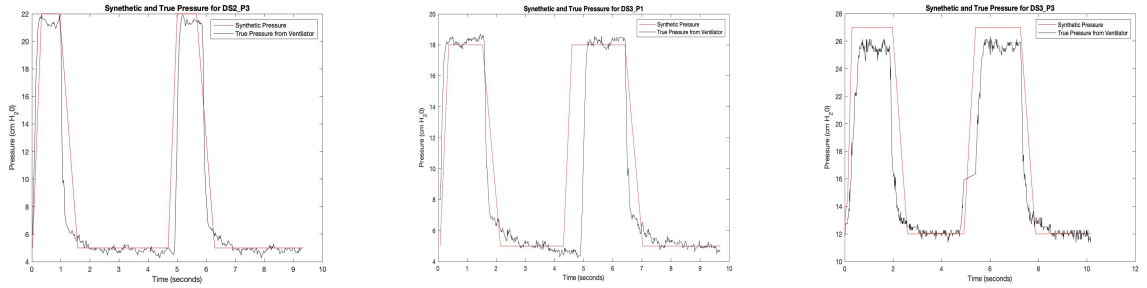


**Figure 6.7:** Left: pressure curves for date set 2 patient 3. Middle: pressure curves for date set 3 patient 1. Right: pressure curves for date set 3 patient 3. The synthetic pressure curve in red has a rectangular shape where as the pressure curve from the ventilator in black includes noise.

## 6.3 Airway Resistance and Results

Once we have screenshots of ventilators, we use Python to extract the volume curve information based on the HSV of the green ventilator curve. The Python code takes in an image and pulls the pixel locations of a certain HSV color. In this case a green curve with HSV between 100-140. These pixels are then scaled to reflect the horizontal and vertical axis of the ventilator volume. This Python script maps pixel locations to numeric values. The Python code outputs 2 vectors, one that represents time in seconds and another vector that represents volume in liters. We use both these vectors to verify the inverse problem results.

In this section, we will share the results of 32 patients, including a summary of the results via four tables and figures of the airway resistance results. The tables will include resistance values display on the ventilator, the 9-generation resistance vector computationally found from the inverse problem, and the relative error between the true volume from the screenshot and the volume that is output from the forward model. The relative error is measured with the 2-norm:

$$\frac{\left(\sum_{i=1}^{N}|V_i(\vec{R}) - V_i^{vent}|^2\right)^{1/2}}{\left(\sum_{i=1}^{N}|V_i^{vent}|^2\right)^{1/2}} \tag{6.1}$$

where $N$ is the number of elements in the vector. $N$ varies per patient depending on the total number of breaths as well as how many pixels the Python script was able to map. The average number of elements in a vector for the 32 patients is 766. The $2-$norm relative errors describe the errors between the true lung volume from the ventilator and the RCCB lung model predicted volume. The average $2-$norm relative error for all 32 patients was 38.79% while the minimum $2-$norm relative error was 18.66%, and the maximum $2-$norm relative error was 64.07%.

We state the data set and the patient number in the table based on our own book-keeping method. For example, the patient ID DS7_P2 represents data set 7 patient 2. We choose a nine–generation system based on availability of resistance vectors values found in literature to use as test values as well as ease in matrix size. If a screenshot of a volume curve does not complete the entire breath, we remove the last incomplete breath. For example, in figure 4.1, the volume curve data we pull is only of 2 complete breaths as we do not have complete information of the third exhale. Figure 6.8 shows the volume curve we pull from the patient's ventilator screenshot from figure 4.1. The Hamilton G5 series does include the total resistance value as a parameter. We compare the ventilated reported total resistance value to the resistance value predicted from the inverse problem.

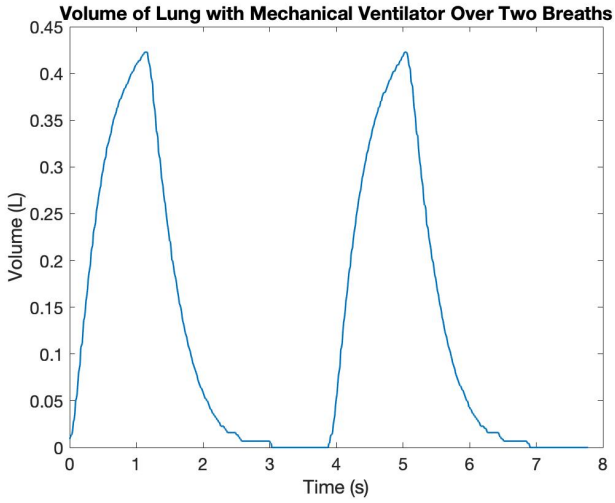


**Figure 6.8:** A volume curve of the first two breaths taken from the ventilator screenshot seen in figure 4.1. Using a Python script, we are able to recreate this curve by processing pixel information from the ventilator screenshot.

The results from this study can be seen below. The results are presented in the following order: female COVID-19 negative, male COVID-19 negative, female COVID-19 positive, and male COVID-19 positive. The first table, table 6.1 is an overall summary of the number of people in each category as well as their mean age. The second table, table 6.2, is patient data including age, weight, COVID-19 test results at the time the ventilator screenshot was taken, and pulmonary history. Hospitals did not start seeing COVID-19 positive patients until after data set 5. Unfortunately, not all patient information was collected for each patient. The third table, table 6.3, has patient parameters used in the RCCB lung model including the minimum and maximum pressure, airway compliance calculated from the definition, and compliance taken from the ventilator. The fourth table, table 6.4, includes information from the model results as well as the relative error between the ventilator lung volume and the lung volume calculated from the forward problem. All relative errors are reported using the $2-$norm.

In figures 6.9 through 6.20, the results on the left include the ventilator lung volume curve in black and the forward problem volume results in red. These plots show time in seconds versus volume in liters. The right plots are airway resistance vector curves. The horizontal axis represents generation $n$ in the lung from the $0^{\text{th}}$ to the $8^{\text{th}}$ generation. The vertical axis represents the airway resistance in cm $H_20$/L/s. The reported ventilator resistance value is seen on the reconstructed resistance as a red dot.

**Table 6.1:** Subject characteristics for the 32 patients. The notes in this table include $^a$Independent sample T-test and $^b$Chi Square Test of Independence.

| | COVID-19 Negative ($N = 20$) | COVID-19 Positive ($N = 12$) | p-value |
|---|---|---|---|
| Age (years) | 57.4 $\pm$ 18.0 | 56.0 $\pm$ 13.1 | $0.8348^a$ |
| Weight (kg) | 88.2 $\pm$ 38.3 | 72.8 $\pm$ 25.0 | $0.2697^a$ |
| Sex Female | 9 (45%) | 5 (41.7%) | $0.854^b$ |
| Sex Male | 11 (55%) | 7 (58.33%) | |

**Table 6.2:** Table of summary of 32 patients. Patient ID is for booking keeping only. Information is broken up by patient sex and patient COVID-19 result. Any blanks in table are patients unknowns.

| Patient ID | Age | Sex | Weight (Kg) | ETT | COVID-19 | Pulmonary history |
|---|---|---|---|---|---|---|
| DS2_P3 | | Female | | 7.0 | Negative | |
| DS3_P1 | | Female | | 7.5 | Negative | |
| DS3_P2 | | Female | | 7.5 | Negative | |
| DS3_P3 | | Female | | 7.5 | Negative | |
| DS4_P1 | | Female | | 7.5 | Negative | |
| DS6_P1 | | Female | | 7.5 | Negative | |
| DS6_P2 | | Female | | 7.5 | Negative | |
| DS16_P1 | 79 | Female | 37.49 | 7.5 | Negative | No known history |
| DS19_P1 | 60 | Female | 67.5 | 7.5 | Negative | Smoker, 1 pack per day; |
| DS2_P5 | | Male | | 6.0 | Negative | |
| DS2_P7 | | Male | | 7.5 | Negative | |
| DS2_P8 | | Male | | 7.5 | Negative | |
| DS7_P1 | 32 | Male | 80.1 | 8.0 | Negative | No known history |
| DS7_P2 | 79 | Male | 72.5 | 7.0 | Negative | No known history |
| DS13_P1 | 73 | Male | 74.3 | 8.0 | Negative | Reactive Airway Disease |
| DS17_P1 | 49 | Male | 126.9 | 7.5 | Negative | No known history |
| DS19_P2 | 48 | Male | 77.1 | 7.5 | Negative | No known history |
| DS19_P3 | 54 | Male | 93.8 | 7.0 | Negative | No known history |
| DS20_P1 | 70 | Male | 176.9 | 8.0 | Negative | OHS |
| DS20_P2 | 30 | Male | 75 | 7.5 | Negative | No known history |
| DS15_P1 | 67 | Female | 48.5 | 7.0 | Positive | No known history |
| DS18_P1 | 61 | Female | 82.1 | 7.5 | Positive | No known history |
| DS18_P2 | 42 | Female | 101.5 | 8.0 | Positive | Asthma, Smoker |
| DS22_P1 | 58 | Female | 43.15 | 7.5 | Positive | Asthma |
| DS25_P1 | 77 | Female | 24.48 | 7.5 | Positive | No known history |
| DS7_P5 | 35 | Male | 87.3 | 8.0 | Positive | Asthma |
| DS8_P2 | 70 | Male | 86.1 | 8.0 | Positive | No known history |
| DS9_P1 | 54 | Male | 78.1 | 7.5 | Positive | No known history |
| DS11_P1 | 58 | Male | 58.3 | 8.0 | Positive | No known history |
| DS12_P1 | 62 | Male | 107.3 | 8.0 | Positive | No known history |
| DS12_P2 | 36 | Male | 90 | 8.0 | Positive | Asthma |
| DS12_P3 | 52 | Male | 66.3 | 7.5 | Positive | No known history |

**Table 6.3:** Table of patient input parameters for the RCCB lung model. Any blanks are unknown parameters as data was not available.

| Patient ID | Min/Max Pressure (cm $H_20$) | Calculated Compliance | Ventilator Compliance | Triggered breath |
|---|---|---|---|---|
| DS2_P3 | 5/22 | .0464 | .0365 | No |
| DS3_P1 | 5/18 | .0592 | .0414 | No |
| DS3_P2 | 5/17 | .04 | .0307 | No |
| DS3_P3 | 12/27 | .0208 | .0274 | No |
| DS4_P1 | 5/18 | .056 | .0559 | No |
| DS6_P1 | 6/22 | .0272 | .025 | No |
| DS6_P2 | 6/18 | .0496 | .0344 | No |
| DS16_P1 | 10/23 | .0352 | .0388 | No |
| DS19_P1 | 10/21 | .0304 | .0314 | No |
| DS2_P5 | 4/21 | .0432 | .0313 | No |
| DS2_P7 | 5/14 | .032 | .0589 | No |
| DS2_P8 | 11/29 | .0384 | .0325 | No |
| DS7_P1 | 8/17 | .0496 | .0408 | No |
| DS7_P2 | 8/41 | .0336 | .0269 | No |
| DS13_P1 | 7/15 | .0592 | .0614 | No |
| DS17_P1 | 5/22 | .0432 | .0478 | No |
| DS19_P2 | 5/20 | .04 | .041 | No |
| DS19_P3 | 5/14 | .0512 | .0514 | No |
| DS20_P1 | 5/12 | .056 | .0947 | No |
| DS20_P2 | 5/14 | .0528 | .0538 | No |
| DS15_P1 | 5/22 | .0272 | .0197 | No |
| DS18_P1 | 12/30 | .024 | .0158 | No |
| DS18_P2 | 24/38 | .0208 | .0203 | No |
| DS22_P1 | 12/32 | .0176 | .0186 | No |
| DS25_P1 | 14/33 | .0192 | .0184 | No |
| DS7_P5 | 20/33 | .032 | | No |
| DS8_P2 | 7/15 | .0496 | .0396 | No |
| DS9_P1 | 14/31 | .024 | .027 | No |
| DS11_P1 | 10/26 | .0272 | .0232 | No |
| DS12_P1 | 13/20 | .0272 | .0213 | No |
| DS12_P2 | 20/30 | .0176 | .0291 | No |
| DS12_P3 | 7/40 | .0112 | .0073 | No |

**Table 6.4:** Table of inverse problem outputs including resistance vector.

| Patient ID | Ventilator Resistance | Resistance Vector (cm $H_20$/L/s) | Relative Error (%) |
|---|---|---|---|
| DS2_P3 | 13 | $[6.23; 6.83; 6.54; 5.56; 4.48; 3.32; 2.1; 1; 9.769\text{e}{-5}]$ | 31.67% |
| DS3_P1 | 11 | $[5; 5.4; 5.3; 4.77; 3.95; 3; 1.76; 0.82; 3.8\text{e}{-8}]$ | 40.01% |
| DS3_P2 | 15 | $[7.2; 7.7; 7.5; 6.8; 5.78; 4.56; 2.99; 1.47; 2.9\text{e}{-5}]$ | 49.71% |
| DS3_P3 | 11 | $[4.6; 5.85; 6.3; 6; 5.27; 4.1; 2.56; 1.2; 0.001]$ | 53.47% |
| DS4_P1 | 18 | $[8.4; 9.5; 9.47; 8.5; 7; 5.1; 2.88; 0.94; 2.9\text{e}{-8}]$ | 33.93% |
| DS6_P1 | 15 | $[7.2; 7.7; 7.5; 6.8; 5.8; 4.6; 3; 1.5; 0.001]$ | 46.57% |
| DS6_P2 | 14 | $[6.69; 7.2; 7; 6.45; 5.5; 4.4; 2.94; 1.47; 0.0004]$ | 24.69% |
| DS16_P1 | 12 | $[5.2; 6.4; 6.77; 6.4; 5.6; 4.36; 2.8; 1.33; 0.001]$ | 36.5% |
| DS19_P1 | 7 | $[2.77; 3.6; 3.99; 3.85; 3.4; 2.77; 1.78; 0.84; 0.0001]$ | 53.4% |
| DS2_P5 | 18 | $[7.67; 8.78; 8.9; 8; 6.6; 4.8; 2.68; 0.84; 4.5\text{e}{-7}]$ | 30.72% |
| DS2_P7 | 9 | $[3.9; 4.6; 4.85; 4.56; 3.98; 3.2; 2; 0.98; 0.0001]$ | 64.07% |
| DS2_P8 | 12 | $[4; 4.97; 5.2; 4.77; 4; 2.97; 1.62; 0.711; 1.824\text{e}{-11}]$ | 45.43 % |
| DS7_P1 | 10 | $[4.48; 5.13; 5.28; 4.9; 4.27; 3.4; 2.2; 1.05; 0.0001]$ | 31.35% |
| DS7_P2 | 21 | $[10.1; 11.1; 10.98; 9.89; 8.3; 6.4; 4.3; 2.34; 0.5]$ | 18.66% |
| DS13_P1 | 8 | $[3.3; 4.1; 4.4; 4.21; 3.696; 2.98; 1.9; 0.912; 0.0001];$ | 41.26% |
| DS17_P1 | 17 | $[7.9; 9; 9.2; 8.3; 6.9; 5.2; 3.35; 1.576; 0.001];$ | 31.81% |
| DS19_P2 | 14 | $[6.7; 7.2; 7.05; 6.4; 5.45; 4.3; 2.8; 1.35; 0.001]$ | 37.12% |
| DS19_P3 | 13 | $[6.24; 6.84; 6.5; 5.5; 4.4; 3.27; 2.04; 0.96; 0.0001]$ | 42% |
| DS20_P1 | 20 | $[8.1; 9.25; 9.4; 8.6; 7.3; 5.7; 3.86; 2.14; 0.5]$ | 19.98% |
| DS20_P2 | 12 | $[5.18; 6.35; 6.77; 6.45; 5.62; 4.4; 2.81; 1.33; 0.001]$ | 43.72% |
| DS15_P1 | 16 | $[7.33; 8.53; 8.73; 7.9; 6.6; 5.02; 3.2; 1.5; 0.01]$ | 31.92% |
| DS18_P1 | 12 | $[5.18; 6.35; 6.77; 6.45; 5.62; 4.4; 2.81; 1.33; 0.001]$ | 30.34% |
| DS18_P2 | 8 | $[3.3; 4.1; 4.42; 4.2; 3.7; 2.98; 1.9; 0.9; 0.0001]$ | 37.91% |
| DS22_P1 | 28 | $[13.67; 14.67; 14.4; 13.1; 11.35; 9.3; 7; 4.71; 2.4]$ | 41.89% |
| DS25_P1 | 11 | $[4.6; 5.85; 6.3; 6; 5.3; 4.1; 2.6; 1.2; 0.001]$ | 40.92% |
| DS7_P5 | 16 | $[7.3; 8.53; 8.74; 7.95; 6.7; 5.1; 3.3; 1.6; 0.1]$ | 38.64% |
| DS8_P2 | 9 | $[4.3; 4.6; 4.2; 3.64; 2.95; 2.2; 1.38; 0.665; 1.557\text{e}{-6}]$ | 34.26% |
| DS9_P1 | 12 | $[5.48; 6.1; 5.9; 4.99; 4; 2.94; 1.8; 0.84; 1.035\text{e}{-5}]$ | 43.75% |
| DS11_P1 | 8 | $[3.8; 4.1; 3.76; 3.25; 2.6; 1.97; 1.2; 0.588; 1.094\text{e}{-05}]$ | 42.87% |
| DS12_P1 | 10 | $[4.48; 5.1; 5.28; 4.9; 4.27; 3.4; 2.2; 1.05; 0.0001]$ | 31.52% |
| DS12_P2 | 8 | $[3.3; 4.1; 4.4; 4.2; 3.696; 2.98; 1.9; 0.912; 1.11\text{e}{-5}]$ | 50.19% |
| DS12_P3 | 4 | $[1.6; 1.9; 1.9; 1.76; 1.48; 1.14; 0.7329; 0.3618; 5.63\text{e}{-6}]$ | 40.45% |

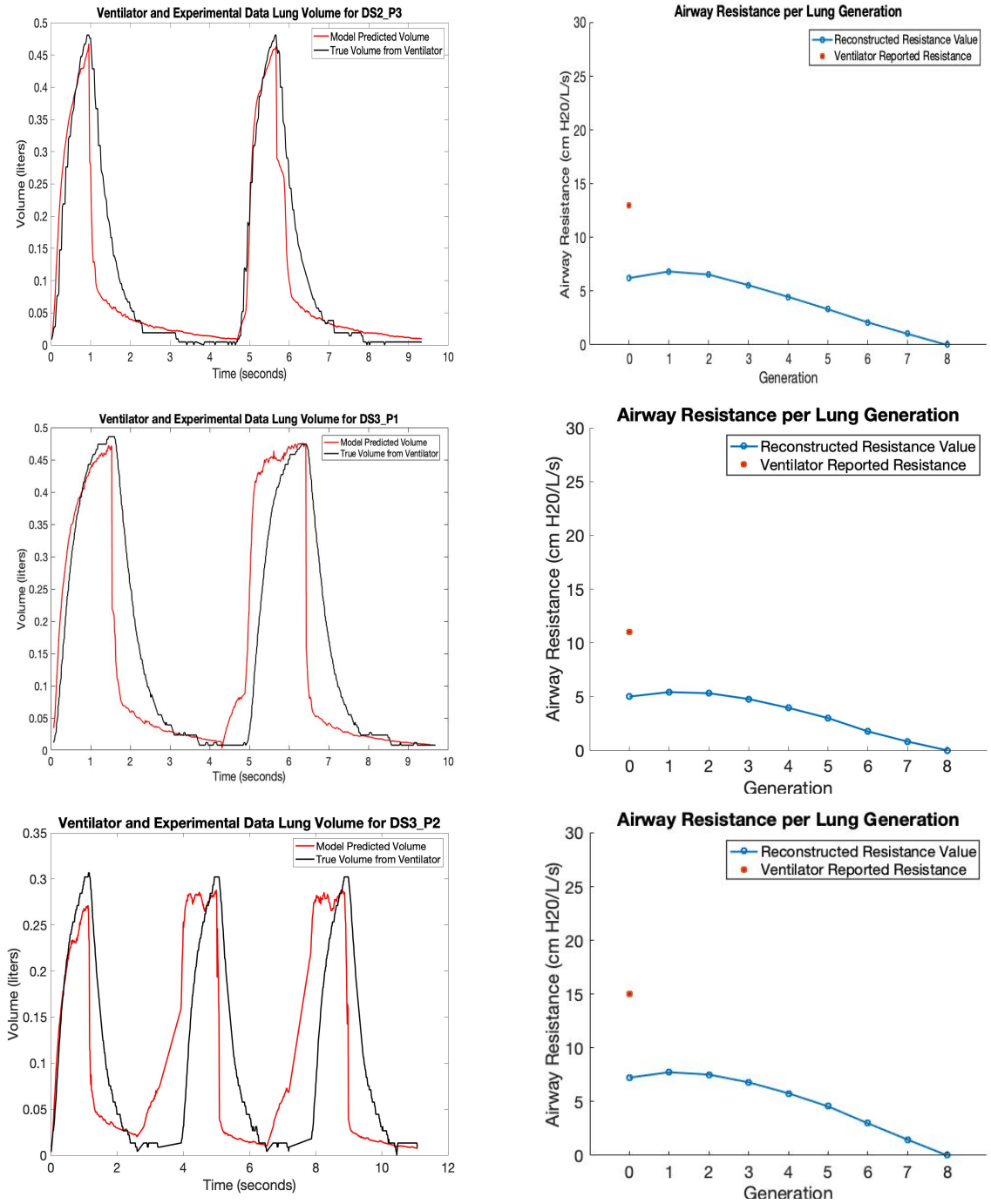


**Figure 6.9:** Top row: plots for DS2_P3 with 2−norm relative error of 31.67%. The ventilator resistance value for DS2_P3 is 13 cm $H_20$/L/s. The resistance values found from the model totaled to 12.4 cm $H_20$/L/s. Second row: plots for DS3_P1 with 2−norm relative error of 40.01%. The ventilator resistance value for DS3_P1 is 11 cm $H_20$/L/s. The resistance values found from the model totaled to 10.0083 cm $H_20$/L/s. Third row: plots for DS3_P2 with 2−norm relative error of 49.71%. The ventilator resistance value for DS3_P2 is 15 cm $H_20$/L/s. The resistance values found from the model totaled to 14.4 cm $H_20$/L/s. All patients are female COVID negative.

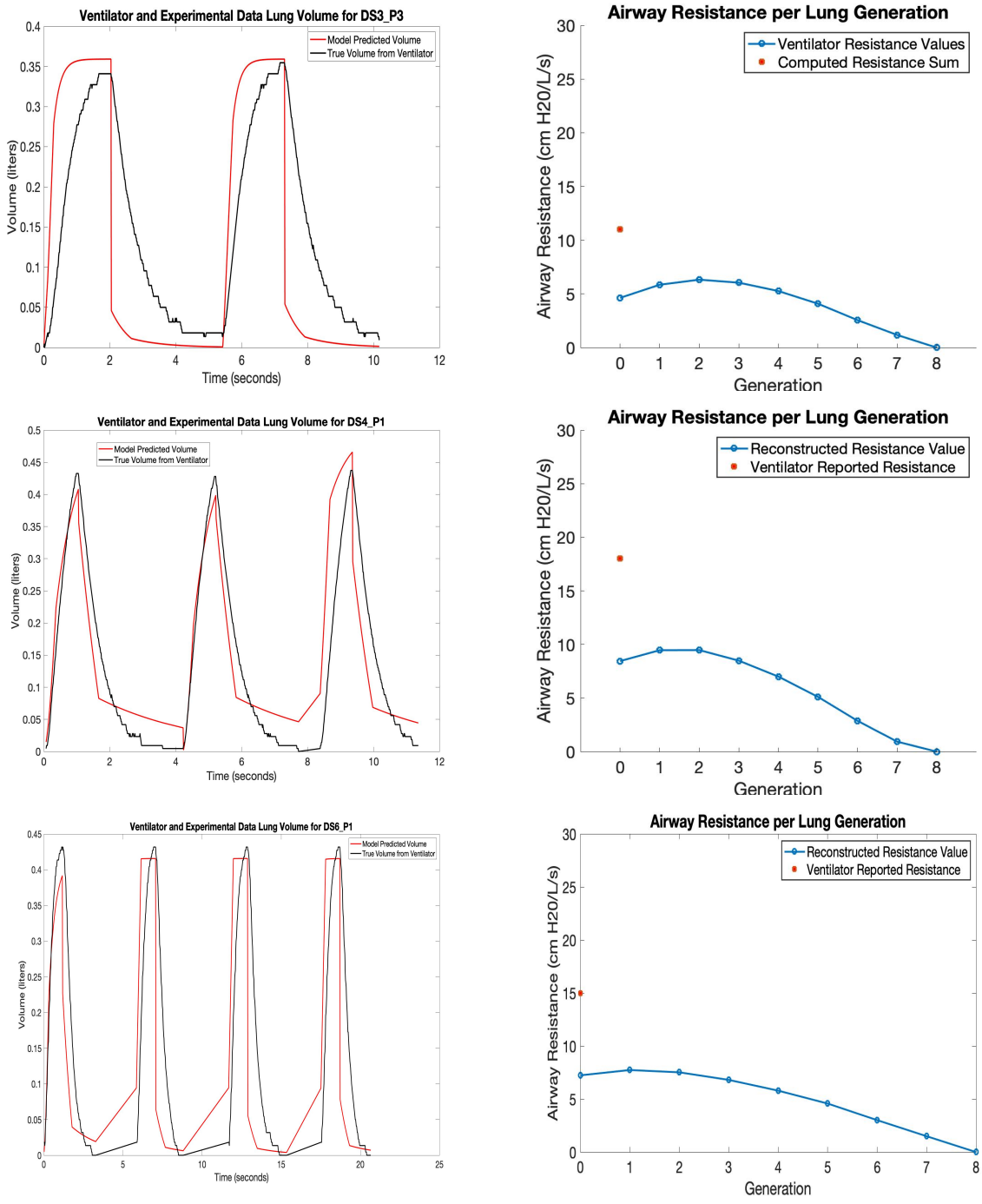


**Figure 6.10:** First row: plots for DS3_P3 with 2−norm relative error of 53.47%. The ventilator resistance value for DS3_P3 is 11 cm $H_20$/L/s. The resistance values found from the model totaled to 10.4 cm $H_20$/L/s. Second row: plots for DS4_P1 with 2−norm relative error of 33.93%. The ventilator resistance value for DS4_P1 is 18 cm $H_20$/L/s. The resistance values found from the model totaled to 17.2604 cm $H_20$/L/s. Third row: plots for DS6_P1 with 2−norm relative error of 46.57%. The ventilator resistance value for DS6_P1 is 15 cm $H_20$/L/s. The resistance values found from the model totaled to 14.4 cm $H_20$/L/s. All patients are female COVID negative.

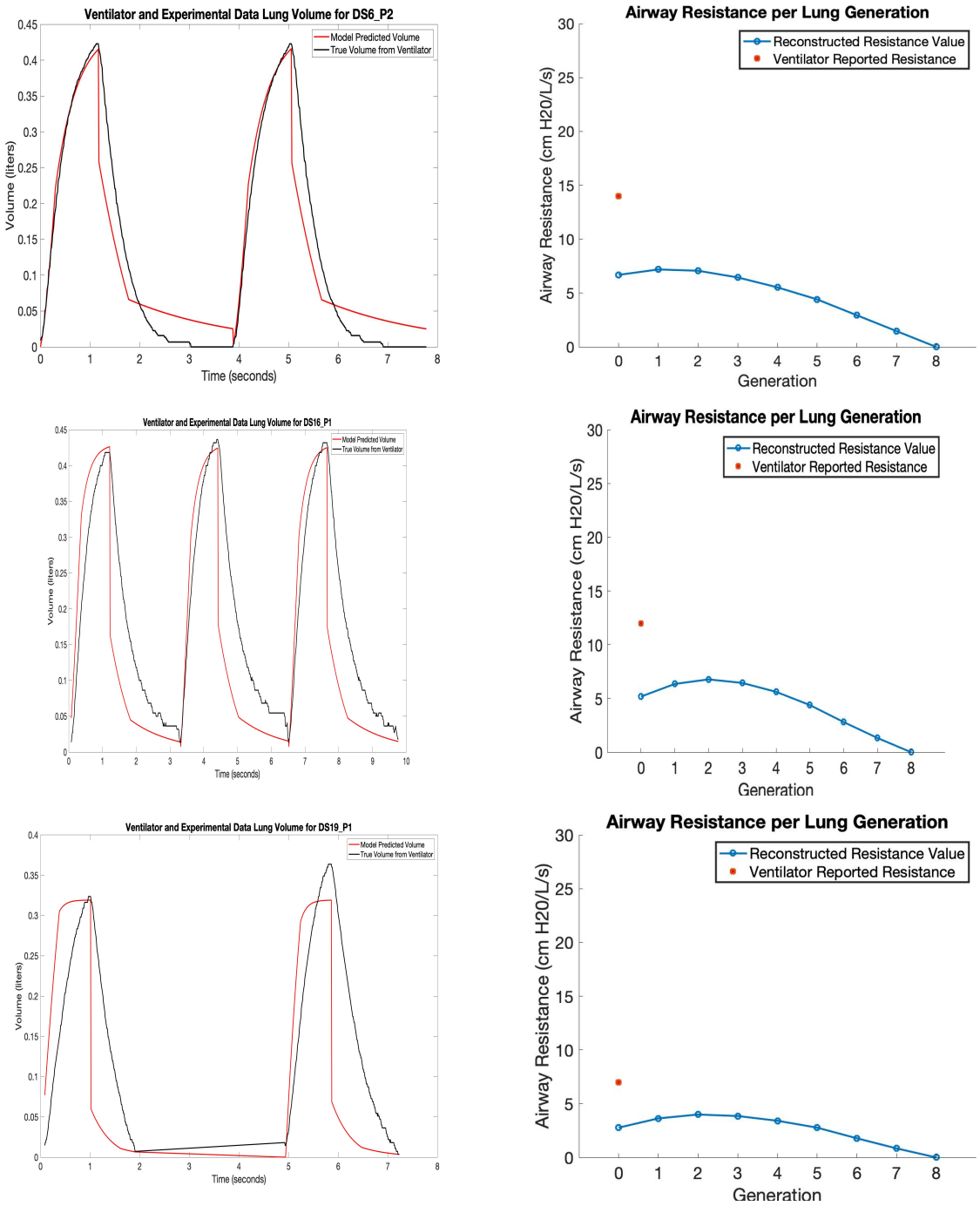


**Figure 6.11:** First row: plots for DS6_P2 with 2−norm relative error of 24.69%. The ventilator resistance value for DS6_P2 is 14 cm $H_20$/L/s. The resistance values found from the model totaled to 13.4 cm $H_20$/L/s. Second row: plots for DS16_P1 with 2−norm relative error of 36.5%. The ventilator resistance value for DS16_P1 is 12 cm $H_20$/L/s. The resistance values found from the model totaled to 11.4 cm $H_20$/L/s. Third row: plots for DS19_P1 with 2−norm relative error of 53.40%. The ventilator resistance value for DS19_P1 is 7 cm $H_20$/L/s. The resistance values found from the model totaled to 6.4 cm $H_20$/L/s. All patients are female COVID negative.

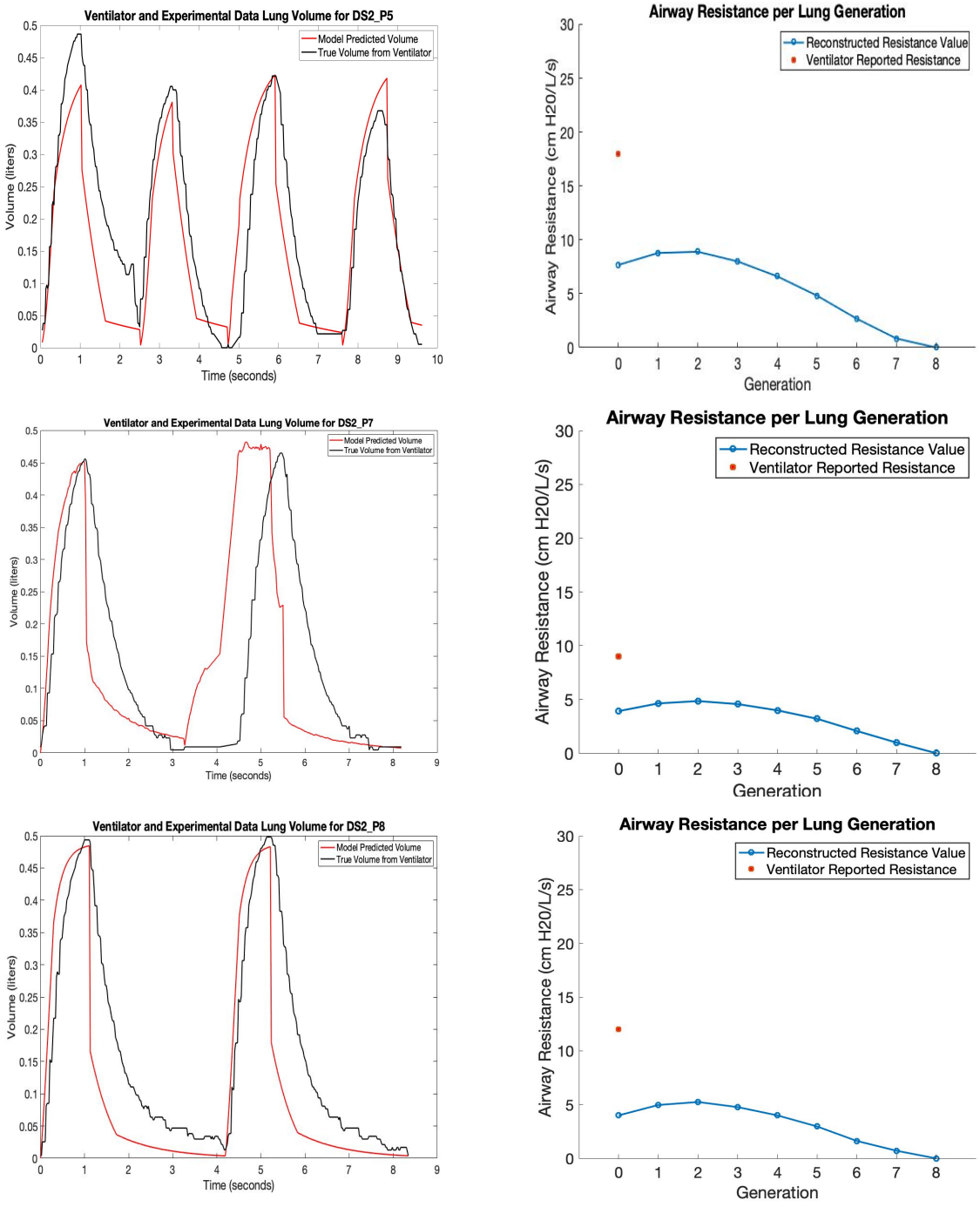


**Figure 6.12:** First row: plots for DS2_P5 with 2−norm relative error of 30.72%. The ventilator resistance value for DS2_P5 is 18 cm $H_20$/L/s. The resistance values found from the model totaled to 15.8947 cm $H_20$/L/s. Second row: plots for DS2_P7 with 2−norm relative error of 64.07%. The ventilator resistance value for DS2_P7 is 9 cm $H_20$/L/s. The resistance values found from the model totaled to 8.4 cm $H_20$/L/s. Third row: plots for DS2_P8 with 2−norm relative error of 45.43%. The ventilator resistance value for DS2_P8 is 12 cm $H_20$/L/s. The resistance values found from the model totaled to 8.7646 cm $H_20$/L/s. All patients are male COVID negative.

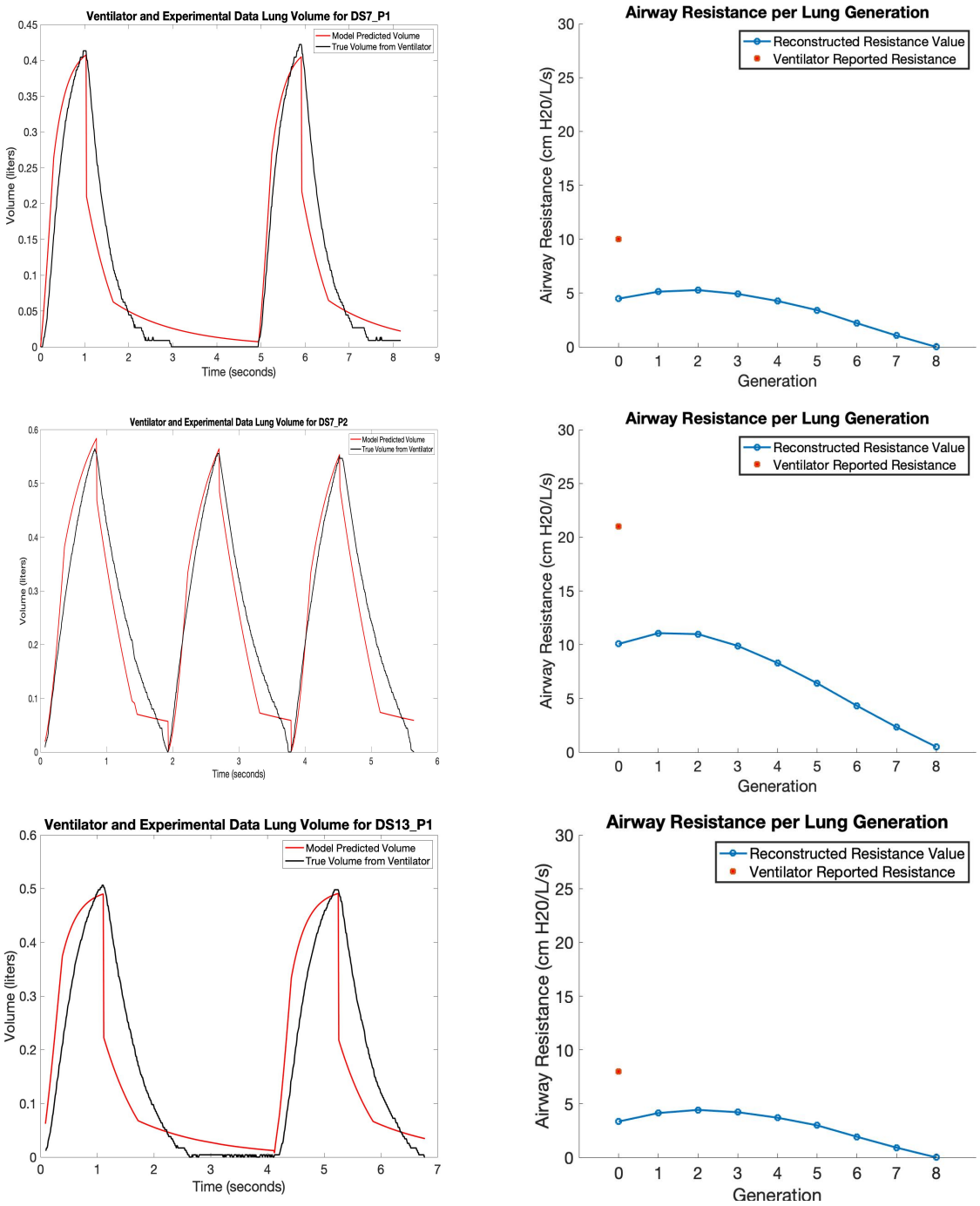


**Figure 6.13:** First row: plots for DS7_P1 with 2−norm relative error of 31.35%. The ventilator resistance value for DS7_P1 is 10 cm $H_20$/L/s. The resistance values found from the model totaled to 9.4 cm $H_20$/L/s. Second row: plots for DS7_P2 with 2−norm relative error of 18.66%. The ventilator resistance value for DS7_P2 is 21 cm $H_20$/L/s. The resistance values found from the model totaled to 20.4 cm $H_20$/L/s. Third row: plots for DS13_P1 with 2−norm relative error of 41.26%. The ventilator resistance value for DS13_P1 is 8 cm $H_20$/L/s. The resistance values found from the model totaled to 7.4 cm $H_20$/L/s. All patients are male COVID negative.

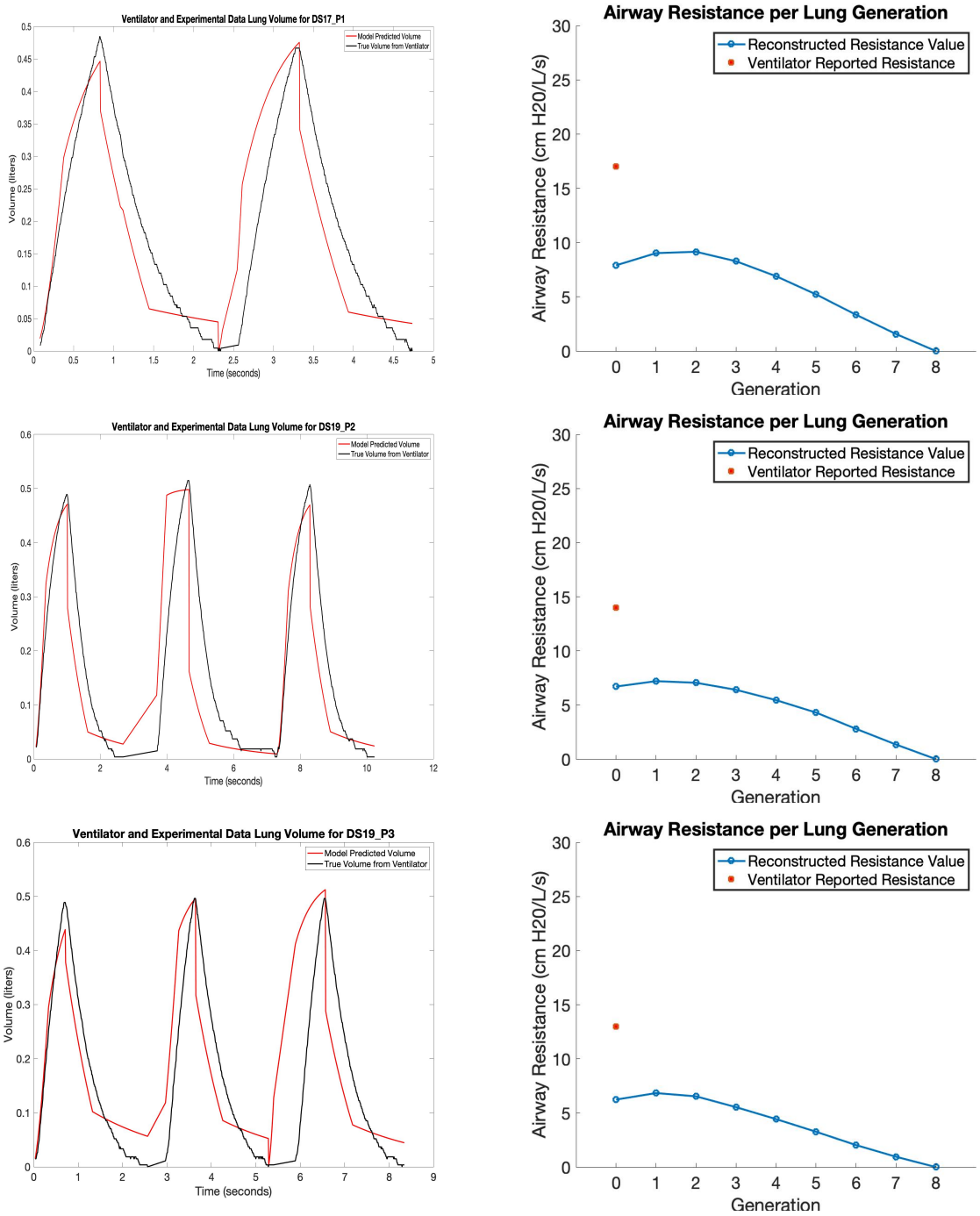


**Figure 6.14:** First row: plots for DS17_P1 with 2−norm relative error of 31.81%. The ventilator resistance value for DS17_P1 is 17 cm $H_20$/L/s. The resistance values found from the model totaled to 16.4 cm $H_20$/L/s. Second row: plots for DS19_P2 with 2−norm relative error of 37.12%. The ventilator resistance value for DS19_P2 is 14 cm $H_20$/L/s. The resistance values found from the model totaled to 13.4 cm $H_20$/L/s. Third row: plots for DS19_P3 with 2−norm relative error of 42%. The ventilator resistance value for DS19_P3 is 13 cm $H_20$/L/s. The resistance values found from the model totaled to 12.4 cm $H_20$/L/s.

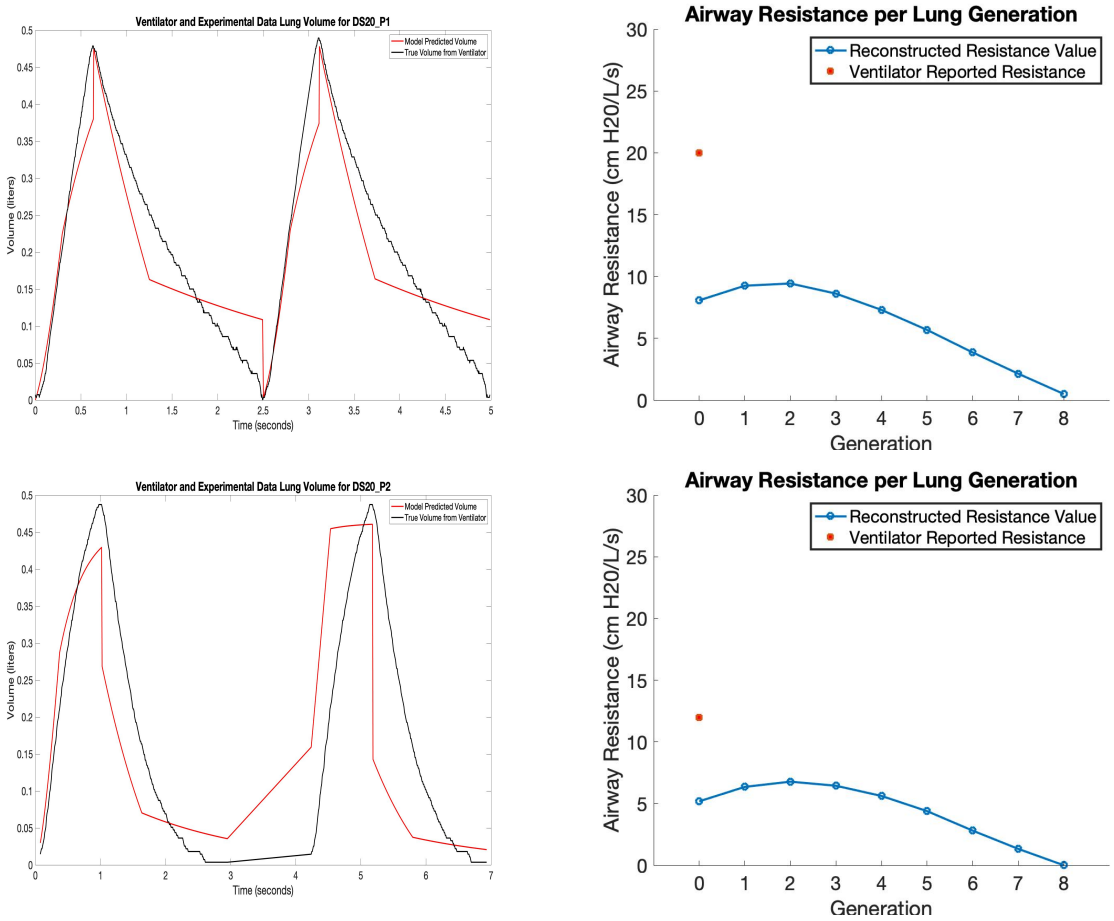


**Figure 6.15:** First row: plots for DS20_P1 with $2-$norm relative error of 19.98%. The ventilator resistance value for DS20_P1 is 20 cm $H_20$/L/s. The resistance values found from the model totaled to 16.8456 cm $H_20$/L/s. Second row: plots for DS20_P2 with $2-$norm relative error of 43.72%. The ventilator resistance value for DS20_P2 is 13 cm $H_20$/L/s. The resistance values found from the model totaled to 11.4 cm $H_20$/L/s. All patients are male COVID negative.

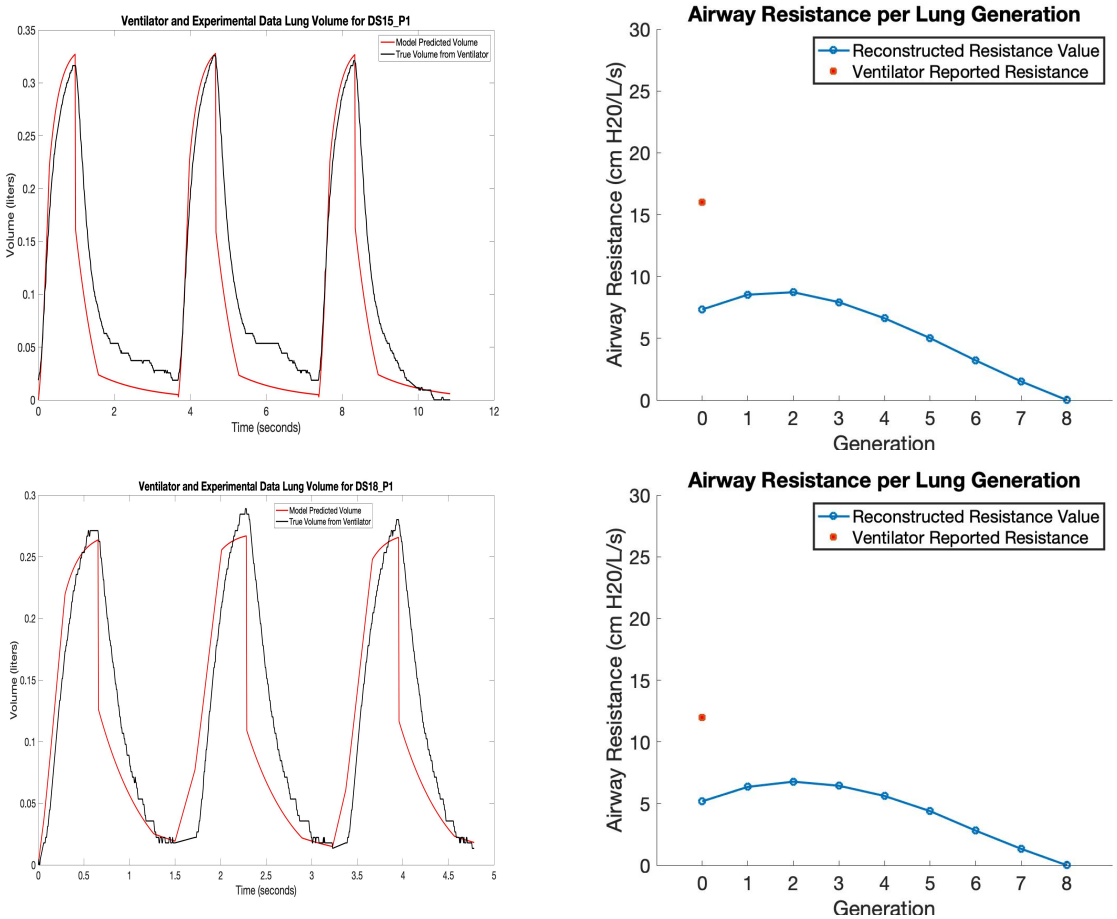


**Figure 6.16:** First row: plots for DS15_P1 with $2-$norm relative error of 31.92%. The ventilator resistance value for DS15_P1 is 16 cm $H_20$/L/s. The resistance values found from the model totaled to 15.4 cm $H_20$/L/s. Second row: plots for DS18_P1 with $2-$norm relative error of 30.34%. The ventilator resistance value for DS18_P1 is 12 cm $H_20$/L/s. The resistance values found from the model totaled to 11.4 cm $H_20$/L/s. Both patients are female COVID positive.

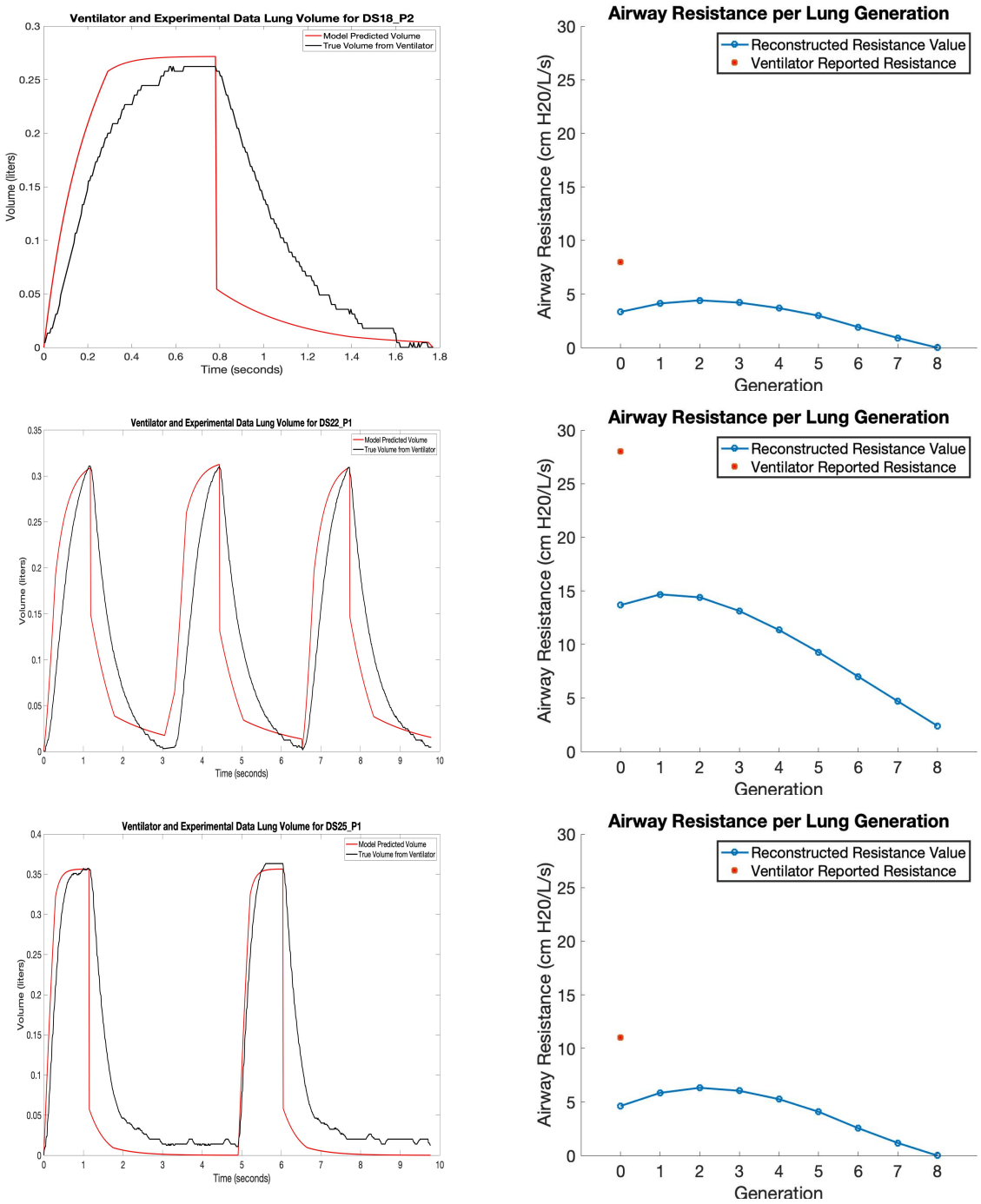


**Figure 6.17:** First row: plots for DS18_P2 with 2−norm relative error of 37.91%. The ventilator resistance value for DS18_P2 is 8 cm $H_20$/L/s. The resistance values found from the model totaled to 7.4 cm $H_20$/L/s. Second row: plots for DS22_P1 with 2−norm relative error of 41.89%. The ventilator resistance value for DS22_P1 is 28 cm $H_20$/L/s. The resistance values found from the model totaled to 27.4 cm $H_20$/L/s. Third row: plots for DS25_P1 with 2−norm relative error of 40.92%. The ventilator resistance value for DS25_P1 is 11 cm $H_20$/L/s. The resistance values found from the model totaled to 10.4 cm $H_20$/L/s. All three patients are female COVID positive.

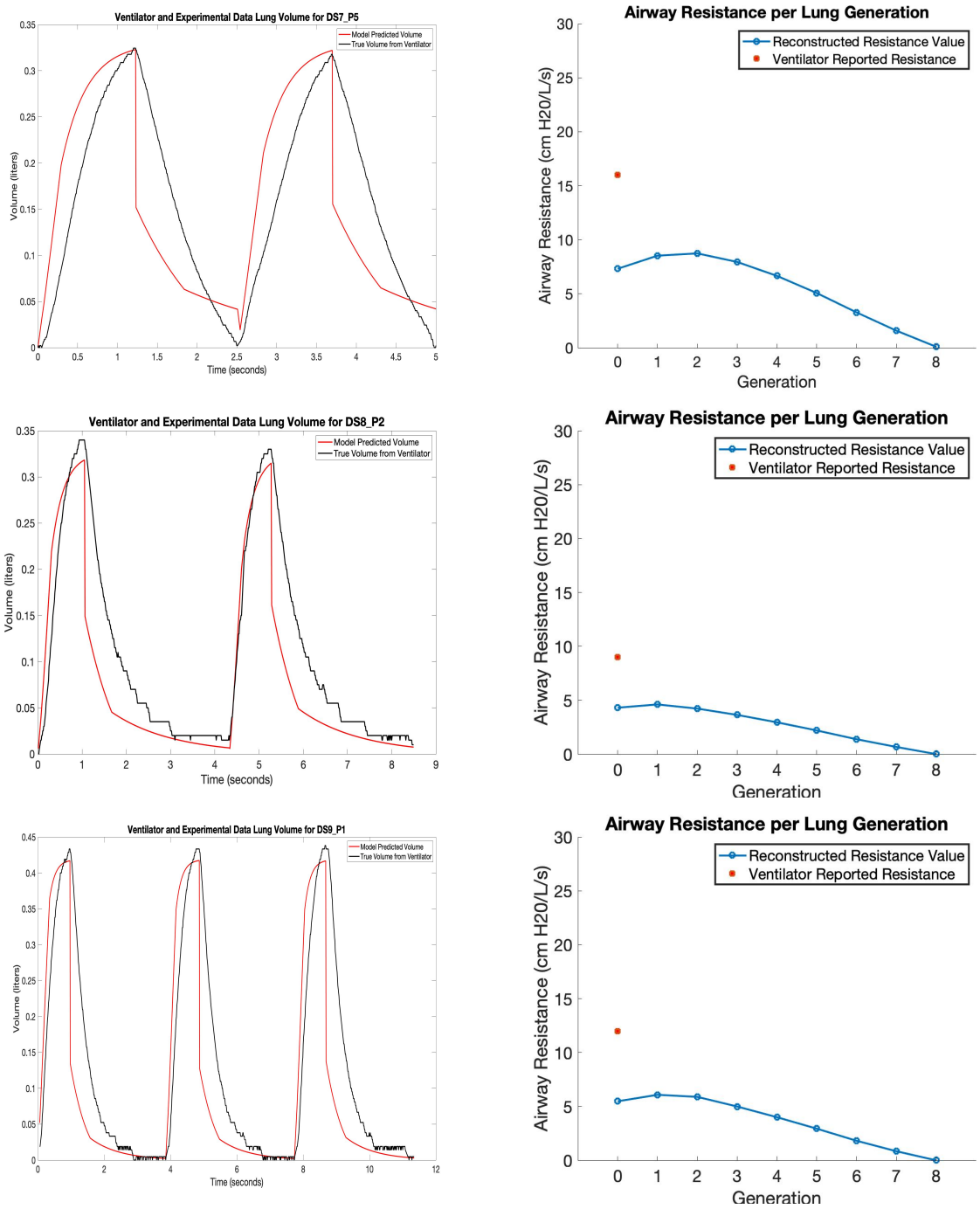


**Figure 6.18:** First row: plots for DS7_P5 with 2−norm relative error of 38.64%. The ventilator resistance value for DS7_P5 is 16 cm $H_20$/L/s. The resistance values found from the model totaled to 15.4 cm $H_20$/L/s. Second row: plots for DS8_P2 with 2−norm relative error of 34.26%. The ventilator resistance value for DS8_P2 is 9 cm $H_20$/L/s. The resistance values found from the model totaled to 8.4 cm $H_20$/L/s. Third row: plots for DS9_P1 with 2−norm relative error of 43.75%. The ventilator resistance value for DS9_P1 is 12 cm $H_20$/L/s. The resistance values found from the model totaled to 10.9883 cm $H_20$/L/s. All three patients are male COVID positive.

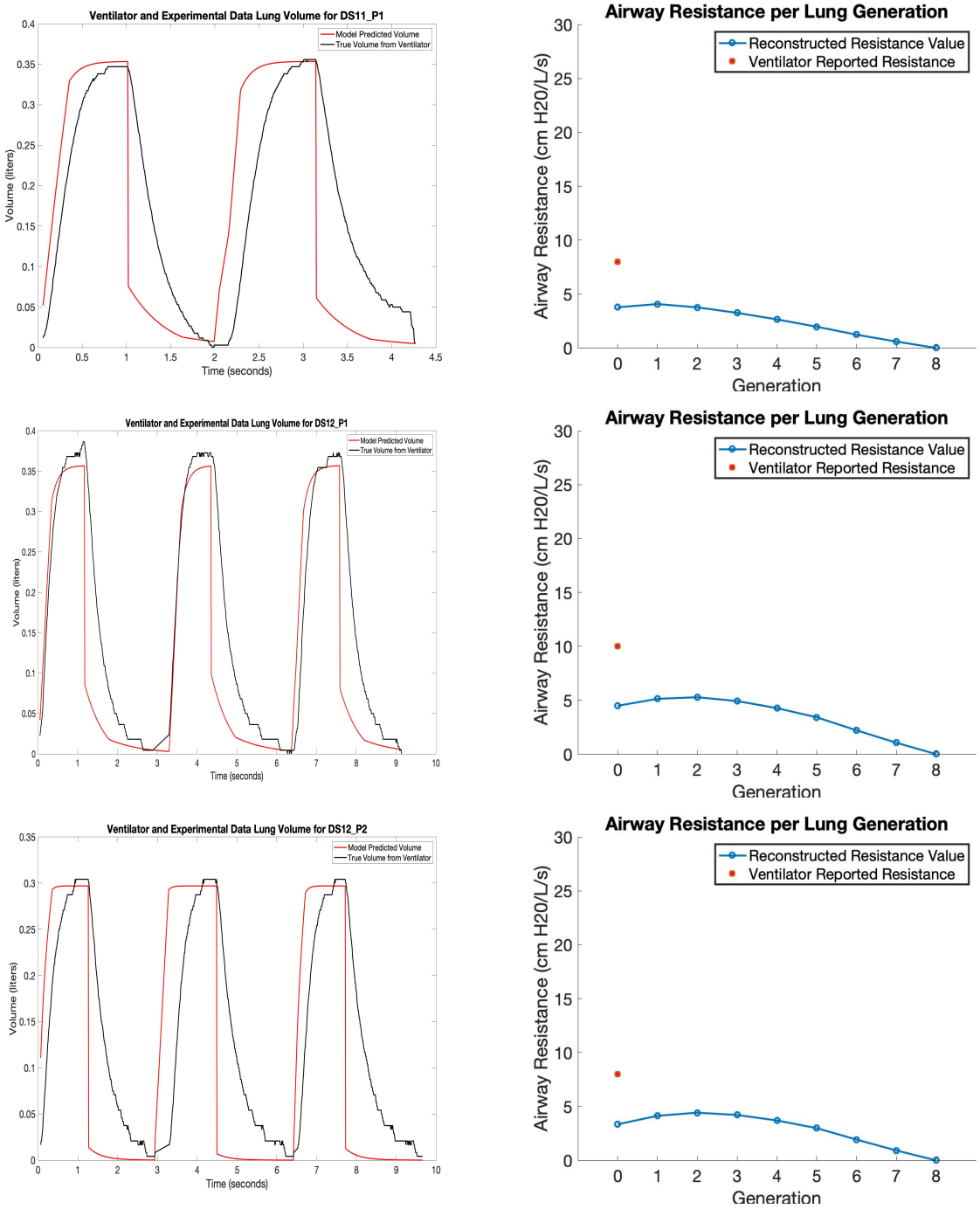


**Figure 6.19:** First row: plots for DS11_P1 with 2−norm relative error of 42.87%. The ventilator resistance value for DS11_P1 is 8 cm $H_20$/L/s. The resistance values found from the model totaled to 7.4 cm $H_20$/L/s. Second row: plots for DS12_P1 with 2−norm relative error of 31.52%. The ventilator resistance value for DS12_P1 is 10 cm $H_20$/L/s. The resistance values found from the model totaled to 9.4 cm $H_20$/L/s. Third row: plots for DS12_P2 with 2−norm relative error of 50.19%. The ventilator resistance value for DS12_P2 is 8 cm $H_20$/L/s. The resistance values found from the model totaled to 7.4 cm $H_20$/L/s. All patients are male COVID positive.

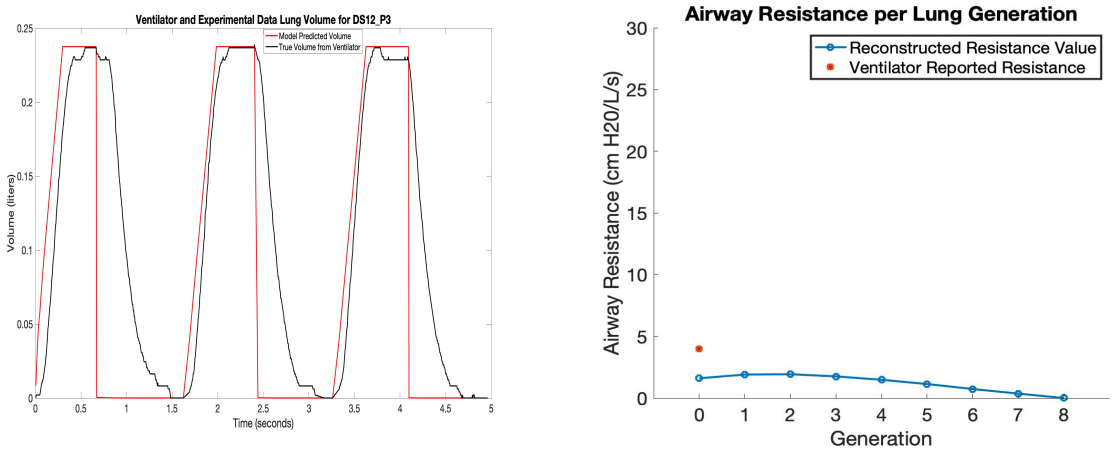


**Figure 6.20:** Plots for DS12_P3, a male COVID positive, with $2-$norm relative error of $40.45\%$. The ventilator resistance value for DS12_P3 is 4 cm $H_20$/L/s. The resistance values found from the model totaled to 3.4 cm $H_20$/L/s.

## 6.4 Sensitivity Analysis

A sensitivity analysis for the parameters of compliance and resistance was performed to study the relationship between the two parameters. For the analysis, 8 patients were studied from three different subgroups of our results. Two of the eight patients had a reported high resistance vector results with values decreasing inside the resistance vector from 14 to 2 cm $H_20$/L/s with a total resistance adding up to 20.4 and 27.4 cm $H_20$/L/s. Two of the eight patients had a reported low resistance vector results with values decreasing inside the resistance vector from 3 to 0 cm $H_20$/L/s with a total resistance adding up to 3.4 and 6.4 cm $H_20$/L/s. The remaining four patients were pulled from the middle range with resistance vector values between 8 and 0 cm $H_20$/L/s summing up to between 12-15 cm $H_20$/L/s. The percent relative change in compliance was calculated by dividing the range of tested compliance values by the calculated compliance value. Based on the sensitive analysis, a $95.28\%$ average relative change in compliance corresponds to a $2.76 \pm 5.54\%$ relative change in the resistance value in the first six entries of the resistance vector. However, the last three elements in the nine generation resistance vector were more sensitive to compliance. With the same $95.28\%$ average relative change in compliance a $18.97 \pm 34.27\%$ relative change in the resistance value in the last three entries of the resistance vector.

## 6.5 Statistical Analysis

The relationship between patient sex and airway resistance as well as COVID-19 diagnosis and airway resistance were analyzed. Patients were grouped into one of four categories: female COVID-19 negative, male COVID-19 negative, female COVID-19 positive, and male COVID-19 positive.

The statistical analysis was completed and written by Dr. Kim McFann, a Project Coordinator and Biostatistician at UCHealth's Medical Center of the Rockies. Please note all forms of $R_i$ represent the $i^{\text{th}}$ element in the airway resistance vector where $R_0$ is the first element and $R_8$ is the ninth and final element.

Thirty-two patients were enrolled in this study, 14 females (43.8%) and 18 males (56.2%). Categorical variables were compared using Chi Square Test of Independence while continuous variables were compared using Independent Sample T-tests with the exception of the vector of resistances in each generation of the bronchial tree all the way down to the alveoli. For this analysis MANOVA was used to analyze the series of dependent variables between COVID-19 negative and positive participants [48]. For all analysis, $p < 0.05$ is considered significant. The primary hypothesis was:

$H_0$: There is no significant difference in the airway resistance between COVID-19 negative and positive patients.

$H_A$: There is a significant difference in the airway resistance between COVID-19 negative and positive patients.

Of the 32 patients, 12 were positive for COVID-19 by a polymerase chain reaction test. We compare COVID-19 negative patients to positive patients. Resistance values $R_0 - R_8$ demonstrate decreasing resistance along the bronchial tree by generation; however, there was no difference in resistance between those who were negative and those who were COVID-19 positive ($p = 0.2270$).

We notice in table 6.5, the average resistance value for generation 0–6 ($R_0 - R_6$) is higher for COVID-19 negative patients compared to COVID-19 positive patients. However, the $p$-value for resistance between COVID-19 positive and negative patients is 0.2270 which is not significant

**Table 6.5:** A comparison of COVID-19 positive and negative patients. The notes in the table include †Endotracheal tube diameter, Ventilator Reported resistance value, $^a$Independent sample T-test, $^b$Chi Square Test of Independence, and *MANOVA p-value for the vector of resistance. $R_i$ represent the $i^{th}$ element in the airway resistance vector where $R_0$ is the first element in the vector and $R_8$ is the ninth and final element in the vector.

| | COVID-19 Negative ($N = 20$) | COVID-19 Positive ($N = 12$) | p-value |
|---|---|---|---|
| Calculated Compliance (cm $H_20$/L) | $0.04 \pm 0.01$ | $0.02 \pm 0.01$ | $< 0.0001^a$ |
| ETT Diameter† | $7.4 \pm 0.4$ | $7.7 \pm 0.3$ | $0.06365^a$ |
| Max Pressure (cm $H_20$) | $20.3 \pm 6.6$ | $29.2 \pm 7.3$ | $0.0012^a$ |
| Min Pressure (cm $H_20$) | $6.6 \pm 2.4$ | $13.2 \pm 5.8$ | $< 0.0001^a$ |
| Compliance (cm $H_20$/L) | $0.04 \pm 0.02$ | $0.02 \pm 0.01$ | $0.0004^a$ |
| Ventilator Resistance (cm $H_20$/L/s) | $13.5 \pm 3.8$ | $11.8 \pm 6.1$ | $0.3504^a$ |
| $R_0$ (cm $H_20$/L/s) | $6.1 \pm 1.9$ | $5.4 \pm 3.1$ | $0.2270^*$ |
| $R_1$ (cm $H_20$/L/s) | $6.9 \pm 2.0$ | $6.2 \pm 3.2$ | $0.2270^*$ |
| $R_2$ (cm $H_20$/L/s) | $7.0 \pm 1.9$ | $6.2 \pm 3.2$ | $0.2270^*$ |
| $R_3$ (cm $H_20$/L/s) | $6.3 \pm 1.6$ | $5.7 \pm 3.0$ | $0.2270^*$ |
| $R_4$ (cm $H_20$/L/s) | $5.4 \pm 1.4$ | $4.9 \pm 2.6$ | $0.2270^*$ |
| $R_5$ (cm $H_20$/L/s) | $4.1 \pm 1.0$ | $3.8 \pm 2.1$ | $0.2270^*$ |
| $R_6$ (cm $H_20$/L/s) | $2.6 \pm 0.7$ | $2.5 \pm 1.6$ | $0.2270^*$ |
| $R_7$ (cm $H_20$/L/s) | $1.2 \pm 0.4$ | $1.3 \pm 1.1$ | $0.2270^*$ |
| $R_8$ (cm $H_20$/L/s) | $0.1 \pm 0.2$ | $0.2 \pm 0.7$ | $0.2270^*$ |
| Relative 2-norm | $38 \pm 10.10\%$ | $36.92 \pm 9.17\%$ | N/A |

enough to claim COVID-19 negative patients will have higher resistance value. We also notice, the standard deviation for COVID-19 positive patients is higher for all resistance values per generation compared to COVID-19 negative patients.

There were significant differences between groups for calculated compliance ($p < 0.0001$), maximum pressure ($p = 0.0012$), minimum pressure ($p < 0.0001$) and ventilator reported compliance ($p = 0.0004$). Maximum and minimum pressures were higher in COVID-19 positive patients, while calculated compliance ($p < 0.0001$) and ventilator reported compliance ($p = 0.0003$) were lower. Table 6.5 shows a comparison between COVID-19 positive and COVID-19 negative patients. Based on the statistical analysis, sex and COVID-19 status do not play a role in airway resistance values. Examining table 6.5, we can see the average resistance value of each generation ($R_0 - R_8$). Overall, the average values have very little difference between COVID-19 negative and

COVID-19 positive patients. There is a significant difference for pressure and compliance between COVID-19 negative and COVID-19 positive patients.

For the 32 patients, the ventilator reported resistance value varied from 4 cm $H_20$/L/s to 28 cm $H_20$/L/s. The RCCB lung model found the total airway resistance in the lung for all patients to be between 3.4 cm $H_20$/L/s and 27.4 cm $H_20$/L/s. On average, the first element in the resistance vector, which represents the trachea, was $44.51 \pm 3.44\%$ of the reported resistance value. The second element, $R_1$ was $51.27 \pm 2.43\%$ of the ventilator reported value. $R_2$ was found to be on average $52.10 \pm 3.60\%$ of the ventilator reported value, $R_3$ was $47.72 \pm 4.75\%$ of the ventilator reported value, $R_4$ was $40.58 \pm 5.05\%$ of the ventilator reported value, $R_5$ was $31.50 \pm 4.69\%$ of the ventilator reported value, $R_6$ was $20.13 \pm 3.51\%$ of the ventilator reported value, $R_7$ was $9.67 \pm 2.35\%$ of the ventilator reported value, and $R_8$ was $0.44 \pm 1.6\%$ of the ventilator reported value. These percent values add up to over $100\%$ as the resistance is defined in series.

Based on the statistical analysis, sex and COVID-19 results do not play a role in airway resistance values. Examining table 6.5, we can see the average resistance value of each generation ($R_0 - R_8$). Overall, the average values have very little difference between COVID-19 negative and COVID-19 positive patients. There is a significant difference for pressure and compliance between COVID-19 negative and COVID-19 positive patients.

## 6.6 Discussion

A goal for this study is to determine the airway resistance in the bronchial tree through ventilator output data. We observe and determine if there is a relationship between the total airway resistance value on the ventilator compared to the airway resistance vectors from the inverse problem. We wish to determine whether sex is a parameter that influences the values of the resistance vector, and so we investigate whether there is a statistical correlation.

We study the relationship between patient sex and COVID-19 result for airway resistance. We grouped each patient into one of four categories: female COVID-19 negative, male COVID-19 negative, female COVID-19 positive, and male COVID-19 positive. In figure 6.21 we see all 32

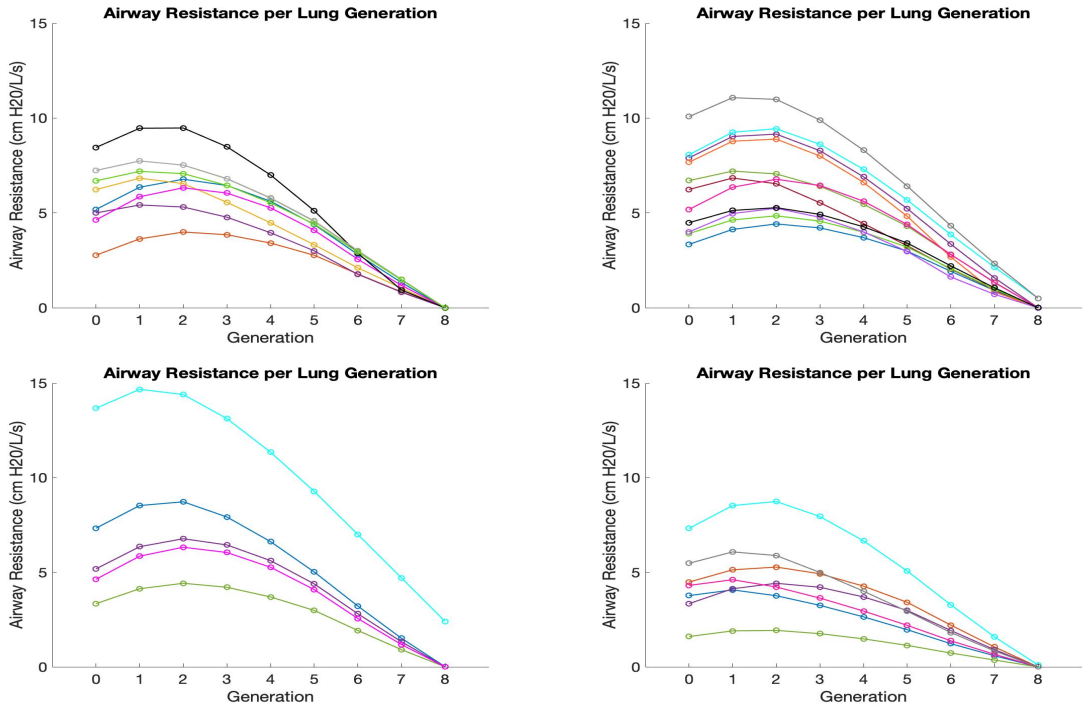


**Figure 6.21:** Top Left: A plot of all female COVID-19 negative resistance vectors. Top Right: A plot of all male COVID-19 negative resistance vectors. Bottom Left: A plot of all female COVID-19 positive resistance vectors. Bottom Right: A plot of all male COVID-19 positive resistance vectors.

resistance vectors grouped in each category. From the statistical analysis, gender and COVID-19 results do not play a role in airway resistance values. Examining table 6.5, we can see the average resistance value of each generation. Overall, the average values have very little difference between COVID-19 negative and COVID-19 positive patients. We did find a significant difference for pressure and compliance between COVID-19 negative and COVID-19 positive patients. In the future, we can explore the relationship between COVID-19 test result, compliance, and airway resistance.

The results in section 6.3 demonstrate that the RCCB lung model can predict shape, amplitude, and breathing intervals in the ventilator volume curves with good visual accuracy. Since there is currently no method for measuring resistance values along the bronchial tree, the estimated values can only be validated in combination with the forward model output of ventilation volume. Since

the Hamilton G5 Operator Manual [7] only provides total airway resistance, future work is needed to determine the accuracy and utility of the reconstructed airway resistance values.

The grouping by sex and COVID-19 diagnosis in the plots of the airway resistance vectors in figure 6.21 reveal that, although there is some common vector grouping, visually there does not appear to be a connection between resistance vector and sex or COVID-19 diagnosis of the patient, which is consistent with the statistical analysis. The patients' resistance vector results in figure 6.21 supports this.

The RCCB lung model has several limitations. As mentioned, this multi-compartment lung model assumes the lung has a dichotomous structure. This assumption is not accurate for a true lung as one branch may lead to three or more other branches. However, each patient's actual lung structure is unknown, and relaxing this assumption would significantly complicate the model. This model also assumes left/right symmetry of the lung as well as linearity in the compliance and resistance matrices. These assumptions are made in the absence of regional lung information for each patient. Having access to regional lung information through lung imaging will allow for asymmetries in airflow to be considered in an updated model. Asymmetries in airflow can be added in this multi-compartment lung model through compliance, pressure, and volume parameters.

Limitations of the study include incomplete pressure data and limited number of breaths from the ventilator screenshots. All 32 patients' ventilator information were collected while the patient was in the supine position or laying on their back. For this study, we did not collect patient height, so we do not know the role height may play in airway resistance in the bronchial tree. Limitations of the study include incomplete pressure data and limited number of breaths from the ventilator screenshots

Our results show each element of the resistance vector plays a role in the overall shape of the lung volume. The last three elements of the resistance vector control the shape of the volume peak, rather the peak looks more plateau in shape or more curvature is determined the last elements in the resistance vector. The smaller the last elements are, the more of a plateau you have, while the

larger, the more curvature you have. The first three elements in the resistance vector control the height of the volume peak.

Spontaneous breathing is a mode in mechanical ventilation where patients can trigger their own breathing. In patient triggering, the patient overrides the machine's breath. These triggered breaths can lead to a different expected volume curve that the RCCB lung model must account for as the start of an inhale may be irregular. During a triggered breath, the ventilator and respiratory muscles work together to generate the applied pressure [49]. This new pressure value may affect the accuracy of the RCCB lung model. This study did not include patients with spontaneous breaths.

### 6.6.1 Specific Data Results

There were a few results that stand out. These results can be seen in the supplementary data. Synthetic pressure can affect the overall results as the true patient time versus pressure curve may have been different than the synthetic pressure curve we used. Synthetic pressure curves as well as translating volume curves from screenshots with an average number of time points per breath play a role in results like Patient ID: DS3_P2, DS2_P7, DS 20_P1, and DS12_P2 which all had on average, a range of 0.0202 L/cm $H_20$ between calculated and ventilator compliance.

Patients with especially low minimum and maximum pressure values also stood out. This may be because the slope or change in pressure between the two pressure values is different than the one calculated using the synthetic pressure curves. Patients DS2_P7, DS19_P2, DS19_P3, DS20_P1, and DS20_P2 all had the lowest minimum pressure values of 4 or 5 cm $H_20$. Patients DS12_P3, DS19_P1, and DS18_P2 had small reported ventilator resistance values of 4, 7 and 8 cm $H_20$/L/s, respectively.

Patients DS19_P2 and DS19_P3 are both male COVID-19 negative with the first element in the resistance vector, $R_0$ the resistance value in the trachea, being in the top seven resistance values. For DS19_P2, $R_0$ was 47.89% of the reported ventilator resistance value and for DS19_P3, $R_0$ was 47.97% of the reported ventilator resistance value which was in the top four values. Both patients

had a low-pressure value and close reported and calculated compliance values. For DS20_P1, the sum of the resistance vector was 16.8456 cm $H_20$/L/s, however, the ventilator reported resistance value was 20 cm $H_20$/L/s so each element in the vector could be at a higher value. For DS7_P5, the reported compliance value was unknown so we cannot compare the calculated compliance value to the true compliance value.

# Part II Reconstruction of Airway Resistance in an Asymmetric Lung

# Chapter 7

# Forward Problem for an Asymmetric Lung

The RCCB model for symmetric lungs includes assumptions that are not real world accurate, such as a dichotomous structure and left/right lung symmetry. Since we do not know the branching structure for each patient, we assume an easier to work with dichotomous structure. Acknowledging left/right asymmetries better models the lung in the presence of pathologies, especially when modeling patients on mechanical ventilators. Developing a model that includes lung asymmetries leads to a more accurate model but does involve working with a more complex system.

In this chapter, we introduce a RCCB multi-compartment lung model for asymmetric lungs that uses regional information. We give a brief background on the medical imaging technique electrical impedance tomography (EIT) to explain one way to capture and determine regional lung information. We then detail how to handle some complexities that arise from this asymmetric version of the RCCB model. Finally, we discuss the limitations this model has.

## 7.1 RCCB Lung Model for an Asymmetric Lung

The RCCB lung model that accounts for left/right asymmetries requires regional information, meaning parameters need to be described in terms of generations and airways as opposed to just generations. This allows us to work with parameters of vectors (generations) or matrices (airways).

We define pressure, $P(t)$, as a $2^n \times 2^n$ matrix where the elements inside the matrix describe pressure in each airway at each time $t$. Compliance, $C(t)$, is a $2^n \times 2^n$ matrix dependent on time, where elements describe the compliance per each airway. Note that equation (4.8) defines a way to convert a generation resistance vector to a $2^n \times 2^n$ airway resistance matrix and vice versa. We can translate equation (4.8) to apply to vector and matrix pressure and compliance in a similar way. Defining all parameters of the model as $2^n \times 2^n$ matrices implies the output of the model or volume at any given time will also be a $2^n \times 2^n$ matrix.

The resistor-capacitor circuit based multi-compartment asymmetric lung model that uses regional lung information is:

$$V(t) = \begin{cases} P(t)C(t)\left(\mathbb{I} - e^{-t(RC(t))^{-1}}\right) & \text{for all } t \in [0, T_{in}] \\ P(t)C(t)e^{-t(RC(t))^{-1}} & \text{for all } t \in [T_{in}, T_{total}] \end{cases} \tag{7.1}$$

where $V$ is volume, $P$ is pressure, $C$ is compliance, $R$ is resistance and $V, P, C, R$ are $2^n \times 2^n$ matrices at time $t$. This model satisfies both symmetries and asymmetries within airways, creating a more realistic model.

To collect regional volume information, which will be used to validate the model, we use electrical impedance tomography (EIT). Since EIT tracks changes in ventilation and volume, it is an excellent choice for bedside imaging of patients on mechanical ventilators. However, this asymmetric model does yield other complexities we did not account for in the previous symmetric version of the model (equation (4.9)).

## 7.2 EIT

Electrical impedance tomography, or EIT, is an imaging technique where electrodes are placed on the surface of an imaged region and low levels of current are applied below the threshold of human perception. EIT allows us to reconstruct an image of the lungs because conductivity and permittivity vary in the body; specifically, air has a low conductivity and blood has high conductivity [50]. A photo of electrodes on the body is seen in figure 7.1. From these electrodes, we receive measurable voltage distributions and solve an inverse problem for the conductivity distribution in the region of interest [50]. EIT is a helpful medical imaging technique because it is cost effective, portable, and electric currents can propagate through the tissue without damage. This imaging technique is non-invasive and provides real time images of changes in ventilation and pulmonary perfusion [51].

Today, we can collect multiple cross sections of the human lungs by putting two layers or rows of electrodes on a patient, seen in figure 7.1. The first layer is a set of 16 electrodes and collects

data focusing on the top of the lungs. The second row of 16 electrodes is placed underneath the first 16 and collects data on the lower lungs. We will need to make more assumptions to define which generations are in the top or bottom of the lung. For the asymmetric lung model, we used the GE GENESIS EIT system [52] to collect data and reconstruction algorithms from [53, 54] to reconstruct images from the EIT data.

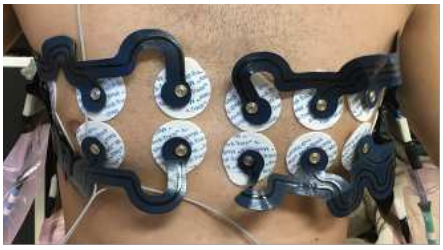

**Figure 7.1:** A photo of 32 electrodes arranged in two rows of 16 on the WEAT (wearable electrode applicator textile) belt designed by GE Research. This photo is taken from [55]. The EIT system used on this healthy volunteer is the GE GENESIS EIT system [52].

## 7.3 Lung Structure

Using EIT allows us to collect regional lung information. EIT data leads to calculating volume per voxel where a voxel is equivalent to a pixel in 3D space. Defining the lung structure or what generation and airway a specific voxel represents is challenging. In this section, we discuss how we define the lung structure. When calculating regional lung volume using EIT, we must know which voxel corresponds to which region. Unfortunately, based on EIT images, seen in figures 7.2 and 7.3, we cannot easily determine which voxel corresponds to which airway or generation. However, we can make educated assumptions to help us define the lung structure.

After calculating the lung volume from EIT data, we are left with voxels that represent lung volume at a given time. Based on the electrode placement of 32 electrodes placed around their chest with 16 on the top and another 16 on the bottom, we determine the overall volume in both the top and bottom lung, and we also define the volume in the left and right lung of each voxel.

Based on lung structure knowledge, we notice the upper lung has fewer airways and branching than the lower lung and the airways branch out both horizontally and vertically as we move along

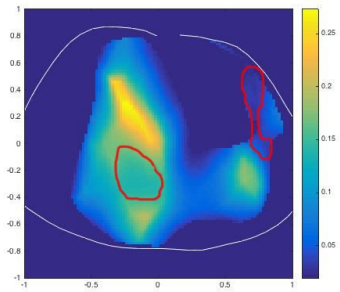

**Figure 7.2:** EIT image showing an unhealthy lung. This image is a ventilation/perfusion ratio map and the regions circled in red are potential regions of air trapping. This image was taken from [56].

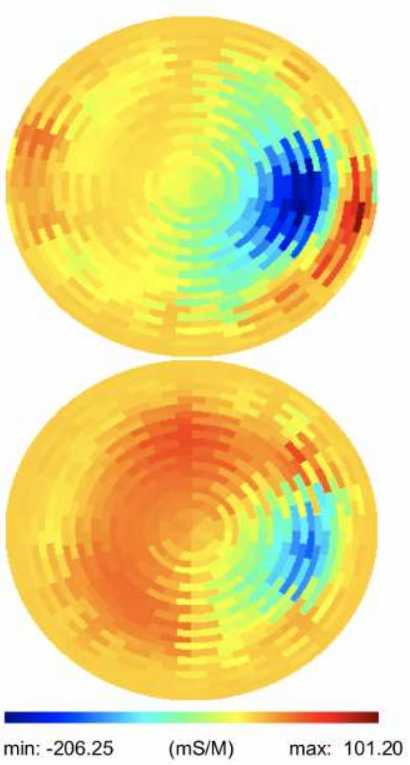


**Figure 7.3:** Two cross sections of EIT images displayed in a DICOM orientation, where the right part of the image is the patient's left. These two EIT images show conductivities. Both images are slices of a 3D reconstruction at full inspiration of an ARDS patient on a mechanical ventilator at University of Colorado Anschutz Medical Campus. Here the blue voxels represent regions of low conductivity relative to the reference image, which was taken at full expiration. The top image represents the upper lung, and the bottom image represents the lower lung. We can see the right lung has little to no volume at the time this data was collected. The EIT system used to collect this data was the GE GENESIS system [52]. This image was reconstructed using algorithms from [53, 54] and the image was taken from [55].

the bronchial tree. Casts of the human lungs from [1], give visuals of the lung structure. Using this knowledge, we define certain airways and branches as being in the upper left, upper right, lower left, or lower right of the lung as these distinctions are apparent in EIT data. Figure 7.4 is an example of a 32 compartment, 5 generation lung with definitions of upper and lower lungs. Notice, in figure 7.4 the color red represents airways in the lower lung while blue airways are defined to be in the upper lung. EIT data does not collect information on generation 0, or the trachea, as the electrodes are not placed that high on the patient. Table 7.1 includes a summary of how many total airways are assumed to be in the upper versus the lower lungs. This is how we define the lung branching for all patients. This definition does assume a dichotomous structure.

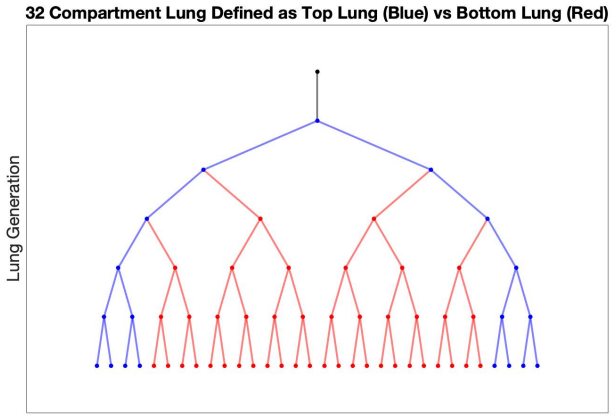


**Figure 7.4:** A depiction of a 32 compartment, 5 generation lung with blue airways defined as upper lung and red airways defined as lower lung. There are less airways in the upper lung than in the lower lung.

One of the challenges at this stage is to define the lung structure for each patient. We have estimates of the volumes as a function of time in each lung section (left, right, lower, upper) from the EIT data, but not necessarily what airway and generation a voxel represents. So, we must define this for each patient's data. The EIT data collected includes the entire cross section of the upper torso including the lungs, heart, and dead space. The cross section is discretized using a Joshua Tree mesh as was used in [53, 54]. An example with numbered voxels is seen in figure 7.5. The top row of 16 electrodes on the belt is placed so that the cross-sectional plane of electrodes

**Table 7.1:** Summary of airways defined to be in the upper versus the lower lung. The trachea or generation 0 is defined to be in neither the lower or upper lung as EIT data cannot collect information on the trachea since it is above the electrode placement.

| Generation | Airways in Upper Lung | Airways in Upper Lung | Airways in Generation |
|---|---|---|---|
| 0 | 0 | 0 | $2^0 = 1$ |
| 1 | 2 | 0 | $2^1 = 2$ |
| 2 | 2 | 2 | $2^2 = 4$ |
| 3 | 2 | 6 | $2^3 = 8$ |
| 4 | 4 | 12 | $2^4 = 16$ |
| 5 | 8 | 24 | $2^5 = 32$ |
| 6 | 16 | 48 | $2^6 = 64$ |
| 7 | 32 | 96 | $2^7 = 128$ |
| 8 | 64 | 192 | $2^8 = 256$ |
| 9 | 128 | 284 | $2^9 = 512$ |
| $\vdots$ | $\vdots$ | $\vdots$ | $\vdots$ |
| 24 | $2^{22} = 4,194,304$ | $2^{24} - 2^{22} = 12,582,912$ | $2^{24} = 16,777,216$ |

aligns with the upper lung. The bottom row of 16 electrodes on the belt is placed so that the cross-sectional plane of electrodes aligns with the lower lung. We define a voxel in the upper lung if it associated with the top row of 16 electrodes and define a voxel in the lower lung if it associated with the bottom row of electrodes. Note that the lower lung has voxels 1 – 496 and the upper lung has voxels 497 – 992. Therefore, each patient has a total of 992 voxels of volume at every time. The height of each voxel is equal to the vertical distance between the upper and lower rows of electrodes, with the vertical center of each voxel at the location of the center of the electrode for that row. All electrodes in each row are assumed to be at the same height.

Even when a patient is inhaling with a volume of larger than zero, many of the 992 voxels in the Joshua Tree mesh still have zero assigned volume as not all voxels are associated with lung space. For example, patient 112, who will be introduced in chapter 9, has a total of 142 voxels defined as lung space in the 992 available options. The number of voxels not used are due to two reasons. One being that not all the area imaged with EIT includes lung, some of the area may be heart or dead space. Another reason there are so many voxels not assigned or associated to lung volume is that many of the patients who are imaged have lung health concerns. Going back to patient 112, the lower right lung volume is completely zero due to the patient's health issues. A

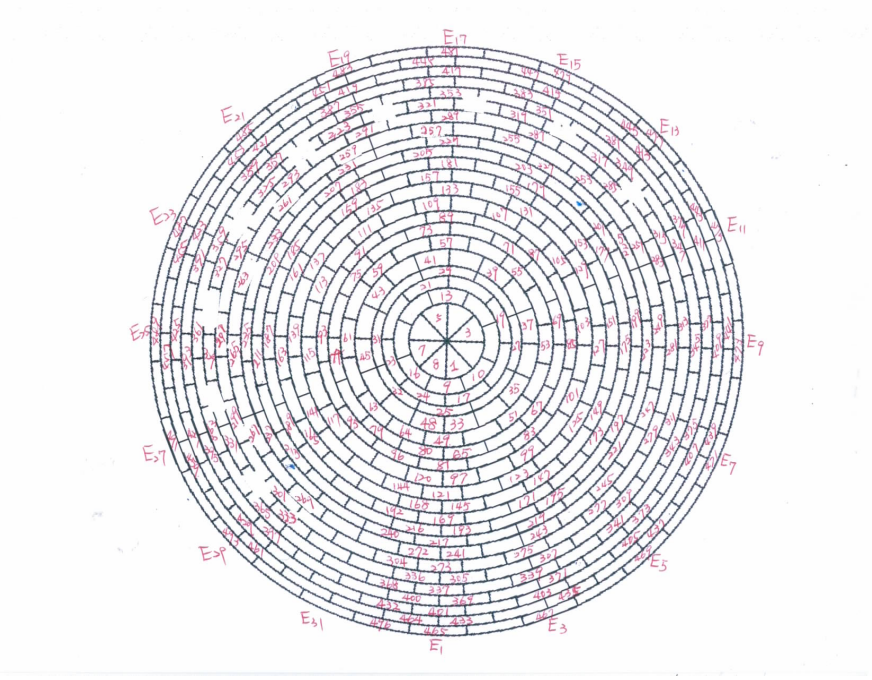

**Figure 7.5:** An example of a Joshua Tree mesh discretization of the lower lung from EIT data. Every other voxel is numbered to keep track.

breakdown of the total volume for all four quadrants of the lung for patient 112 is seen in figure 7.6. More information on the EIT volume discretization as well as validation of EIT volume versus ventilator volume can be seen in [55].

Although we have discretized the domain, we still need to define each voxel in its respective airway. EIT volume data was computed and provided by Nilton Barbosa da Rosa Junior, a member of Dr. Jennifer Mueller's Colorado State University lab. Nilton defined each voxel to be in one of the following categories: lower left lung, lower right lung, upper left lung, or upper right lung. The left versus right part of the lung comes from dividing the Joshua Tree mesh in half, straight through the middle. Some voxels were defined in both the left and right lung. These cases come from voxels close to both the left and right side and happened only near the middle of the Joshua Tree mesh. For these overlapping cases we split the volume at every time in that voxel in half to assign half to the left lung and half to the right lung. For example voxels 13 and 39 from figure 7.5, we assume half the volume in the voxel is in the right lung and the other half is in the left lung

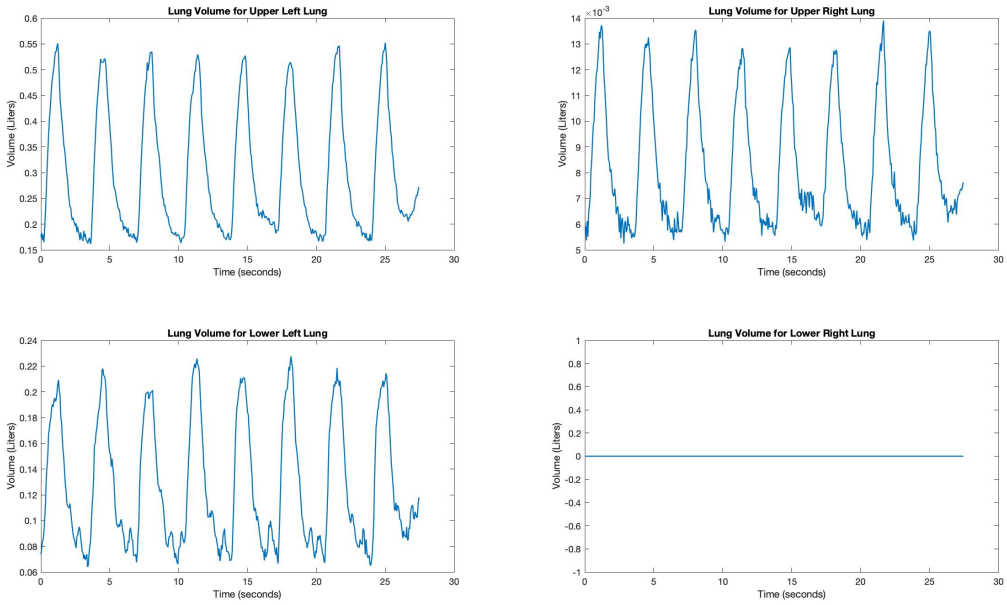


**Figure 7.6:** Four volume plots for EIT patient 112 broken down by upper left lung, upper right lung, lower left lung, and lower right lung. All four plots were reconstructed from EIT data. Note the varying volume scales for the vertical axis.

for every time point. Using figure 7.5, we define voxels 5 – 8 in the lower right lung and voxels 1 – 4 in the lower left lung.

These definitions and constructions allow us to define voxels into the four categories of locations: lower/upper lung and left/right lung. From casts of lungs, we understand the general structure of the lung including the expected location of the heart. Based on the layout of the lungs, we define the main bronchi or generation 1 of the lungs to be toward the middle of the Joshua tree mesh. In every generation, we number the airways as we would read, from left to right, the lower airway numbers are in the left lung and the larger numbers are in the right lung. An example of this can be seen in figure 4.2, where the first airway in the second generation is in the left lung and the fourth airway in the second generation is in the right lung. As we move lower in the bronchial, the airway size gets smaller and so we must reflect this in how we assign voxels.

An example of defining voxels as part of an airway is seen in table 7.2 for patient 112's lower left lung. We can apply this general idea to all patients so that we know the volume in each airway

**Table 7.2:** Summary of the voxels for EIT patient 112 lower left lung only. In this case we look at a 4 generation or 16 compartment system. The voxel values are coming from the Joshua tree mesh seen in figure 7.5.

| Generation | Airway | Joshua Tree mesh Voxel Values (1-496) |
|---|---|---|
| 2 | 2 | 68, 69, 83, 84, 101, 102, 103, 104 |
| 3 | 2 | 128, 152, 153, 176, 177 |
| 3 | 3 | 126, 127, 150, 151, 174, 175, |
| 3 | 4 | 124, 125, 149, 172, 173 |
| 4 | 3 | 201, 252, 253, 282 |
| 4 | 4 | 200, 225, 251 |
| 4 | 5 | 199, 224, 250, 282 |
| 4 | 6 | 198, 223, 249 |
| 4 | 7 | 222, 247, 248 |
| 4 | 8 | 197, 221 |

at every given time. This allows us to work with a matrix of volumes at a given time as opposed to the total lung volume at a given time as we did in chapter 6.

In chapter 6, we introduced a study that used lung volume from mechanical ventilator data to predict generation lung resistance. The lung volume on mechanical ventilators is used to ensure patients are receiving oxygen correctly. With the asymmetric version of the RCCB lung model introduced in this chapter, we rely on volume from EIT data. The work in [55] studies one example of comparing the sum of the time-dependent EIT-derived lung volumes per voxel with the time-dependent total lung volume from the ventilator. We take this work as an assumption that the lung volumes calculated from the EIT data are a good approximation to the true volumes.

## 7.4 Pressure Drop

Previously we assumed pressure is equal throughout every airway in the lung. However, that is not accurate. Pressure varies depending on the generation and stage of inhale and exhale. We know the total pressure curve increases and then plateaus during inhalation; during exhalation the total pressure decreases and then plateaus as seen in figure 6.4. We can break this up further by generation.

During inhalation, when the pressure is increasing, the lung generation versus pressure curve will be decreasing and concave up. This means there is a higher pressure value in the trachea and first few generations than the lower generations. As we increase in time, the pressure continues to increase and the concavity of the generation versus pressure curve will decrease, allowing for the pressure difference between generations to decrease. When the total lung pressure plateaus, the pressure in generation $0$ is equal to the pressure in generation $23$ and every generation in-between. Therefore, the generation versus pressure curve will be a straight line.

During exhalation, when the pressure is decreasing, the end airways, or generation $23$, will decrease at a slower rate than the generations toward the trachea. Therefore, as we move through exhalation, the generation versus pressure curve will be an increasing, concave down shape until the exhalation is plateaued. In which case, the generation versus pressure curve will be a straight line.

We know the overall shape of the generation versus pressure curve at any given time, so we should ensure this is true for the asymmetric model. One way to ensure our pressure per generation holds this shape is by defining the concavity depending on where the patient is in a breath and adding it to the model. Since we know regional lung information, we can also define the pressure as a matrix for each given time instead of a vector of generations. We calculate these pressure values at each time and for each element in the pressure matrix, $P_{i,j}$, where $i$ represents row and $j$ represents column. Using the definition of airway resistance, $R = \frac{\Delta P}{\dot{V}}$, and forward differences, we define pressure at a given time, such that $\Delta P = \frac{R\Delta V}{\Delta t}$.

## 7.5 Model Limitations

This RCCB lung model has some limitations, the biggest of which is the assumption of each patient's lung structure. Although we can apply the same logic and steps to defining the lung structure for each patient, we would only be finding the general branch of each EIT data point. EIT data allows us to estimate what is happening in each quadrant of the lung (lower, upper, left, right) and our assumption of the lung structure leads to predicting certain aspects of the lung in the

correct general area. The asymmetric model provides us with more information than the previous symmetric RCCB lung model, and we can study how asymmetries in the lung, regardless of overall location, affect parameters like airway resistance.

Now that we have an asymmetric model and understand the assumptions we are making, the next step is to set up an inverse problem to determine airway resistance in each generation for each patient. The optimization algorithm and inverse problem steps vary when compared to the inverse problem for the RCCB model, in chapter 5.

# Chapter 8

# Inverse Problem for an Asymmetric Lung

Now that we have an asymmetric version of the RCCB lung model that includes regional information, we update the inverse problem. We treat the inverse problem as an algorithm with multiple steps. Since we do not know regional pressure, resistance, or compliance, we use previous techniques from section 6.1 as initial guesses for each variable.

We initialize pressure and compliance matrices as we previously did with the intention of updating them based on definition after we know more about airway resistance. After initializing the airway resistance vector, pressure, and compliance, we run through the inverse optimization problem once. Once we solve for resistance, we update pressure and compliance variables by their definition to account for regional information and then run the optimization problem again.

This algorithm allows us to start with information we know, then update the information to include and account for the regional information. By updating variables to reflect the regional changes, we can predict better values for resistance. A summary for the algorithm is in Algorithm 1. The overall inverse problem from equations (5.9) and (5.10), does not change, but the model $V(\vec{R})$ is updated to equation 7.1. As we see in Algorithm 1, we iterate through a total of 6 times; once as an initial symmetric case (step 2 through step 6) and five times when updating pressure and compliance for asymmetries (step 7 through step 11). The stopping criteria in this algorithm is based on number of steps and there are no stopping criteria in regards to tolerance. Tables of L2 norm differences between iterations can be found in section 9.2.

Pressure at each time $t$ can now be calculated by leveraging its relationship to resistance. Resistance is defined by the change in pressure divided by air flow rate, $R = \frac{\Delta P}{\dot{V}}$. Each element $P_{ij}$ of the pressure matrix $P$ can be calculated at a given time $t_k$ by

$$P_{ij}(t_k) - P_{ij}(t_{k-1}) = \frac{R_{ij}(V_{ij}(t_k) - V_{ij}(t_{k-1}))}{t_k - t_{k-1}} \tag{8.1}$$

**Algorithm 1** An algorithm for the asymmetric inverse problem.

1: Get the volume in each voxel from EIT data
2: Initialize the symmetric airway resistance matrix
3: Initialize $P(t)$ =diag$(P_{total}/2^n)$ ▷ define pressure at each time as symmetric diagonal matrix
4: Initialize $C(t)$ =diag$(C_{total}/2^n)$ ▷ define compliance at each time as symmetric diagonal matrix
5: Compute the solution to the inverse problem
6: Return initial $\vec{R}$ define as $\vec{R}_{current}$
**for** i=1 to 5 **do**
    7: define $\vec{R}_{current}$ as $\vec{R}_{previous}$
    8: Update $P(t)$ using equation 8.1
    9: Update $C(t)$ using equation 8.2
    10: Compute the solution to the inverse problem
    11: Return $\vec{R}$ and define as $\vec{R}_{current}$
**end for**

where $i$ represents rows and $j$ represents columns of the respective matrix with $i, j \leq 2^n$, $k$ is the element in the discretized time vector, $P$ is pressure, $R$ is resistance, and $V$ is volume.

We update compliance at each time as a matrix both through the definition and the asymmetric pressure matrix calculation from equation (8.1). Compliance is defined as $C = \frac{\Delta V}{\Delta P}$ such that each element of the compliance matrix $C_{i,j}$ can be calculated at a given time $t_k$ by

$$C_{ij}(t_k) = \frac{V_{ij}(t_k) - V_{ij}(t_{k-1})}{P_{ij}(t_k) - P_{ij}(t_{k-1})} \tag{8.2}$$

where $i$ represents rows and $j$ represents columns of the respective matrix with $i, j \leq 2^n$, $P$ is pressure, and $V$ is volume. Elements $P_{i,j}$ come from equation (8.1). We utilize the calculated volume from EIT, or $V_{meas}$, to represent the volume $V$ as we know regional lung volume information.

## 8.1 Inverse Crime

Now that we have an inverse problem algorithm that accounts for asymmetries, we must verify that it is constructed correctly. We use the inverse crime to verify the model and to find the best regularization parameter. For the inverse crime, we created synthetic "true" volume data for a $2^4$ compartment lung using a resistance vector of $\vec{R} = [8.5, 10, 7.5, 2, .75]$, inhale and exhale times of

1.5 seconds and 2.5 seconds respectively, a total compliance value of $0.0356$ L/cm $H_20$, minimum pressure of 5 cm $H_20$, and maximum pressure of 25 cm $H_20$. We use the minimum and maximum pressure values to create synthetic pressure seen in figure 8.1. Figure 8.2 includes the forward model generated volume data. The generated volume data in the inverse crime was based off a symmetric lung since no data was collected prior to the inverse crime construction and we were not sure how the asymmetries in the lungs would appear in the EIT data. This model was designed to work with both the asymmetric lung and symmetric lung case. Since we apply this model to asymmetric lungs, once we had a regularization parameter from the inverse crime, we empirically checked the results of patients with varying regularization parameters to verify the best choice. Using Algorithm 1 to solve the inverse crime, we iterate the inverse problem 6 times.

We ran the inverse problem for a range of regularization parameters including $\alpha = 10^k$ where $k = \{-8, -7, \ldots, 7, 8\}$. Figure 8.3 includes the L-curve for the regularization parameters where the horizontal axis is the natural log of the 2-norm of the difference between the output of the forward model and the true volume, $V_{meas}$. The vertical axis is the natural log of the 2-norm of the resistance vector, $\vec{R}$. From the L-curve, in figure 8.3, we can see the corner appears at $\alpha = 0.1$. We then zoom in around the corner to get a closer look at what is happening and tested regularization parameters $\alpha = \{0.005, 0.01, 0.02, 0.03, \ldots, 0.08, 0.09, 0.1, 1, 10\}$ which gave us the L-curve seen in figure 8.4. The inverse crime results of $\alpha = 0.1$ gave us a 2-norm relative error of 5.46%, while the regularization parameter of $\alpha = 0.01$ gave us a 2-norm relative error of 0.4%. We chose a regularization parameter of $\alpha = 0.01$ as it is the best value based on the inverse crime. We note that the L-curve is not always a reliable way to find the regularization parameter. The inverse crime volume results with $\alpha = 0.01$, as well as resistance vectors from the inverse crime, can be found in figure 8.5.

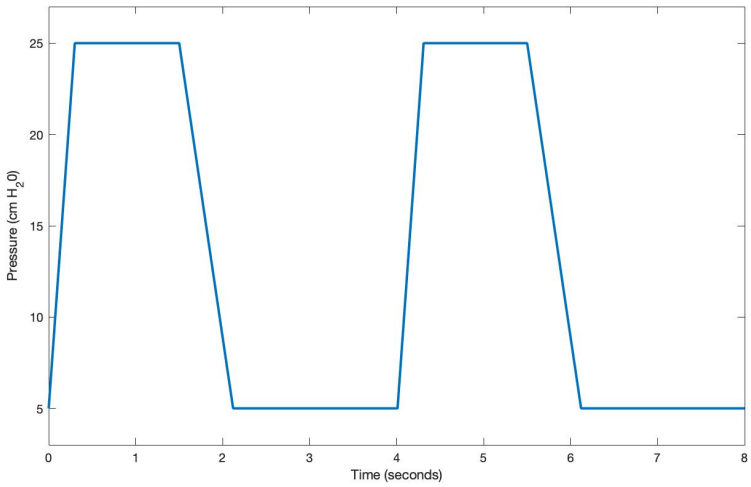


**Figure 8.1:** A synthetic pressure curve created for the inverse crime with an inhale time of 1.5 seconds, an exhale time of 2.5 seconds, a minimum pressure of 5 cm $H_20$, and a maximum pressure of 25 cm $H_20$.

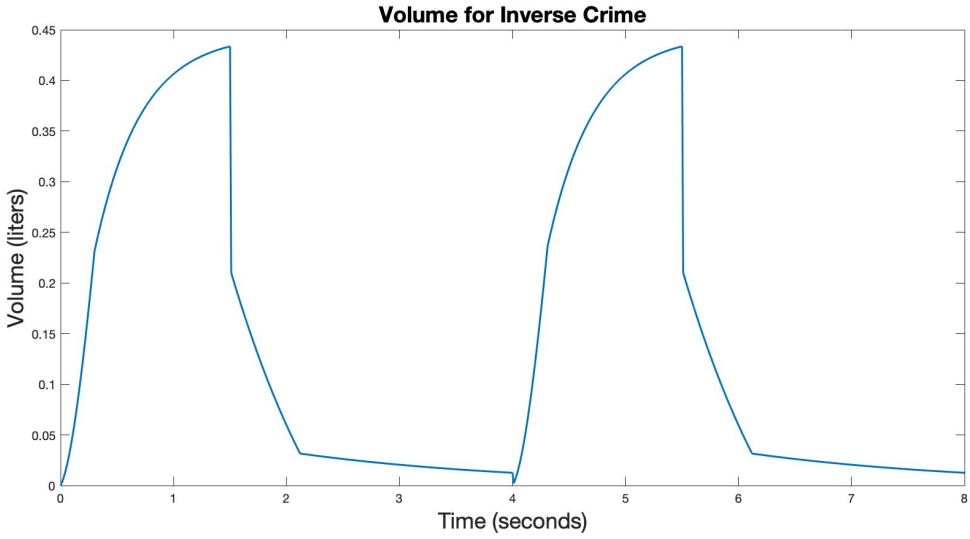


**Figure 8.2:** A synthetic total volume curve created for the inverse crime from the forward model. Parameters include a resistance vector of $[8.5, 10, 7.5, 2, .75]$, inhale and exhale times of 1.5 seconds and 2.5 seconds respectively, a total compliance value of $0.0356$ L/cm $H_20$, minimum pressure of 5 cm $H_20$ and maximum pressure of 25 cm $H_20$.

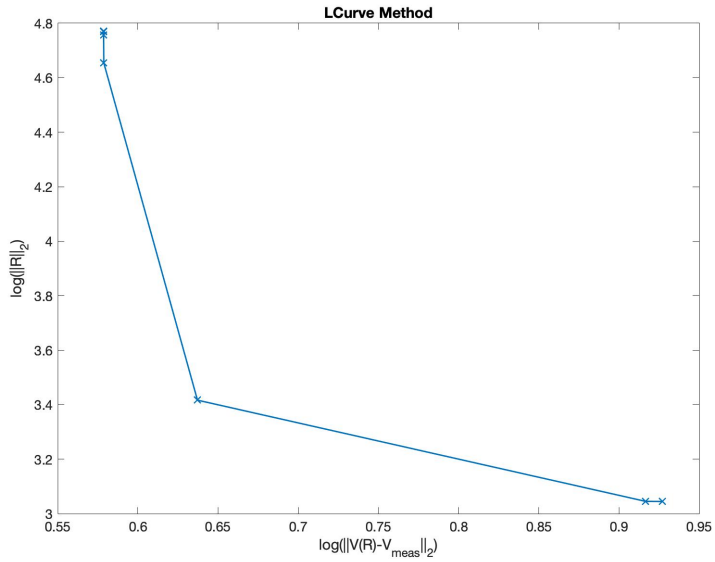


**Figure 8.3:** A graph of the L-curve with regularization parameters of $\alpha = 10^k$ where exponent $k = \{-8, -7, \ldots, 7, 8\}$. The horizontal axis is the natural log of the 2-norm of the difference between the output of the forward model and the true volume, $V_{meas}$. The vertical axis is the natural log of the 2-norm of the resistance vector, $\vec{R}$. Here the corner appears at $\alpha = 0.1$. We also notice the small overall scale of both the axis.

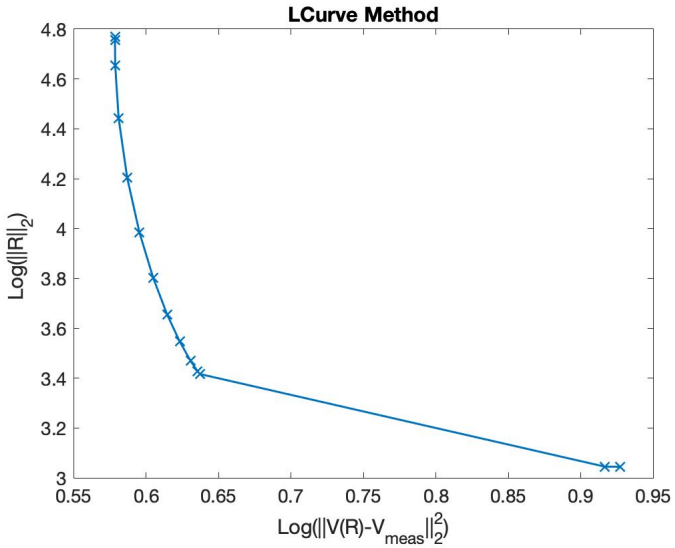


**Figure 8.4:** A graph of the L-curve. The horizontal axis is the natural log of the 2-norm of the difference between the output of the forward model and the true volume, $V_{meas}$. The vertical axis is the natural log of the 2-norm of the resistance vector, $\vec{R}$. We also notice the small overall scale of both the axises. The regularization parameters are $\alpha = \{0.005, 0.01, 0.02, 0.03, \ldots, 0.08, 0.09, 0.1, 1, 10\}$. Here the corner appears at $\alpha = 0.1$.

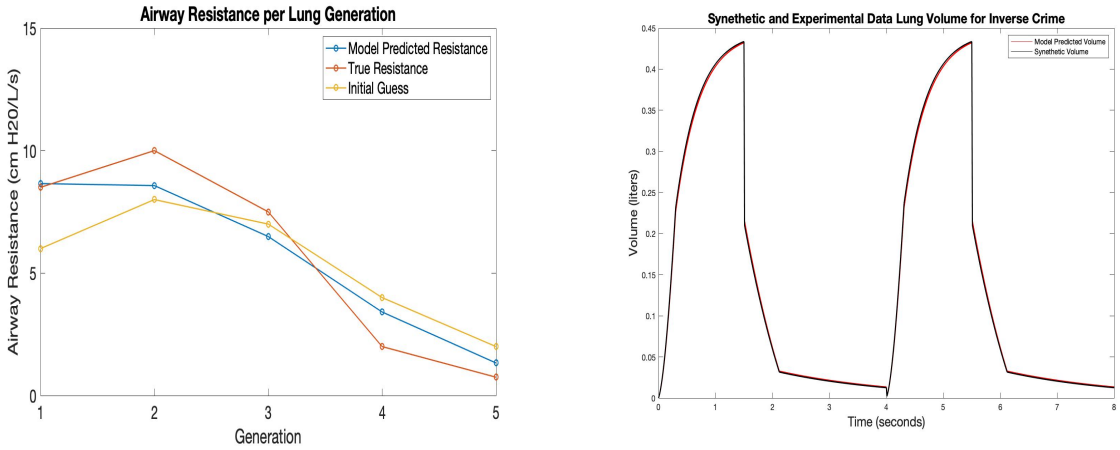


**Figure 8.5:** Left: Resistance vector results for inverse crime including: the initial guess of the resistance vector (yellow) used in the optimization problem, the true resistance vector (red) used to create the volume curve, and the model predicted resistance vector (blue). In this image, we work with a $2^4$ compartment model. Right: A time (seconds) versus volume (liters) plot. True synthetic volume results are in black and the model predicted volume results are are in red. The 2-norm relative error between the volume results is $0.79\%$.

# Chapter 9

# Medical Imaging and Airway Resistance

Acute Respiratory Distress Syndrome (ARDS) is a lung injury that allows fluid to leak into the lungs and may induce trouble breathing or necessitate the use of mechanical ventilators. ARDS is a clinical condition "characterized by a consistent recognizable pattern of lung injury" [57]. It usually develops after a lung injury has already occurred and can lead to complications like pneumonia, pulmonary embolism, and acute renal failure [14]. ARDS, "remains a significant contributing factor to morbidity in the traumatically injured patient" [14]. The severity of ARDS has prompted many studies on the prevention of the disease. These studies consider the genetics of patients and examine mechanical ventilator parameters [14, 57].

We conduct a study to learn more about ARDS patients' lung parameters. We reconstruct the airway resistance in the bronchial tree of 5 ARDS patients undergoing mechanical ventilation while laying supine. We estimate the airway resistance throughout the lungs by solving the inverse problem for an asymmetric lung model, as presented in chapter 7 using regional lung information obtained by way of lung imaging. This study uses electrical impedance tomography (EIT), mechanical ventilator data, and the asymmetric resistor-capacitance circuit based (RCCB) multi-compartment lung model to estimate the airway resistance of a 5-generation lung model for 5 patients. Since we collected EIT data, we can estimate regional ventilation in the upper and lower lung. We use the regional lung information to define the asymmetric parameters in the RCCB lung model. We update the parameters to include asymmetries based on generation and airway.

In this chapter, we apply the asymmetric model with regional information, introduced in chapter 7 to real world patients. We describe the data collection process, the results of the real world data applied to the asymmetric RCCB lung model, the conclusions, and any planned or suggested future changes to this model and study.

## 9.1 Data Collection

We collect lung information of mechanically ventilated patients using the GE GENESIS EIT system [52] and mechanical ventilator screenshots. Data from the EIT machine were reconstructed using algorithms from [53,54]. After producing and testing a model that describes lung volume at a given time, we apply the model to real world data. The goal of this study is to apply the asymmetric RCCB lung model to estimate patients' airway resistance values throughout each branch in the bronchial tree.

Due to safety regulations during the COVID-19 pandemic, the doctors and medical professionals in charge of the care for patients at UCHealth-Anschutz Medical Campus collected both the mechanical ventilator screenshots and the EIT data. We use data collected from January 2022 to March 2022. Members of Dr. Jennifer Mueller's lab at Colorado State University (CSU) trained the UCHealth-Anschutz Medical Campus team on how to properly prep and collect EIT data from patients. Members of the data collection team from UCHealth-Anschutz Medical Campus included Patrick (Pj) Offner, a Professional Research Assistant, and Dr. Ellen L. Burnham, a Professor of Medicine and Director of the Medical Intensive Care Unit at the UCHealth-Anschutz Medical Campus.

The GE GENESIS EIT machine collects voltage data at 18 frames/second during ventilation [52]. After reconstructing the data, we can recognize when a patient is inhaling and exhaling as well as regional ventilation information. More on this can be found in [55]. Ventilation data provides us with information that includes possible lung asymmetries or diseased areas the patient may have. This information can then be added to the RCCB lung model to help us determine the airway resistance. Ventilator lung volume information can be used to validate total lung volume from EIT data.

Four of the five patients in this study used the Hamilton G5 series ventilator, as in chapter 6, whereas one patient used the Covidien Puritan Bennett 980 series ventilator. The Puritan Bennett can show and collect the same information as the Hamilton ventilator. Examples of the screenshots of the Puritan Bennett ventilator are provided in figure 1.2. As with Study 1, compliance, minimum

and maximum pressure, and total lung volume were collected for each patient from ventilator screenshots. However, Study 2 collected ventilator pressure curve data as well.

For all five mechanically ventilated patients, we collected 3D EIT data while the patient was supine. All patients in this study were COVID-19 negative with ARDS. Data collected for each patient included age, gender, race, ethnicity, height, weight, diagnosis or reasoning behind ventilation, mechanical ventilator screenshots, and EIT data. The study was conducted in accordance with the amended Declaration of Helsinki. Data were collected at Anschutz Hospital in Aurora, Colorado under the approval of the institutional review board (COMIRB approval number 21-3315). We received only deidentified data.

The mechanical ventilator screenshots collected the same parameters from the study found in chapter 6 including the ventilator volume curve for up to four breaths, the total pressure curve for up to four breaths, total resistance, the minimum and maximum pressure, and total compliance. We convert and use parameters similarly to what is done in chapter 6. As in the previous study, we use the total resistance as a constraint in the optimization problem (equation 7.1). Also as in Study 1, we take the total compliance value and divide it by $2^n$ where $n$ is the number of generations.

We create time dependent pressure curves synthetically. Like the previous study, we know the minimum and maximum pressure and general shape of the pressure curve. However, there are still some unknowns which we avoid by synthetically generating pressure for the initial pressure and updating this value over time. The data provided for each patient in this study contained a total pressure curve and the reported minimum and maximum pressure at one time snapshot from the ventilator. We used the ventilator pressure curve to determine the average times during inhalation and exhalation when the pressure increased and decreased, respectively. We then used the minimum pressure, maximum pressure, and average times to create the synthetic pressure curve.

The way we define and find synthetic pressure is the same as what was done in Study 1; however, we found the average time for one breath for each patient instead of applying one average value to all patients. Unlike in the previous study, for this study, we defined a total compliance

both during inhalation and exhalation. The total compliance per both inhalation or exhalation is used as the initial compliance in Algorithm 1. The inhalation and exhalation compliance matrix will update as we run through Algorithm 1.

The use of synthetically generated pressure curves provides us with several benefits over measured pressure curves. If we did use ventilator measured pressure, it would require the assumption that each breath is identical. We would make this assumption because the EIT volume data had an average of 6 breaths per patient whereas the ventilator screenshots pressure and volume data had an average of two breaths per patient. Concatenating multiple repeating ventilator pressure curves still presents the challenge of synchronizing the time and element size to the EIT volume data. As we showed in chapter 6, synthetic pressure yields acceptable results. Once we had a pressure curve, we broke it up into a pressure matrix, as described in chapter 6. The pressure matrix is created by dividing the total pressure value at each time by $2^n$ and putting that value in a diagonal $2^n \times 2^n$ matrix. These diagonal pressure matrices, based on ventilator pressure values, were the initial generated pressure matrices and were redefined as iterations increased as seen in Algorithm 1.

From section 6.3 and screenshots of ventilators in figures 1.1 and 1.2, one sees that ventilator volume curves have a minimum value of zero. We note that the lung volume for mechanically ventilated patients is not actually zero liters since the lung is not physically completely empty. A mechanical ventilator defines the volume at the end of an exhale as zero, but EIT lung volume data consider the total lung volume at any given time, so volume is never zero. Since we are modeling lungs on a mechanical ventilator, it is important the volume data reflects this. To account for this leftover non-zero volume in EIT data, we shift EIT volume data by defining its minimum volume as zero. For example, if an EIT volume curve ranges from 0.2 – 0.7 L, to account for the patient being on a mechanical ventilator starting at volume 0 L, we shift the EIT volume curve to 0 – 0.5 L.

We collected EIT data to have a more complete understanding of the lungs. We used ventilator screenshots to verify the total lung volume computed from the EIT images. We computationally

estimated the lung volume from EIT data and used the regional distributions of air in the lung to update the RCCB lung model. Once we obtained all volume data, we applied the RCCB model to approximate the airway resistance values of the patients on mechanical ventilators. All data collected was used in the inverse problem (equation (7.1)) with Algorithm 1 to predict the airway resistance in the lung.

Structural similarity Index (SSIM) is a way to measure the similarities between two images by comparing three feature of the image: luminance, contrast, and structure [58]. We can use this same idea to compare the overall structure of the EIT volume curve and model predicted volume curve, focusing only on structure since they are line plots. In SSIM, structure is defined as:

$$s(x, y) = \frac{\sigma_{xy} + k}{\sigma_x \sigma_y + k} \tag{9.1}$$

where $x$ and $y$ are images, $\sigma_x$ and $\sigma_y$ are standard deviations of images $x$ and $y$, $\sigma_{xy}$ is the cross covariance of images $x$ and $y$, and $k$ is a constant defined as $4.5 \times 10^{-4}$, based on work from [44,58]. By construction, the closer to the number one the output of equation (9.1) is, the closer the curves are.

## 9.2 Results

In this section, we share the results from the data of five ARDS patients, including a summary of the results via five tables and two figures of the airway resistance results. The tables include patient background, parameter information, and a five-generation resistance vector computed from the inverse problem. We also include the 2-norm relative error (equation (6.3)) and the structure SSIM error measure (equation (9.1)) between the volume from computed EIT, treated as ground truth, and the volume output from the forward model with the reconstructed airway resistance values. The average EIT volume vector size for the 5 patients was 353 $\pm$ 186 elements with an average of 55 $\pm$ 15 elements per breath. The average 2-norm relative error between the total lung volume estimated from the EIT images and the RCCB lung model predicted volume for the five

patients was $37.55 \pm 12.06\%$. The minimum 2-norm relative error was $27.93\%$ while the maximum 2-norm relative error was $58.06\%$. The average structure SSIM error between the total lung volume estimated from the EIT images and the RCCB lung model predicted volume for the five patients was $0.8243 \pm 0.1170$. The closest structure SSIM error was $0.9313$ while the furthest structure SSIM error was $0.6275$.

The de-identified patient ID, for bookkeeping only, is stated as EIT_Number. For example, EIT_112 represents Patient 112 from the EIT study. For this study, we chose a five generation system based on runtime or the asymmetric model. The asymmetric version of the RCCB lung model has asymmetric matrices with non-zero elements of size $2^n \times 2^n$ at each time with an average of 353 $\pm$ 186 time points per patient. If $n = 9$, like in Study 1, every parameter will be a positive $2^9 \times 2^9$ asymmetric matrix at every time point. The run time then increases from seconds, for the symmetric model version, to hours to a day for the asymmetric model version. For every patient in this study, time zero starts at the start of an inhale.

Table 9.1 includes a summary of the patients' background including age, sex, height, weight, and primary diagnosis or reason for being ventilated. Table 9.2 includes parameters used as initial guesses in the model like minimum pressure, maximum pressure, and inhalation and exhalation compliance from the ventilator. Table 9.3 includes the ventilator total resistance, the model predicted resistance vector, and the sum of the resistance vector. Table 9.4 reports the relative errors between the EIT lung volume and the lung volume calculated from the forward problem using the computer resistance vector. Table 9.5 includes the 2-norm relative error of resistance vector results between iterations of Algorithm 1 for all five patients.

Figures 9.1 and 9.2 include the results of Algorithm 1 for all five patients. The plots on the left display the reconstructed five generation resistance curve for each patient. The horizontal axis represents generation $n$ in the lung from the $0^{\text{th}}$ to the $4^{\text{th}}$ generation. The vertical axis represents the airway resistance in cm $H_20$/L/s. The images on the right include the EIT lung volume curve in black and the forward problem volume results in red. These plots show time in seconds versus volume in liters.

**Table 9.1:** Summary of patient information including age (years), patient sex, and primary diagnosis for being on a ventilator.

| Patient ID | Age | Sex | Height (cm) | Weight (Kg) | Primary Diagnosis |
|---|---|---|---|---|---|
| EIT_111 | 47 | Male | 182.9 | 67.6 | Upper GI bleed |
| EIT_112 | 73 | Male | 182.9 | 71.7 | Pulmonary Edema |
| EIT_116 | 52 | Male | 177.8 | 70.6 | ARDS and rhinovirus |
| EIT_120 | 68 | Male | 160 | 65.2 | Alveolar Hemorrhage |
| EIT_122 | 62 | Male | 180.3 | 68.9 | Sepsis |

**Table 9.2:** Table of patient input parameters for the RCCB lung model taken from the ventilator. All values represent the total lung.

| Patient ID | Min/Max Pressure (cm $H_20$) | Ventilator Inhale Compliance (L/cm $H_20$) | Ventilator Exhale Compliance (L/cm $H_20$) |
|---|---|---|---|
| EIT_111 | 5/17 | 0.07 | 0.11 |
| EIT_112 | 5/16 | 0.035625 | 0.04417 |
| EIT_116 | 8/19 | 0.0552 | 0.06846 |
| EIT_120 | 5/14 | 0.19 | 0.335 |
| EIT_122 | 5.2/14 | 0.0405 | 0.06 |

**Table 9.3:** Table of inverse problem outputs including resistance vector. The second column is the total resistance value (cm $H_20$/L/s) reported from ventilator screenshots. The third column is the resistance vector output from Algorithm 1. The total computed resistance value (cm $H_20$/L/s), in the fourth column, is the sum of the elements in the resistance vector from column 3, found using equation (5.6).

| Patient ID | Ventilator Resistance | Resistance Vector (cm $H_20$/L/s) | Computed Total Resistance |
|---|---|---|---|
| EIT_111 | 10 | $[5.78; 6.34; 4.22; 0.31; 0.001]$ | 10.045 |
| EIT_112 | 16 | $[8.88; 9.5; 6.13; 1.75; 0.3758]$ | 15.4 |
| EIT_116 | 10 | $[5.79; 6.35; 4.22; 0.2872; 0.001]$ | 10.06 |
| EIT_120 | 2 | $[0.69; 1.1; 1.097; 0.34; 0.0716]$ | 1.5651 |
| EIT_122 | 11 | $[6.03; 7.07; 5.39; 1.88; 0.214]$ | 11.1578 |

**Table 9.4:** Table of inverse problem relative errors. The relative error in the second column is the 2-norm relative error between the lung volume curve from EIT reconstructions and the RCCB lung volume output using the resistance vector from table 9.3. The third column is the structure SSIM error, with a value of closer to one meaning more similar structure.

| Patient ID | 2-norm Error (%) | Structure SSIM Error |
|---|---|---|
| EIT_111 | 38.29% | 0.8197 |
| EIT_112 | 32.17% | 0.8797 |
| EIT_116 | 27.93% | 0.9313 |
| EIT_120 | 58.06% | 0.6275 |
| EIT_122 | 31.3% | 0.8633 |

**Table 9.5:** Table of 2-norm relative error of resistance vector results between iterations of Algorithm 1 for all patients.

| | 2-norm relative error (%) | | | | |
|---|---|---|---|---|---|
| Patient ID | EIT_111 | EIT_112 | EIT_116 | EIT_120 | EIT_122 |
| Iteration 1 to 2 | 38.42% | 19.15% | 2.87% | 23.02% | 5.0109E−6% |
| Iteration 2 to 3 | $6.4115e^{-4}$% | 1.1911E−4% | 2.87% | 13.61% | 1.5711E−6% |
| Iteration 3 to 4 | 5.8801E−4% | 2.0410E−5% | 0.66% | 3.4% | 8.8284E−7% |
| Iteration 4 to 5 | 5.7435E−4% | 2.6716E−6% | 0.59% | 3.37% | 2.2823E−7% |
| Iteration 5 to 6 | 5.6130E−4% | 9.6670E−7% | 0.53% | 0.0% | 6.0198E−8% |

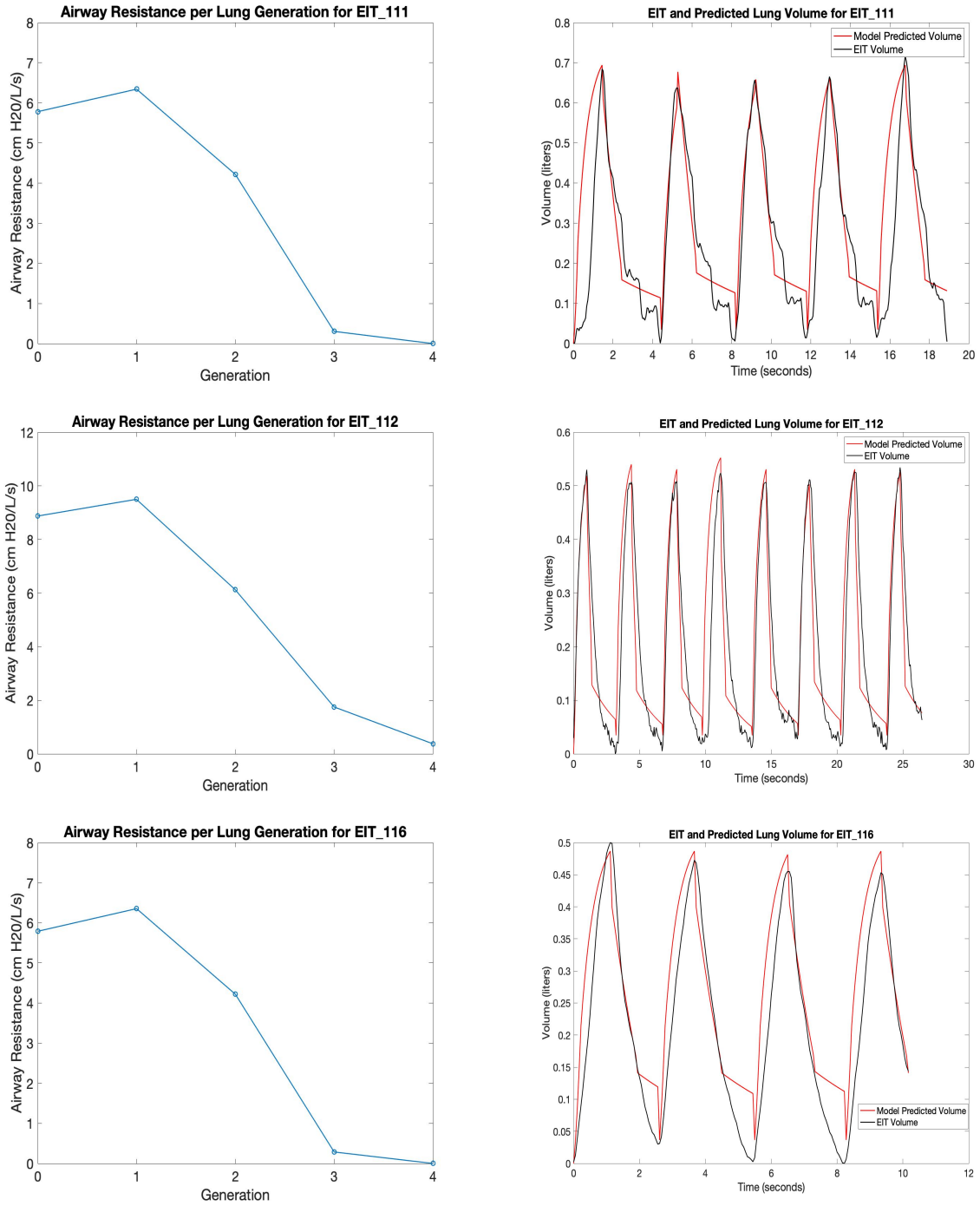


**Figure 9.1:** Top row: plots for EIT_111 with a ventilator total resistance value of 10 cm $H_20$/L/s and a total resistance value from the reconstructed airway vector of 10.0446 cm $H_20$/L/s. Second row: plots for EIT_112 with a ventilator total resistance value of 16 cm $H_20$/L/s and a total resistance value from the reconstructed airway vector of 15.3999 cm $H_20$/L/s. Third row: plots for EIT_116 with a ventilator total resistance value of 10 cm $H_20$/L/s and a total resistance value from the reconstructed airway vector of 10.0589 cm $H_20$/L/s.

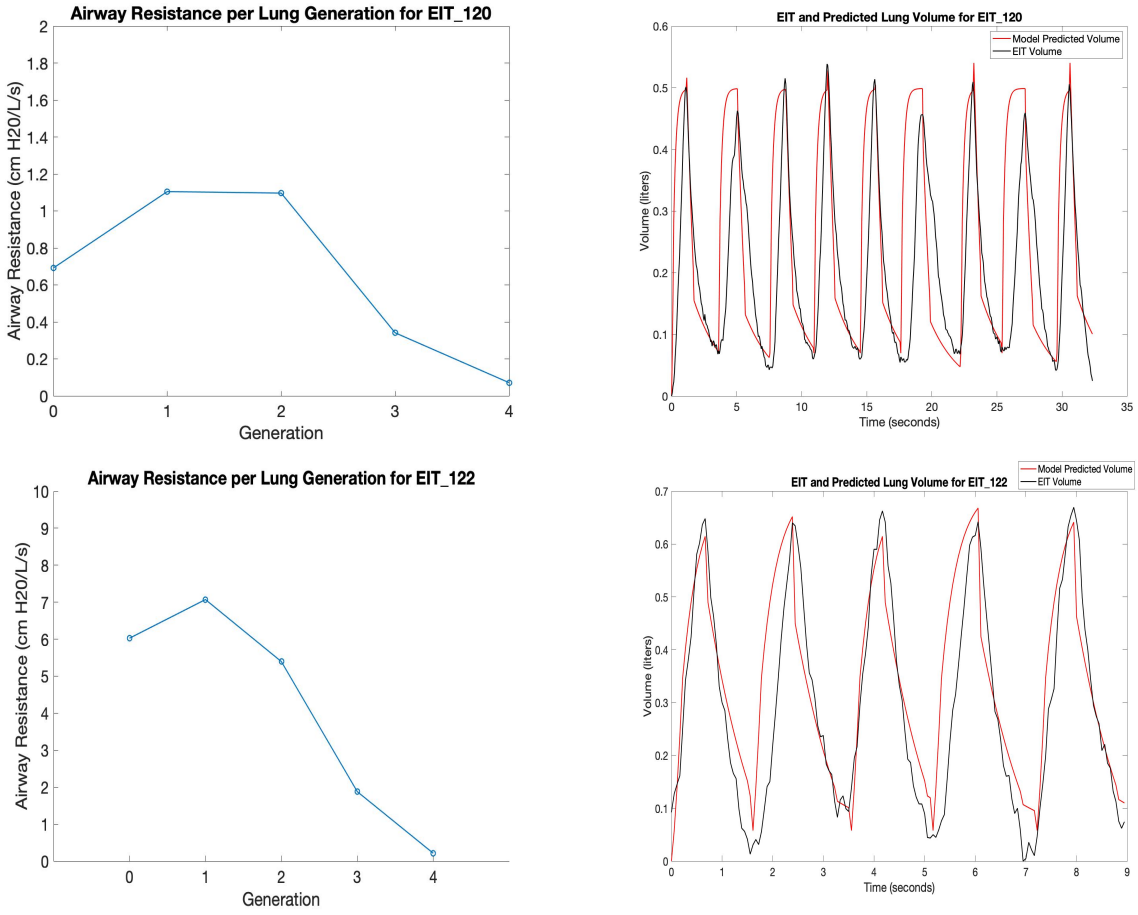


**Figure 9.2:** Top row: plots for EIT_120 with a ventilator total resistance value of 2 cm $H_20$/L/s and a total resistance value from the reconstructed airway vector of 1.5651 cm $H_20$/L/s. Second row: plots for EIT_122 with a ventilator total resistance value of 11 cm $H_20$/L/s and a total resistance value from the reconstructed airway vector of 11.1578 cm $H_20$/L/s.

## 9.3 Discussion

Results for this study are seen in figure 9.1 and 9.2. These figures demonstrate the consistency of the asymmetric model and optimization problem when predicting airway resistance. For this study, the average ventilator reported total resistance value was $9.8 \pm 5.02$ cm $H_20$/L/s whereas the average model predicted total resistance value was $9.65 \pm 5.03$ cm $H_20$/L/s. On average, the first element of the resistance vector, which represents the resistance in the trachea, was $52.11 \pm 9.90\%$ of the total resistance value. The second element of the resistance vector, $R_1$, was $61.17 \pm 3.83\%$ of the total reported resistance value. Element 3, or $R_2$ of the five element resistance vector averages

$45.31 \pm 6.58\%$ of the total resistance value. Element 4, $R_3$, had on average $10.20 \pm 7.06\%$ of the total ventilator resistance value. Finally, the last element of the resistance vector, $R_4$, had an average of $1.58 \pm 1.55\%$ of the total resistance value. These percent values add up to over 100% as resistance was defined in series. A summary of the results and outputs of the model is found in table 9.6. A summary of all resistance vectors is seen in figure 9.3.

**Table 9.6:** An average of initial parameters and output results of the five male COVID-19 negative ARDS patients from this study.

| Parameter | Average |
|---|---|
| Inhalation Compliance | $0.078265 \pm 0.06389$ L/cm $H_20$ |
| Exhalation Compliance | $0.123526 \pm 0.120695$ L/cm $H_20$ |
| Maximum Pressure | $16 \pm 2.1232$ cm $H_20$ |
| Minimum Pressure | $5.64 \pm 1.3321$ cm $H_20$ |
| Ventilator Reported Resistance | $9.8 \pm 5.02$ cm $H_20$/L/s |
| $R_0$ | $5.433 \pm 2.955$ cm $H_20$/L/s |
| $R_1$ | $6.0745 \pm 3.0652$ cm $H_20$/L/s |
| $R_2$ | $4.211 \pm 1.9213$ cm $H_20$/L/s |
| $R_3$ | $0.9124 \pm 0.82478$ cm $H_20$/L/s |
| $R_4$ | $0.1326 \pm 0.1613$ cm $H_20$/L/s |
| 2-norm Relative Error | $37.55 \pm 12.06\%$ |
| structure SSIM Error | $0.8243 \pm 0.1170$ |

In contrast to Study 1, this study utilizes a model that considers asymmetries in the lung. However, the summary of results, seen in section 9.2, are presented by generation and do not yet reflect these asymmetries. Figure 9.5 includes the resistance values per each airway during inhalation. Comparing figure 9.5 and EIT_112 resistance vector results from table 9.3, we see the results for each airway add up to the generational values. As mentioned in section 7.3, based on the

EIT reconstruction, patient EIT_112 has no airflow in the right lung. All five patients' computer resistance value results are found in figures 9.4 - 9.8.


**Figure 9.3:** Resistance vector outputs from Algorithm 1 for all five male COVID-19 negative ARDS patients in this study.

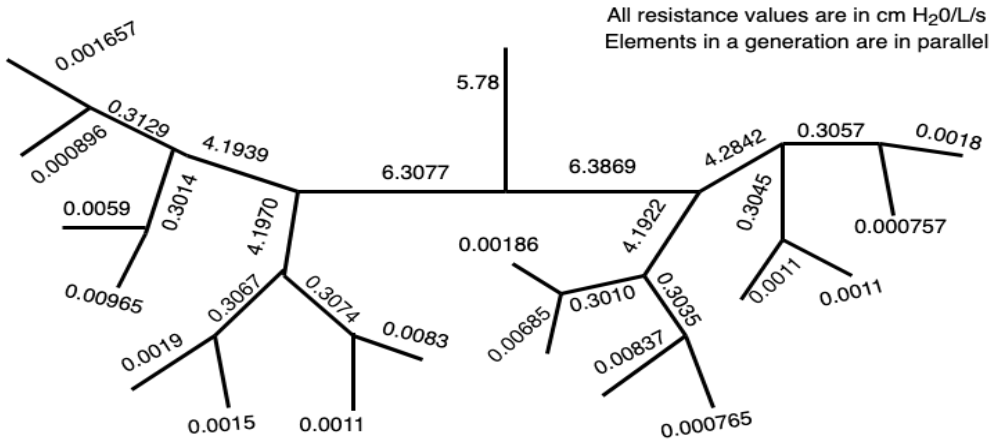


**Figure 9.4:** Resistance values for each airway for EIT_111. Although the branch volumes in a generation were similar, we still see the asymmetries that we did not account for in the first study come through.

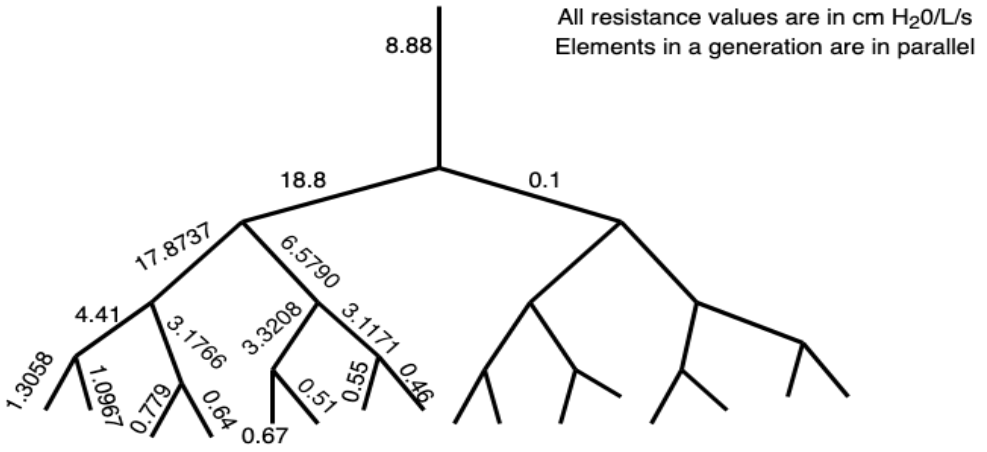


**Figure 9.5:** Resistance values for each airway for EIT_112. Notice the asymmetries that we did not account for in the first study. For EIT_112, the volume of the right lower lung is zero and not receiving any flow or gas. When the flow is zero this means resistance is infinite, by definition. We can relate this to an insulator in circuits as the perfect insulator has infinite resistance.

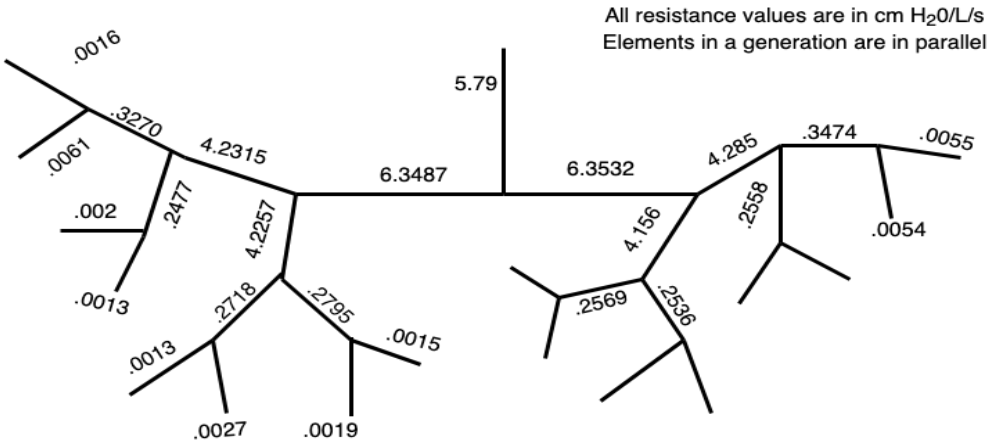


**Figure 9.6:** Resistance values for each airway for EIT_116. Notice the asymmetries that we did not account for in the first study. For EIT_116, the volume of the right lower lung was less compared to the other quadrants and we accounted for this by defining a few branches to have zero airflow.

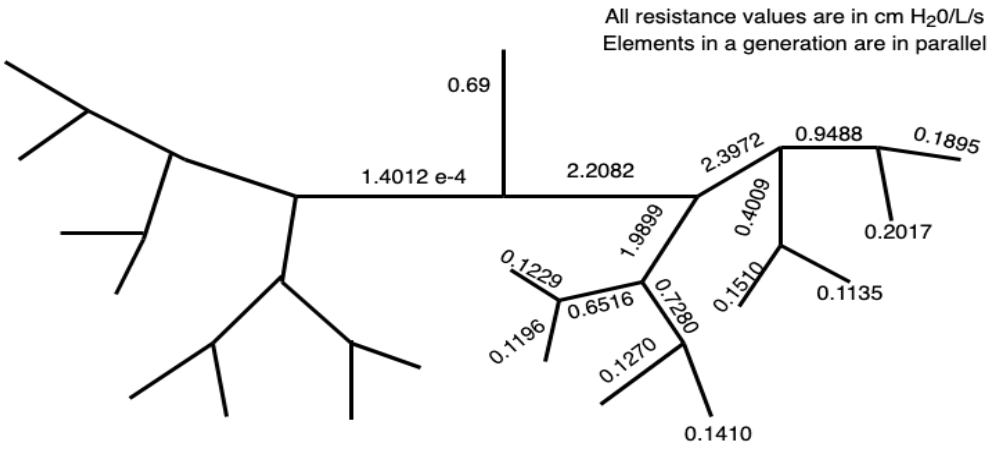


**Figure 9.7:** Resistance values for each airway for EIT_120. Notice the asymmetries that we did not account for in the first study. For EIT_120, the volume of the left lung is zero and not receiving any flow or gas. When the flow is zero this means resistance is infinite. We can relate this to an insulator in circuits as the perfect insulator has infinite resistance.

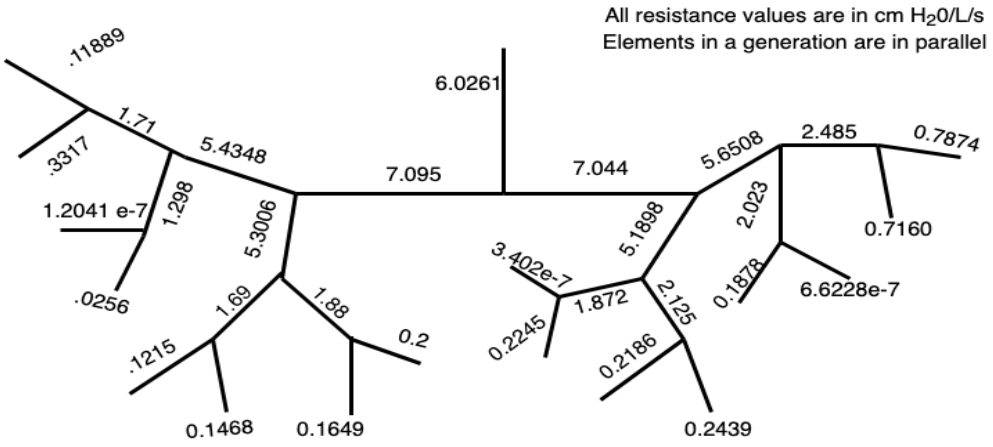


**Figure 9.8:** Resistance values for each airway for EIT_122. Although the branch volumes in a generation were similar, we still see the asymmetries that we did not account for in the first study come through.

In this study, we tested the modified asymmetric RCCB lung model to account for regional lung information. Thus one would expect the results in this study to be more accurate than the results seen in section 6.3. There were 5 male COVID-19 negative participants in Study 2 and 11 in Study 1. For the first study, the 11 patients had an average minimum pressure value of $6.18 \pm 2.09$ cm

$H_20$ while the 5 males in Study 2 had an average of $5.64 \pm 1.33$ cm $H_20$ minimum pressure from the ventilators. The maximum average pressure value from the ventilator for the 11 patients in Study 1 was $19.91 \pm 8.56$ cm $H_20$ while the average in Study 2 was $16 \pm 2.12$ cm $H_20$. The average ventilator reported total resistance for Study 1 male COVID-19 negative patients was $14 \pm 4.427$ cm $H_20$/L/s and from table 9.6, we see the average reported total resistance value from Study 2 was $9.8 \pm 5.02$ cm $H_20$/L/s. In the first study, the average 2-norm lung volume relative error for the 11 patients was $36.96 \pm 12.73\%$ whereas Study 2 had an average relative error of $37.55 \pm 12.06\%$. We notice the average 2-norm relative error was lower in Study 1 with the original RCCB lung model compared to Study 2 with the asymmetric RCCB lung model. However, there was an outlier in Study 2, which we will discuss in section 9.3.1. If we remove the outlier, patient EIT_120, from the average relative error calculation for Study 2 patients, the relative error calculation is updated to $32.42 \pm 4.32\%$.

We calculate the SSIM error using equation 9.1 to the 11 patients from Study 1 and the five patients from Study 2. For Study 1, the average structure measure was $0.8370 \pm 0.1027$ whereas the average structure metric for Study 2 was $0.8243 \pm 0.1170$. However, once we removed the outlier EIT_120 who had a structure measure of $0.6275$, the lowest of all 16 patients we compare, the average structure difference for Study 2 was $0.8735 \pm 0.0461$. Based on this information, we can see the asymmetric RCCB lung model of 5-generations performs with better consistency than the 9-generation study results of the symmetric RCCB lung model used in the first study.

The goal of Study 2 is to better predict airway resistance in the lung and to create a more realistic model. With a better understanding of airway resistance, we can optimize ventilator settings for patients and hopefully better understand what is happening in the lungs without the need for ionizing imaging technologies. Although the asymmetric model introduced in chapter 7 shows promise of predicting airway resistance correctly, there are still some limitations.

We were able to collect patient height in this study, but we did not account for height in the model. We assume all patients' lung size and shape are similar regardless of patient height or weight. We also assume a more simplistic structure of the lungs. Although we have regional

information and asymmetry knowledge, we assume specific structure in addition to regional information. Like the study in chapter 6, this asymmetric model assumes a dichotomous structure. While a non-dichotomous structure is more realistic, it introduces more complexity to the model. In the future, applying this model to patients participating in pulmonary lung function tests while collecting EIT data may better predict which airways are blocked. Other limitations to this study include possible inaccuracies in the EIT-derived regional lung volumes, and errors in synthetic pressure curves and compliance values from the ventilator.

### 9.3.1 Outliers and Special Cases

Even though this study had only five subjects in it, two of the five had special cases arise when analyzing and running the data. The reported ventilator resistance value for patient EIT_120 was far smaller than those of other male COVID-19 negative patients in both studies. For patient EIT_116, there was a larger overall volume difference between the minimum and maximum volume compared to other male COVID-19 negative patients.

For EIT_120, the reported ventilator resistance value was $R_{vent} = 2$ cm $H_20$/L/s, whereas the other four patients in this study had total reported resistance values ranging from 10 – 16 cm $H_20$/L/s. In Study 1, the smallest overall reported resistance value was 4 cm $H_20$/L/s for all 32 patients, but the smallest reported resistance value for a male COVID-19 negative patient was 8 cm $H_20$/L/s. The overall range of total resistance values for the 11 male negative patients in Study 1 was 8 – 21 cm $H_20$/L/s. Also, as discussed in chapter 5, the patient from Study 1 with $R_{vent} = 4$ had special definitions for $\vec{R}_{min}$ and $\vec{b}$, or the parameter that controlled concavity seen in equation (5.9). The same was true for EIT_120. We know this was an outlier because $R_{vent} = 4$ was considerably low for Study 1, and an outlier itself, so any value less than 4 would also be an outlier.

In the special case of EIT_120, we defined the upper and lower bounds of $R_{vent} = 2$ to be $\vec{R}_{max} = [2; 2; 2; 1; 1]$ and $\vec{R}_{min} = 1\text{e}^{-6} * [1; 1; 1; 1; 1]$, respectively. We also defined the vector $\vec{b}$, that controls concavity as $[-0.5; -0.7; 1; 0.7; 0.5]$. The results for EIT_120 are seen in figure 9.2.

We see the overall shape of the resistance vector does not match our expectations; instead of a peak near the first few generations, there is a plateau. This shape most likely results from our definition of $\vec{b}$, which necessarily differs from the other four patients. Hence, we consider EIT_120 to be an outlier.

For patient EIT_116, the volume results differ from those of previous patients. EIT_116 had a minimum lung volume of 0 liters and a maximum lung volume of 1 liters, causing the total lung volume difference to be 1 L or 1000 mL. Other patients in this study had a volume difference of $0.5$ or $0.6$ liters. In the first study, the 11 male COVID-19 negative patients had a volume difference of 0.4 – 0.6 liters.

Figure 9.9 shows the true volume from EIT data of EIT_116. Figure 9.1 shows the volume of EIT_116 scaled by $\frac{1}{2}$ to reflect a volume difference close to 0.5 L. This scaling is based on the expectation of a maximum lung volume difference of 0.5L since the patient is being ventilated. We conjecture that EIT_116's volume difference was so large due to a varying input parameter. Like the other four patients in this study, we used the compliance, pressure, and total resistance values found on the ventilator screenshots as inputs to the model for EIT_116. We surmise at least one of these initial parameters changed between when ventilator screenshots were taken and when EIT data were collected.

To test this, consider patient EIT_116 with the original EIT maximum volume of 1L and all other parameters including $\vec{b}$ and compliance values the same. If we update the minimum and maximum pressure values to 20 and 40 cm $H_20$, the model yields the results in figure 9.10. We know from table 9.1 all patients except EIT_116 in this study had a minimum pressure value of 5 or 5.2 cm $H_20$ and a maximum pressure value between 14 – 17 cm $H_20$. In the first study, the male COVID-19 negative patients had a minimum pressure value between 4 – 11 cm $H_20$ and a maximum pressure value between 12 – 41 cm $H_20$. All 32 patients in Study 1 had a range of 4 – 24 cm $H_20$ for minimum pressure and a range of 12 – 41 cm $H_20$ for maximum pressure. So, a minimum total pressure of 20 cm $H_20$ and a maximum total pressure of 40 cm $H_20$, although not common, is possible. To compute the plot in figure 9.10, we essentially doubled the pressure

values. Although the results of patient EIT_116 are still within the margin of error when not scaled, we choose to scale appropriately to match with the information given and what we know of lung volume for patients on ventilators.

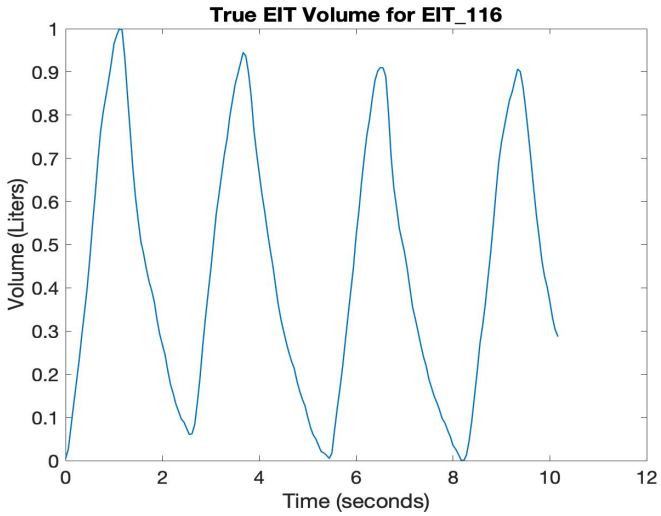


**Figure 9.9:** True volume for patient EIT_116. The plot is in time (seconds) versus volume (liters). The overall volume difference is 1 L from start of inhale to end of inhale.

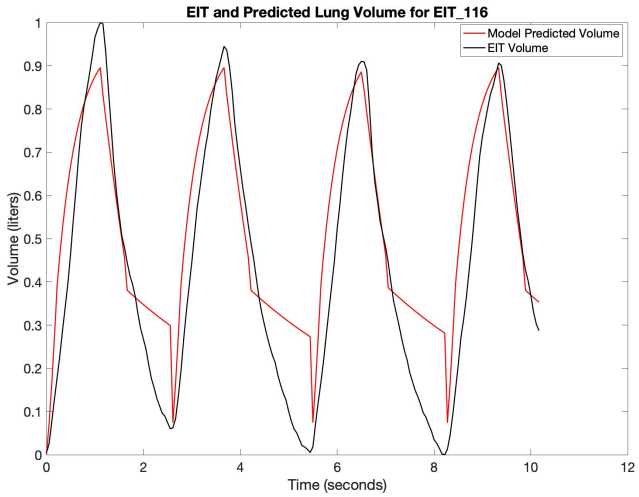


**Figure 9.10:** EIT_116 volume results for original EIT volume but doubled pressure value.

In chapter 7, we presented a multi-compartment lung model that accounts for asymmetries. We tested this model on five male ARDS patients who used mechanical ventilators to assist in breathing. This study collected lung parameters and regional lung information using EIT. We predicted patients' resistance values in each airway of the lung. Overall, this model yields acceptable results when predicting resistance vector shape and lung volume. Although the model used in this study and introduced in chapter 7 can describe real world lung behavior, we can consider other factors to increase its accuracy. We hope this model may be used to better optimize ventilator settings and better customize a patient's treatment. Determining the location and impact of a non-dichotomous structure would lead to a more realistic model but a harder problem to solve.

Work done in this thesis focuses on computing airway resistance throughout the bronchial tree given total parameter values with only certain regional parameter information. However, all results in this paper have only been validated using total volume information. No validations have been made using true airway resistance values in each branch of the bronchial tree. Before applying this model to help patients on ventilators, it is important to validate the results to true resistance values. Obtaining true airway resistance values per generation and branch is a challenge. To collect true resistance values in the lung, we may be able to use techniques like constructing artificial lungs or using time constants. Once obtained, we can compare computed resistance values from Algorithm 1 to true resistance values collected.

By constructing artificial lungs, like in [59], one could measure multiple parameters in the lung through various sensors placed in each artificial branch. In [59], Pertile focused on measuring pressure, but since the relationship of pressure and resistance, $R = \frac{\Delta P}{\dot{V}}$, is known, one can determine resistance at every sensor point or branch. This method is only as good as the hardware and the construction of the artificial lung.

Another validation technique to find true resistance values in the bronchial tree would be to use EIT and time constants. We know EIT is an imaging tool that can be used to collect regional lung parameters. Time constants, used heavily in electrical circuits, describe the time it takes for a capacitor to go from zero charge to a portion of full charge [36]. For RC circuits, the time constant

is the product of resistance and capacitance. Based on the analogy between electrical circuits and the human lungs, inspiratory time constants for the human lung represent the time it takes for the lung to change from its initial volume to its maximum volume. As a formula, we define $\tau = RC$ where $\tau$ is the time constant, $R$ is the airway resistance, and $C$ is compliance. Using EIT ventilation data, we can determine the time it takes for each branch to change from its initial volume to its maximum volume. We can then solve for the airway resistance matrix $R = \tau C^{-1}$ where $\tau$, $R$, and $C$ are $2^n \times 2^n$ matrices. By using EIT, we assume lung structure and branch location. Also note that compliance depends on time and the equation above does not reflect this so we would be taking an average compliance value. Expiratory time constants can be computer analogously.

These techniques can be used to collect airway resistance values, but each has its own advantages and disadvantages. We note that constructing artificial lungs and using time constants will not guarantee correct information about resistance in each branch. One of the reasons we focused on validating this model through volume data was because true volume data was available and able to be collected whereas we were unable to collect true resistance values for our ventilated patients.

# Chapter 10

# Future Steps and Conclusion

Studying the human lungs is vital for helping medical professionals treat patients with ARDS. Determining the mechanics of the lung will help optimize settings on mechanical ventilators and determining if airway resistance is dependent on gender or COVID-19 results can help patients in the future with COVID-19. Also, learning about the effects of the lungs while lying in various positions can be applied to future ARDS patients. There are many lung mechanic models out there but few focus on modeling respiratory mechanics throughout the entire bronchial tree for mechanically ventilated patients.

Utilizing the developed RC-circuit based multi-compartment lung model, we tested the model using synthetic data and applied an inverse crime to the model. We collected real world lung parameters from patients with ARDS on mechanical ventilators and used this newly developed model with its inverse problem to predict airway resistance. Overall, for a symmetric lung, the model yielded resistance vectors with an average relative 2-norm volume error of $38.79 \pm 9.72\%$. For an asymmetric lung, the average relative 2-norm volume error was $37.55 \pm 12.06\%$.

The study introduced in chapter 6 compares parameters of COVID-19 negative and positive patients. This study found pressure values were higher in COVID-19 positive patients while compliance values were lower for the same group of patients. In chapter 7, we updated the model to account for asymmetries and created an algorithm (Algorithm 1) that depends less on ventilator-provided parameters by defining them as initial guesses and updating them through iterations. In both studies, we found regularization parameters that worked for the inverse crime. In the future, applying an adaptive regularization parameter for each patient may lead to better estimations of airway resistance.

For the asymmetric model, we defined volume voxels to be associated with certain airways. In the future, applying the Horsfield Model knowledge to this lung structure definition process could lead to better defined airways [23]. Horsfield et al. measured lengths and diameters of every airway

in a lung cast. We can use the ratios between various airway lengths and diameters to better define the associated volume voxels from the Joshua Tree mesh. Another way to better define voxels to associated airways is by using CT scans. In some CT scans, we can see where a patient's trachea and bronchi divide. Measuring this length, given it is visible in a CT scan, may also help make a more accurate lung structure.

The model in this thesis can lead to better understanding of the lungs, especially ARDS patients or COVID-19 positive patients. Even though researchers and health organizations have studied COVID-19 and ARDS, there are still many unanswered questions. The overall goal of these studies is to learn more about mechanically ventilated ARDS patients by studying the airway resistance throughout the lungs. Although we introduced a new model, there are still improvements that can be made to the model.

Recognizing the parameters throughout the lungs may yield ventilator settings that better assist the patient. The RCCB lung model requires bifurcated branches which is idealized at the average lung is not perfectly bifurcated. Accounting for non-dichotomous structures would be more realistic to the average patient. Currently the asymmetric version of this model is solved within a few seconds for a 5-generation case, but updating the efficiency of Algorithm 1 could allow for a system that describes more generations. Updating Algorithm 1 to include a tolerance stopping criteria between the current and previous $\vec{R}$ would help improve it. Using values found in table 9.5 may help determine a good additional stopping criteria. In the future, computing resistance and compliance for every airway could allow us to find time constants, which determine the time to remove air from each airway in the lung to better comprehend how blocked an airway is. Knowing time constants could open the opportunity for medical professionals to make informed decisions without the patient undergoing a pulmonary function test.

We can learn more about diseased lungs by examining the RCCB model and the EIT images of ARDS patients. These EIT images can show regional lung information including air trapping or other potential problems in the lungs. For patients that may have air trapping, we could analyze the airway resistance and other lung parameters to determine their relationship. Applying this model

to a study comparing ventilated COVID-19 positive patients who move from supine to prone and back may answer the questions of ventilator protocols for these patients.

At the start of the COVID-19 pandemic, after medical professionals spent time treating patients, some doctors came to the conclusion that the treatment for patients should be based on the disease phenotype and not the usual protocol [10]. A protocol many medical professionals recommended involved transitioning the patient from supine to prone and back again every few hours. Although this study was not able to explore this protocol and how it affected the lung regionally, this would be a good future project.

We can learn more about the lungs and respiratory diseases by studying the lungs of a patient on mechanical ventilators. Creating the RCCB lung model with a symmetric and asymmetric lung version leads us to explore healthy and unhealthy lungs. Like with most mathematical models, there is still room for improvement, but this model gives more opportunity to learn about patients with ARDS.

# Bibliography


[1] John B. West and Andrew M. Luks. *Respiratory Physiology*. Wolters Kluwer, 10 edition, 2016.

[2] P.S. Crooke, S. Hota, J. J. Marini, and J. R. Hotchkiss. Mathematical Models of Passive, Pressure-Controlled Ventilation with Different Resistance Assumptions. *Mathematical and Computer Modeling*, 38:495–502, 2003.

[3] David A Kaminsky. What does airway resistance tell us about lung function? *Respiratory Care*, 57(1):85–99, 2012.

[4] V. C. Madama. Mechanics of ventilation, 1999. Last accessed 19 February 2019. https://ubccriticalcaremedicine.ca/rotating/material/Lecture_1forResidents.pdf.

[5] Scott Goodman. Physiology: Respiratory, 2019. Last accessed 19 February 2019. https://www.kumc.edu/AMA-MSS/Study/phys3.html.

[6] Michelle Mellenthin. Interview Conversation with Michelle, May 2019.

[7] Hamilton Medical, Inc., 4990 Energy Way P.O. Box 30008 Reno, NV 89520, USA. *Hamilton G5 Operator's manual 624074/07 Software version 2.2X*, 3 edition, 7 2012. An optional note.

[8] Covidie. Operator's manual for puritan bennett 980 series ventilator, 2018.

[9] Melina Hosseiny, Soheil Kooraki, Ali Gholamrezanezhad, Sravanthi Reddy, and Lee Myers. Radiology Perspective of Coronavirus Disease 2019 (covid-19): Lessons From Severe Acute Respiratory Syndrome and Middle East Respiratory Syndrome. *Cardiopulmonary Imaging*, 214:1–5, 2020.

[10] Sharon Worcester. Is protocol-driven covid-19 ventilation doing more harm than good? *Medscape*, 2020.

[11] L. Gattinoni, D. Chiumello, P. Caironi, M. Busana, F. Romitti, L. Brazzi, and L. Camporota. Covid-19 pneumonia: different respiratory treatment for different phenotypes? *Intensive Care Medicine*, 46(6):1099–1102, 2020.

[12] L. Gattinoni, S. Coppola, M. Cressoni, M. Busana S. Rossi, and D. Chiumello. Covid-19 does not lead to a typical acute respiratory distress syndrome. *Respiratory and Critical Care Medicine*, 201(10), 2020.

[13] Dan Karbing, Soren Kjaergaard, Steen Andreassen, and Stephan Rees. Mathematical modelling of pulmonary gas exchange. *Modeling Methodology for Physiology and Medicine: Second Edition*, pages 281–309, 12 2013.

[14] Magdalena Bakowitz, Brandon Bruns, and Maureen McCunn. Acute lung injury and the acute respiratory distress syndrome in the injured patient. *Scandinavian journal of trauma, resuscitation and emergency medicine*, 20:54, 08 2012.

[15] S Ganzert, K Möller, D Steinmann, S Schumann, and J Guttmann. Pressure-dependent stress relaxation in acute respiratory distress syndrome and healthy lungs: an investigation based on a viscoelastic model. *Crit Care*, 13(6):R199, 2009.

[16] L. Gattinoni, D. Chiumello, and S. Rossi. Covid-19 pneumonia: ARDS or not? *Crit Care*, 24:154, 2020.

[17] Jason H. T. Bates. *Lung Mechanics: An Inverse Modeling Aproach*. Cambridge University Press, 2009.

[18] American Lung Association. Measuring your peak flow rate, 2019. Last updated 28 February 2019. https://www.lung.org/lung-health-and-diseases/lung-disease-lookup/asthma/living-with-asthma/managing-asthma/measuring-your-peak-flow-rate.html.

[19] David A Kaminsky. What does airway resistance tell us about lung function? *Respiratory Care*, 57(1):85–99, 2012.

[20] Rachel A. Barry, Daniel S. Fink, Dusty Cole Pourciau, Kasey Hayley, Rachael Lanius, Schuylor Hayley, Eddy Sims, and Andrew J. McWhorter. Effect of Increased Body Mass Index on Complication Rates during Laryngotracheal Surgery Utilizing Jet Ventilation. *Otolaryngology-Head and Neck Surgery*, 157(3):473–477, 2017.

[21] VijaySekhar Cellaboina, Wassim M. Haddad, Hancao Li, and James M. Bailey. Limit cycle stability analysis and adaptive control of a multi-compartment model for a pressure-limited respirator and lung mechanics system. *International Journal of Control*, 83(5):940–955, 2010.

[22] Bettina Bohnhorst and Corinna Peter. Pediatric respiratory physiology. In Prem Puri, editor, *Pediatric Surgery*, chapter 11, pages 181–200. Springer, 2020.

[23] G. Nucci and C. Cobelli. Mathematical models of respiratory mechanics. *Modeling Methodology for Physiology and Medicine*, 2001.

[24] Jorn Kretschmer, Cesar Bibiano, Bernhard Laufer, Paul Docherty, Yeong Shiong Chiew, Daniel Redmond, James Chase, and Knut Moller. Differences in respiratory mechanics estimation with respect to manoeuvres and mathematical models. *Biomedical Physics and Engineering Express*, 3, 01 2017.

[25] Mads Mogensen, Lars Thomsen, Dan Karbing, Kristoffer Steimle, Yichun Zhao, Stephen Rees, and Steen Andreassen. A mathematical physiological model of the dynamics of pulmonary ventilation. *IET Seminar Digest*, 2010:1–6, 01 2010.

[26] Donald Campbell and James Brown. The electrical analogue of lung. *British Journal of Anesthesia*, 35:684–692, 1963.

[27] Pardis Ghafarian, Hamidreza Jamaati, and Seyed Mohammadreza Hashemian. A review on human respiratory modeling. *Tanaffos*, 15(2):61–69, 2016.

[28] Emmanuel Koumoundouros, J. Santamaria, and J. Patterson. The comparison of work of breathing methodologies on a patient model. *Proceedings of the 23rd Annual International Conference of the IEEE*, 1:441–444, 2 2001.

[29] Antonio Albanese, Limei Cheng, Mauro Ursino, and Nicolas W. Chbat. An integrated mathematical model of the human cardiopulmonary system:model development. *American Journal of Physiology - Heart and Circulatory Physiology*, 310(7):899–921, 2015.

[30] Paolo Barbini. Non-linear model of the mechanics of breathing applied to the use and design of ventilators. *Journal of Biomedical Engineering*, 4(4):294 – 304, 1982.

[31] M. A. F. Epstein and R. A. Epstein. Airway flow patterns during mechanical ventilation of infants: A mathematical model. *IEEE Transactions on Biomedical Engineering*, BME-26(5):299–306, 1979.

[32] J.J Marini and PS Crooke. A general mathematical model for respiratory dynamics relevant to the clinical setting. *American Review of Respiratory Disease*, 147(1):14–24, 1993.

[33] Alvin A. Wald, Terence W. Murphy, and Valentino D. B. Mazzia. A theoretical study of controlled ventilation. *IEEE Transactions on Biomedical Engineering*, BME-15(4):237–248, 1968.

[34] Virginie Le Rolle, Nathalie Samson, Jean-Paul Praud, and Alfredo I Hernández. Mathematical modeling of respiratory system mechanics in the newborn lamb. *Acta Biotheoretica*, 61(1):91–107, March 2013.

[35] Marko Topalovic, Eric Derom, Christian R. Osadnik, Thierry Troosters, Marc Decramer, and Wim Janssens. Airways resistance and specific conductance for the diagnosis of obstructive airways diseases. *Respiratory Research*, 16(88), 2015.

[36] Electonic Tutorial. Rc charging and discharging circuits, 2020. Last accessed 17 December 2020. https://www.electronics-tutorials.ws/rc/rc_1.html.

[37] Dean R Hess. Respiratory mechanics in mechanically ventilated patients. *Respiratory Care*, 59(11):1773–1794, 2014.

[38] Johns Hopkins University Office of Academic Computing. Airway resistance, 1995. Last accessed 20 November 2020. http://oac.med.jhmi.edu/res_phys/Encyclopedia/AirwayResistance/AirwayResistance.HTML.

[39] Zareer Tafadar. Compliance resistance and work of breathing, Nov 2014.

[40] Eduardo Gaio and César Melo. A pattern to evaluate airway resistive phenomenon using rohrer's equation. *Advances in Physiology Education*, 31(1):121–121, 2007. PMID: 17327596.

[41] Saing Paul Hou, Nader Meskin, and Wassim M. Haddad. A general multicompartment lung mechanics model with nonlinear resistance and compliance respiratory parameters. In *2014 American Control Conference*, pages 566–571, 2014.

[42] P.S. Crooke, S. Hota, J.J. Marini, and J.R. Hotchkiss. Mathematical models of passive, pressure-controlled ventilation with different resistance assumptions. *Mathematical and Computer Modelling*, 38(5):495–502, 2003.

[43] Hancao Li and Wassim M. Haddad. Optimal determination of respiratory airflow patterns using a nonlinear multicompartment model for a lung mechanics system. *Computational and Mathematical Methods in Medicine*, 2012:1–11, 2012.

[44] MATLAB. *9.0.0.1570001 (R2020b)*. The MathWorks Inc., Natick, Massachusetts, 2020.

[45] Alison M. Wilson, Dana M. Gray, and John G. Thomas. Increases in endotracheal tube resistance are unpredictable relative to duration of intubation. *Chest*, 136(4):1006–1013, 2009.

[46] G. Conti, R. A. De Blasi, A. Lappa, A. Ferretti, M. Antonelli, M. Bufi, and A. Gasparetto. Evaluation of respiratory system resistance in mechanically ventilated patients: The role of the endotracheal tube. *Intensive Care Medicine*, 20(6):421–424, 1994.

[47] Christian Straus, Bruno Louis, Daniel Isabey, François Lemaire, Alain Harf, and Laurent Bronchard. Contribution of the endotracheal tube and the upper airway to breathing workload. *American Journal of Respiratory and Critical Care Medicine*, 157(1):23–30, 1998.

[48] JF Hair. *Multivariate Data Analysis: With Readings*. Pearson College Division, 1979.

[49] Tommaso Mauri, Barbara Cambiaghi, Elena Spinelli, Thomas Langer, and Giacomo Grasselli. Spontaneous breathing: a double-edge sword to handle with care. *Annals of Translational Medicine*, 55(6), 2017.

[50] Jennifer L. Mueller and Samuli Siltanen. *Linear and Nonlinear Inverse Problems with Practical Applications*. Society for Industrial and Applied Mathematics, 2012.

[51] Daniel Fink. Determining Regional Lung Volumes with Electrical Impedance Tomography on Patients Receiving Low-Frequency Jet ventilation, 2018. COMIRB Protocol #: 17-1927.

[52] J Ashe, D Shoudy, G Boverman, J Sabatini, T J Kao, and B Amm. A high precision parallel current drive experimental eit system. In *15th International Conference on Biomedical Applications of Electrical Impedance Tomography*, 2014.

[53] R S Blue, D Isaacson, and J C Newell. Real-time three-dimensional electrical impedance imaging. *Physiological Measurement*, 21(1):15–26, feb 2000.

[54] Tzu-Jen Kao, Amm. Bruce, David Isaacson, Jonathan Newell, Gary Saulnier, and Jennifer L. Mueller. A 3d reconstruction algorithm for real-time simultaneous multi-source eit imaging for lung function monitoring. *bioRxiv*, 2020.

[55] Nilton Barbosa da Rosa Junior, Jennifer Mueller, Andre Vieira Pigatto, Tzu-Jen Kao, Nancy Stoffel, Cheryl Bromirski, David Davenport, Patrick Offner, and Ellen Burnham. Ventilation

volume of mechanically ventilated patients from eit data on a novel electrode solution: A case study. In *International Conference of Bioelectromagnetism, Electrical Bioimpedance, and Electrical Impedance Tomography*, 2022.

[56] Jennifer Mueller, Peter Muller, Michelle Mellenthin, Rashmi Murthy, Michael Capps, Melody Alsaker, Robin Deterding, Scott Sagel, and Emily Deboer. Estimating regions of air trapping from electrical impedance tomography data. *Physiological Measurement*, 39, 05 2018.

[57] Michael Donahoe. Acute respiratory distress syndrome: A clinical review. *Pulmonary circulation*, 1:192–211, 04 2011.

[58] Zhou Wang, A.C. Bovik, H.R. Sheikh, and E.P. Simoncelli. Image quality assessment: from error visibility to structural similarity. *IEEE Transactions on Image Processing*, 13(4):600–612, 2004.

[59] Joshua Daniel Pertile. *Parameters Governing Airway Pressure Homogeneity During Low Frequency Jet Ventilation*. PhD thesis, University of Colorado, 2019.